AN EXPERIMENTAL STUDY ON THE PERFORMANCE OF BOX TYPE FLOATING BREAKWATERS WITH SCREENS

A THESIS SUBMITTED TO
THE GRADUATE SCHOOL OF NATURAL AND APPLIED SCIENCES
OF
MIDDLE EAST TECHNICAL UNIVERSITY

BY

MUSTAFA ONUR KÜRÜM

IN PARTIAL FULFILLMENT OF THE REQUIREMENTS
FOR
THE DEGREE OF MASTER OF SCIENCE
IN
CIVIL ENGINEERING

JULY 2008

Approval of the thesis:

AN EXPERIMENTAL STUDY ON THE PERFORMANCE OF BOX TYPE FLOATING BREAKWATERS WITH SCREENS

submitted by **MUSTAFA ONUR KÜRÜM** in partial fulfillment of the requirements for the degree of
Master of Science in Civil Engineering Department, Middle East Technical University by,

Prof. Dr. Canan Özgen
Dean, Graduate School of **Natural and Applied Sciences** ______________

Prof. Dr. Güney Özcebe
Head of Department, **Civil Engineering** ______________

Prof. Dr. Ayşen Ergin
Supervisor, **Civil Engineering** ______________

Dr. Işıkhan Güler
Co-supervisor, **Civil Engineering Department** ______________

Examining Committee Members:

Assoc. Prof. Ahmet Cevdet Yalçıner
Civil Engineering, METU ______________

Prof. Dr. Ayşen Ergin
Civil Engineering, METU ______________

Dr. Işıkhan Güler
Civil Engineering, METU ______________

Assoc. Prof. Nuri Merzi
Civil Engineering, METU ______________

Dr. Bergüzar Öztunalı Özbahçeci
Ministry of Transportation, DLH ______________

Date: ______________

I hereby declare that all information in this document has been obtained and presented in accordance with academic rules and ethical conduct. I also declare that, as required by these rules and conduct, I have fully cited and referenced all material and results that are not original to this work.

Name, Last Name: MUSTAFA ONUR KÜRÜM

Signature :

ABSTRACT

AN EXPERIMENTAL STUDY ON THE PERFORMANCE OF BOX TYPE FLOATING BREAKWATERS WITH SCREENS

Kürüm, Mustafa Onur
M.S., Department of Civil Engineering
Supervisor : Prof. Dr. Ayşen Ergin
Co-Supervisor : Dr. Işıkhan Güler

July 2008, 130 pages

In the present thesis the performance of box type floating breakwaters (FBs) with screens under regular waves is examined experimentally in a wave flume. The experiments were conducted in the Coastal and Harbor Engineering Laboratory wave flume, Civil Engineering Department, Middle East Technical University, Ankara. The influence of incident wave characteristics and certain geometric characteristics, such as the width and draft of the structure, on its efficiency is examined. Three different widths of the structure in combination with three different screen (draft) height, a total of nine different cases, of FBs are examined. Results related to transmission and reflection of the incident regular waves on the structure are presented. According to the results, for all structures drafts and structure widths, as h/L increase (wave period and wave height decreases) K_t values decrease. Also, K_t values obtained for chain moored floating breakwaters are larger than the K_t values of fixed cases consistently.

Keywords: Floating breakwater, transmission, reflection, screen, calibration

ÖZ

PERDELİ KUTU TİPİ YÜZEN DALGAKIRANLARIN PERFORMANSININ DENEYSEL ARAŞTIRILMASI

Kürüm, Mustafa Onur
Yüksek Lisans, İnşaat Mühendisliği Bölümü
Tez Yöneticisi : Prof. Dr. Ayşen Ergin
Ortak Tez Yöneticisi : Dr. Işıkhan Güler

Temmuz 2008, 130 sayfa

Bu tezde perdeli kutu tipli yüzen dalgakıranların düzgün dalgaların etkisi altındaki performansı deneysel bir çalışma ile araştırılmıştır. Deneyler Orta Doğu Teknik Üniversitesi, İnşaat Mühendisliği Bölümü, Kıyı ve Liman Laboratuvarı dalga kanalında yapılmıştır. Dalga karakterinin ve yapının genişliği ve kullanılan bariyerlerin derinliği gibi belirli geometrik karakteristik yapı özelliklerinin yüzen dalgakıran üzerindeki etkileri araştırılmıştır. Üç değişik genişlikteki yüzen dalgakıran modeli üç farklı perde derinliği kombinasyonuyla toplam dokuz farklı durum incelenmiştir. Gelen düzgün dalganın geçirim ve yansıtma ile ilgili sonuçları sunulmuştur. Sonuçlara göre bütün yapı genişlikleri ve bariyer derinilikleri için h/L oranı arttıkça geçirgenlik katsayı değerleri azalmaktadır. Ayrıca, zincirle bağlanmış yüzen dalgakıranlardan elde edilen geçirgenlik katsayı değerleri sabitlenmiş yüzen dalgakıranlardan elde edilen değerlerden sürekli olarak daha büyük çıkmıştır.

Anahtar Kelimeler: Yüzen Dalgakıran, geçirgenlik, yansıma, perde, kalibrasyon

To my newborn niece Leyla Güneş...

ACKNOWLEDGMENTS

I would like to express my sincere gratitude to my supervisor Prof. Ayşen Ergin for changing my life. Her enthusiasm about coastal engineering led me to the point where I am today and I am sure her influence on me will lead me further forward throughout my academic life. Her understanding, encouraging and immense engineering knowledge and judgement have provided a good basis for the present thesis. I consider myself very lucky to have met her and worked with her.

I would also like to thank my co-supervisor Dr. Işıkhan Güler for his valuable comments and advice. He monitored my work and encouraged me to go ahead with my thesis. He supported me by spending his precious time to read this thesis and giving critical comments about it.

I would also like to thank Assoc. Prof. Ahmet Cevdet Yalçıner for his support and understanding throughout my thesis studies. We overcame many difficulties together throughout my thesis studies.

I would like to thank Onur Kaçar for showing me the optimum environment to write a thesis, Engin Özkol for opening ”the studio” to me, Emre Maşalacı, Burak Evren, Can Öncül and Deniz Bolayır for their presence in my life. I would like to express my gratitude to my friends for their generous attitude and support. I would like to thank Arif Kayışlı and Yusuf Korkut for the help they provided during unit constructions. Special thanks to Ümit İren and Bodrum Municipality for their support. Lastly, I would like to express my gratitude to my family and my friend Cüneyt Baykal. Without their support, none of this could have been possible.

TABLE OF CONTENTS

LIST OF TABLES

TABLES

LIST OF FIGURES

FIGURES

LIST OF SYMBOLS

a_I	Amplitude of incident wave	44
a_R	Amplitude of reflected wave	44
B	Width of the structure	17
d	Draft	17
D	Structure height (freeboard+draft)	18
f	Frequency	34
F_r	Froude number	20
g	Gravitational acceleration	45
h	Water depth	17
H	Wave height	19
H_i	Incident wave height	6
H_m	Mean wave height	38
H_r	Reflected wave height	6
H_t	Transmitted wave height	6
H_s	Significant wave height	43
k	Wave number	36
K_t	Transmission coefficient	17
K_r	Reflection coefficient	47
l_v	Vert. dist. from bottom to wave board hinge	35
L	Wave length	17
L_{CR}	Wave crest length	18
L_s	Length of the structure	18
S_0	Wave board stroke amplitude	36
t	Time	21
T	Wave period	21
T_m	Model Period	34
V	Volume	21

W	Weight	21
x	Horizontal coordinate	35
y	Horizontal coordinate	35
z	Vertical coordinate	35
$\Delta\ell$	PDistance between two adjacent wave gauges	44
ε_I	Phase angle of incident wave	44
ε_R	Phase angle of reflected wave	44
η_i	i-th point of the surface elevation	42
η_I	Surface elevations of incident wave	44
η_R	Surface elevations of reflected wave	44
σ	Angular frequency	44
ϕ	Velocity potential function	35

CHAPTER 1

INTRODUCTION

1.1 Breakwaters in brief

Since time immemorial, harbors played a deciding role in the extent of prosperity for entire populations. In the early history, naturally sheltered locations (like bays and estuaries) were used as a haven for ships. Soon these sheltered locations, where little wave attack was encountered, became the centers of trade. When the economical importance of harbors increased further more, these harbors became the centers of society as well. Nowadays, space has become very scarce in coastal zones and around harbor areas in particular. However, technological developments made it possible to extend the harbors into the ocean. Often, artificial breakwaters are used to create the sheltered area where harbor activities take place.

The primary function of a breakwater is to attenuate waves to an acceptable level or eliminate their effects altogether. It creates a sheltered region in order to prevent damage to shorelines, harbors, and other natural or man-made structures. Although there are several types of breakwater structures, one can roughly distinguish three main types of breakwaters, which are:

- Conventional (mound) type of breakwaters
- Monolithic type of breakwaters
- Composite type of breakwaters

Conventional (mound) type of breakwaters Mound types of breakwaters are actually no more than large heaps of loose elements, such as gravel and quarry stone or concrete blocks (Figure 1.1).

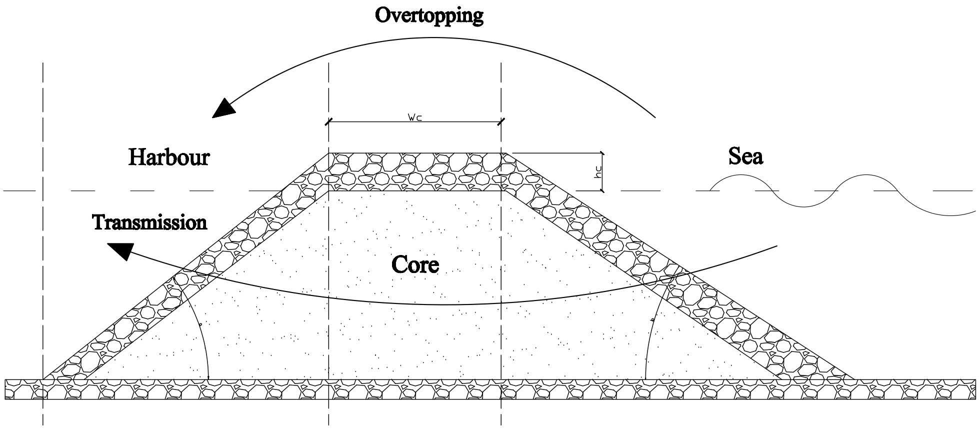

Figure 1.1: Conventional (mound) type of breakwaters

Monolithic type of breakwaters

Monolithic types of breakwaters have a cross section designed in such a way that the structure acts as one solid block. In practice, one may think of a caisson, a block wall, or a masonry structure. Generally this kind of structure is used when space is scarce and local water depths are relatively large (Figure 1.2).

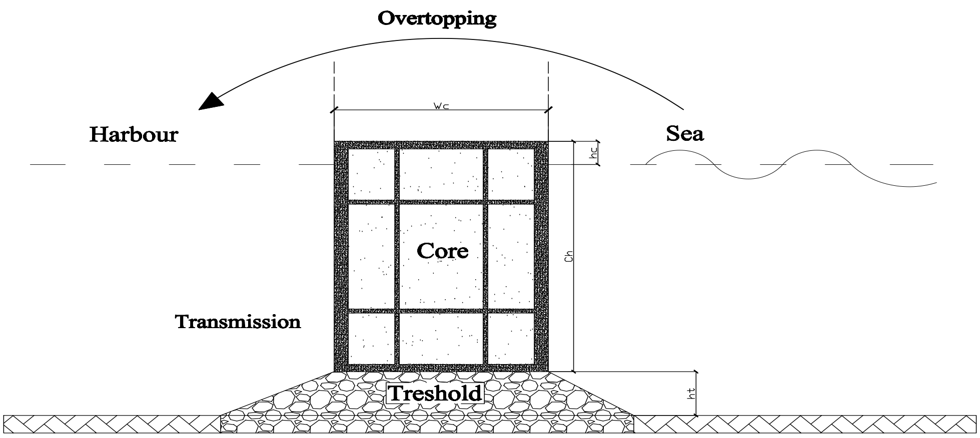

Figure 1.2: Monolithic type of breakwaters

Composite type of breakwaters

A composite type of breakwater is a combination of the conventional and monolithic type of breakwater. When water depths get larger, this kind of structures is often preferred from an economical point of view (Figure 1.3).

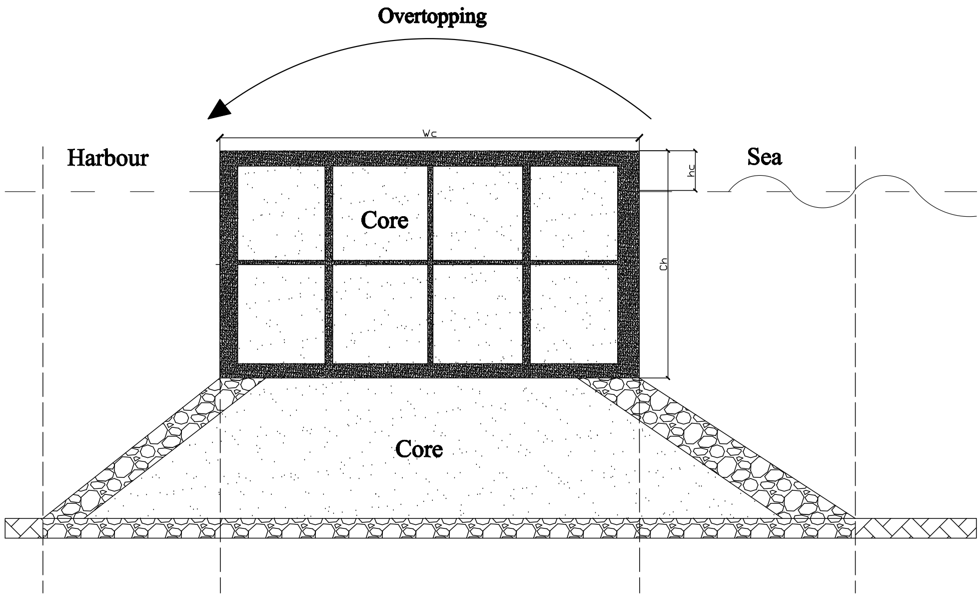

Figure 1.3: Composite type of breakwaters

Although the designs of the breakwaters (Figures 1.1, 1.2, 1.3) differ from one another, a lot of similarities can be distinguished. They are all built to block the incoming waves and to dissipate or reflect the wave energy. They are all fixed structures, designed for a specific location. Bottom-founded structures are limited to a certain maximum water depth since these structures are impossible in deep water environments from a technical as well as an economical point of view [1].

From a military, a humanitarian, a technical and an economical point of view, a new type of breakwater is needed to overcome the restrictions that are associated with fixed breakwaters. This new type of breakwater has to be rapidly installed, transportable, (re-)usable at several locations with different wave conditions and applicable in deep water areas. Several types of unconventional breakwaters have been developed in the past in order to meet these demands, including the floating breakwater (Figure 1.4) [1].

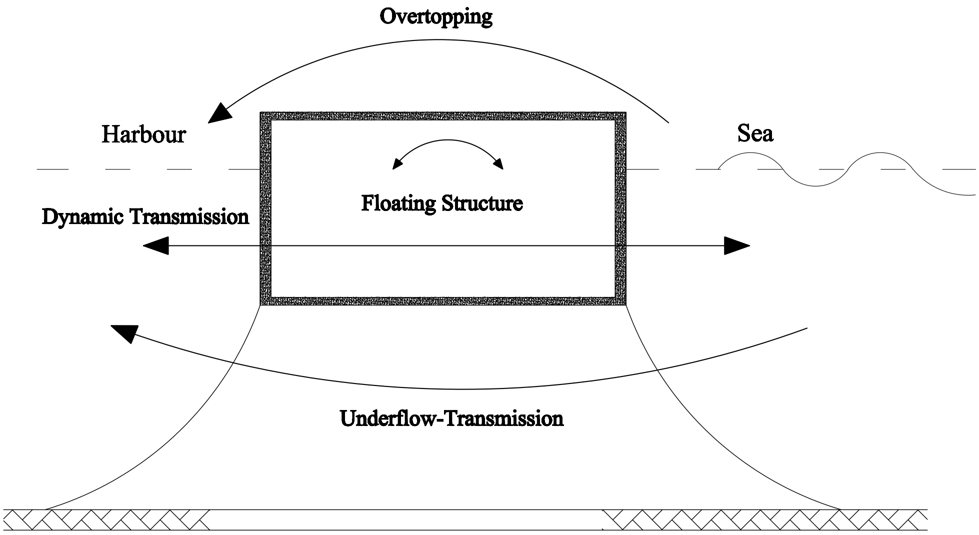

Figure 1.4: Floating type of breakwaters

Although a lot of (theoretical and practical) research has been done on a wide variety of floating breakwater concepts, the appliance of floating breakwaters in real situations is very limited. The complex contribution of the dynamic response to the total wave transmission is the main reason for this. This dynamic response makes a floating breakwater only suitable for a small frequency range. Figures 1.1, 1.2, 1.3, 1.4 show the phenomena that contribute to the two-dimensional wave transmission for several types of breakwaters [1].

1.1.1 Floating Breakwaters

1.1.1.1 Advantages of floating breakwaters

Floating breakwaters represent an alternative solution to protect an area from wave attack, compared to conventional fixed breakwaters. It can be effective in coastal areas with mild wave environment conditions. Therefore, they have been increasingly used aiming at protecting small craft harbors or marinas or, less frequently, the shoreline, aiming at erosion control [2]. The main function of a floating breakwater is to attenuate wave action. Such a structure cannot stop all the wave action. The incident wave is partially transmitted, partially reflected, and partially dissipated. Energy is dissipated due to damping, friction and the generation of eddies at the edges of the breakwater. The breakwater generates a radiated wave which is propagated in offshore and onshore directions. The movement of the breakwater is specified in terms of the anchoring, which defines the degrees of freedom of the breakwater [25].

Some of the conditions that favor floating breakwaters are [2]:

1. Poor foundation: Floating breakwaters might be a proper solution where poor foundations possibilities prohibit the application of bottom supported breakwaters.

2. Deep water: In water depths in excess of 6 m, bottom connected breakwaters are often more expensive than floating breakwaters.

3. Water quality: Floating breakwaters present a minimum interference with water circulation and fish migration.

4. Ice problems: Floating breakwaters can be removed and towed to protected areas if ice formation is a problem. They may be suitable for areas where summer anchorage or moorage is required.

5. Visual impact: Floating breakwaters have a low profile and present a minimum intrusion on the horizon, particularly for areas with high tide ranges.

6. Breakwater layout: Floating breakwaters can usually be rearranged into a new layout with minimum effort.

1.1.1.2 Effectiveness

Floating breakwaters are very effective when their width is of order of half the wavelength and/or when their natural period of oscillation is much longer compared to the wave period. The first requirement is seldom verified, and in this case the performance is uncertain. The performance of a floating breakwater depends on the strongly non-linear interaction of the incident wave (that may partially overtop the module and is in general short-crested and oblique) with the structure dynamics. The interaction becomes complicated by the forces induced by the mooring system and the connections between the modules. Accurate design is necessarily based on the combination of numerical and physical models [2].

1.1.1.3 Types of floating breakwaters

Floating breakwaters are commonly divided into four general categories:

1. Box
2. Pontoon
3. Raft/Mat
4. Tethered float.

The first three types have been much widely investigated by means of physical models and prototype experience, than the last one. Next subsections describes the use of the different types of breakwaters in practice. For design purposes, floating breakwaters can also be separated into two groups:

- Reflective Structures: Box type and pontoon type floating breakwaters are reflective structures.
- Dissipative Structures: Mat type and tethered float type floating breakwaters are dissipative structures.

These two types of actions may be illustrated by Figure 1.5, where H_i, H_r and H_t are the incident, the reflected and the transmitted heights, respectively. This classification is arbitrary, and each structure acts partially in both ways. For each category, some types of floating breakwaters are shown in Figures 1.6 to 1.13.

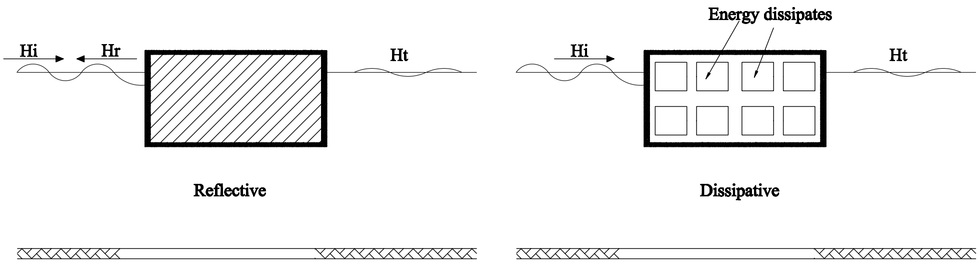

Figure 1.5: Reflective and dissipative actions

Box type floating breakwaters Box type breakwaters (Figure 1.6) are used most frequently. Reinforced concrete modules are either empty inside or, more frequently, have a core of light material (e.g. polystyrene). In the former case the risk of sinking of the structure is not negligible. Usually dimensions are limited to a width of a few meters. Connections are either flexible, allowing preferably only the roll along the breakwater axis, or pre or post tensioned, to make them act as a single unit. In the latter case the efficiency is higher, but the forces between modules are also higher. The modular system as applied and the mooring system are primary points of concern for this kind of structures. Large breakwaters are frequently built with used barges, ballasted to the desired draft with sand or rock.

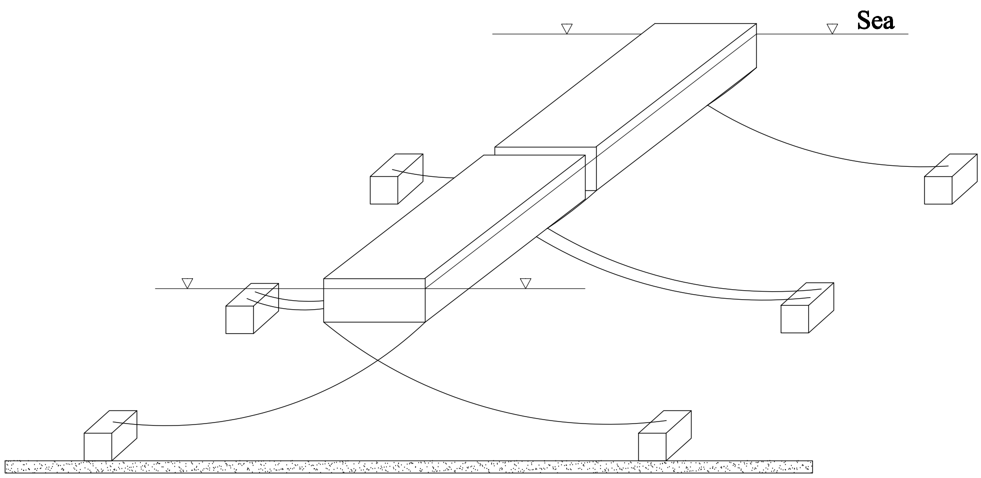

Figure 1.6: Box type floating breakwater

Pontoon type floating breakwaters Raft/Mat type floating breakwaters Pontoon types are effective since the overall width can be of the order of half the wavelength. In this case the expected attenuation of the wave height is significant. In order to increase inertia without increasing the total mass, two single pontoons may be connected to each other, so as to obtain the following structure, Figure 1.7.

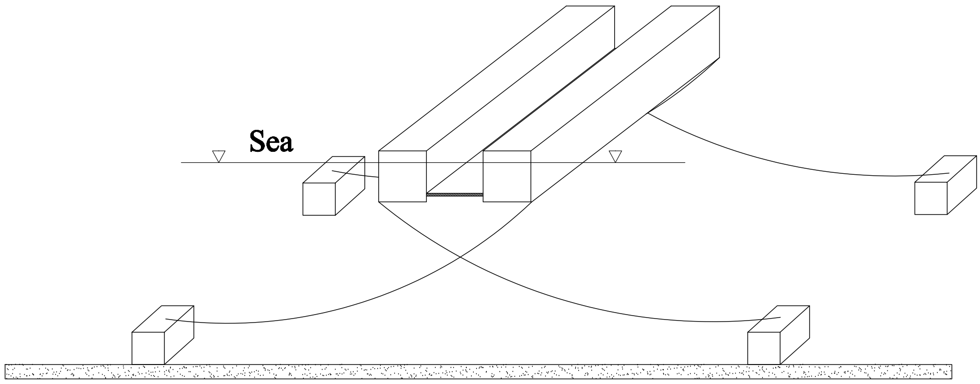

Figure 1.7: Double Concrete Pontoon

Such a breakwater attenuates waves in the same way as a single pontoon, but in addition reduces wave field through turbulence between the two floating bodies. Each float may be constructed of steep pipes filled or partially filled with water [3]. The mass can be concentrated low for stability. This is achieved with catamaran type breakwaters (Figure 1.8)

Another type of double pontoon is the Alaska type floating breakwater [4] which is represented below (Figure 1.9) and where some energy is dissipated by turbulence.

The Canadian A-Frame is another alternative floating breakwater (Figure 1.10), which functions like a reflective system, the rolling motions being important according to the values of the ratio between wavelength and breakwater width.

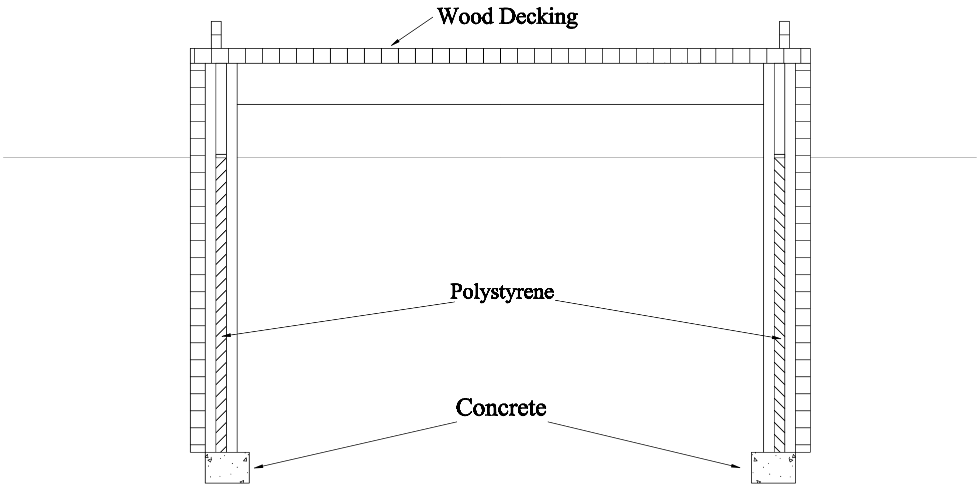

Figure 1.8: Single Pontoon - Catamaran Shape

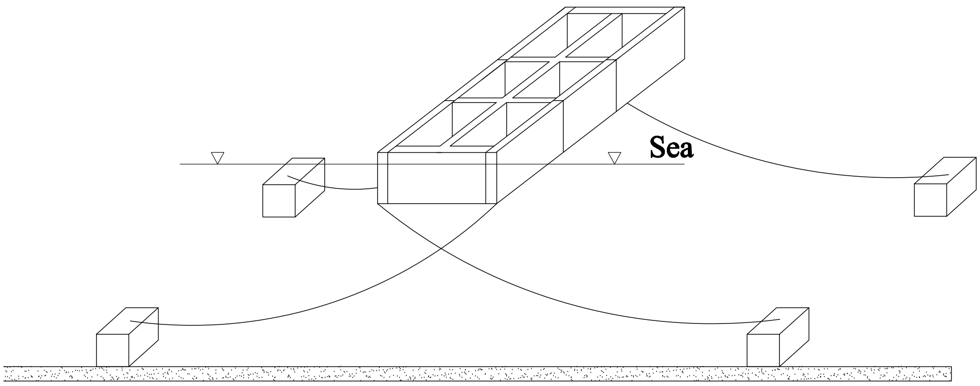

Figure 1.9: Open Compartment - Alaska Type

Raft/Mat type floating breakwaters Within the mat category, the most used are made with tires. Although less effective, they have a low cost, they can be removed more easily, they can be constructed with unskilled labor and minimal equipment, they are subjected to lower anchor loads, they reflect less and they dissipate relatively more wave energy. Raft type floating breakwaters (Figure 1.11) consist of independent hulls or pontoons moored lengthwise to the direction of wave attack and loosely interconnected by cables or chains having a gap width between hull units approximately equal to hull width [5].

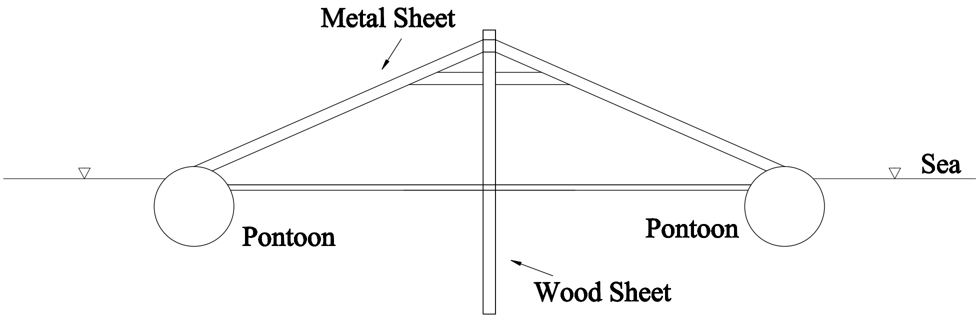

Figure 1.10: A Frame Type

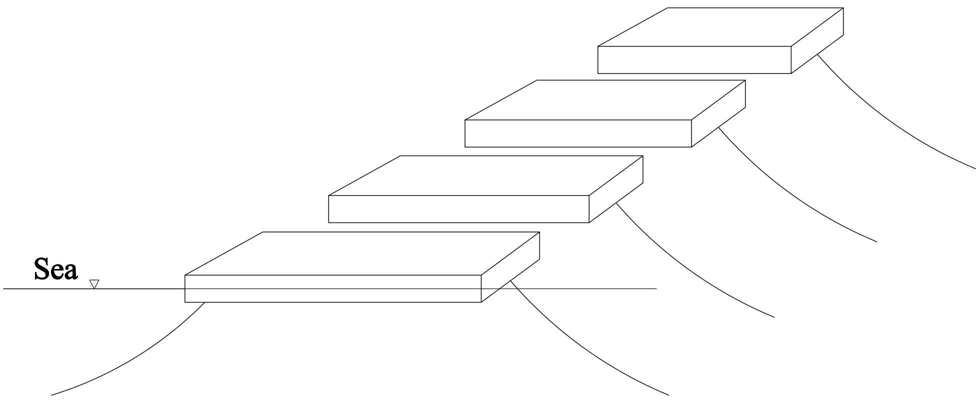

Figure 1.11: Raft Type

Truck tires, sometimes filled with floatation material (e.g. polystyrene or polyurethane), have been used to construct floating mat type breakwaters which attenuate short period waves. Different systems have been designed and patented [6]; some of them are composed exclusively of tires (Goodyear, etc.), others are constructed with poles of beams (Pole-Tire) (Figure 1.12). All influence wave propagation in at least three ways:

- Their mass, inertia and damping characteristics induce a first attenuation, as the reflective systems do;
- They form a semi flexible sheet which tends to follow the fluctuations of the water surface. Provided wave lengths are short enough and the rigidity of the structure is high enough so that restoring forces may be important, this sheet will limit surface vertical displacements;

- Their porosity generates drag forces which contribute to energy losses.

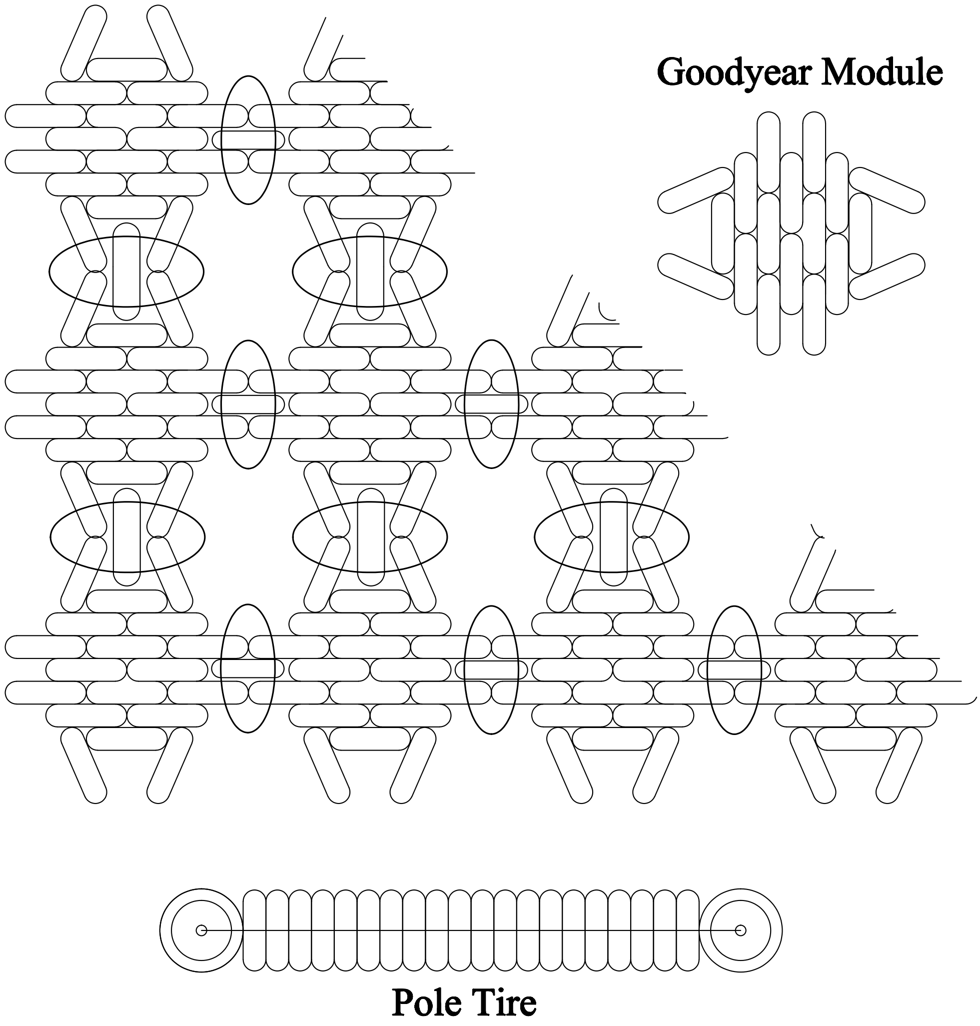

Figure 1.12: Goodyear - Pole Tyre Floating Breakwater

Tethered floating breakwaters Tethered float types are seldom used. A tethered float breakwater [7] consists of a field of independent floats moored to the sea bottom. The mooring lines are always in tension due to high buoyancy of the floats, and the line length is equal or little than the water depth (Figure 1.13)

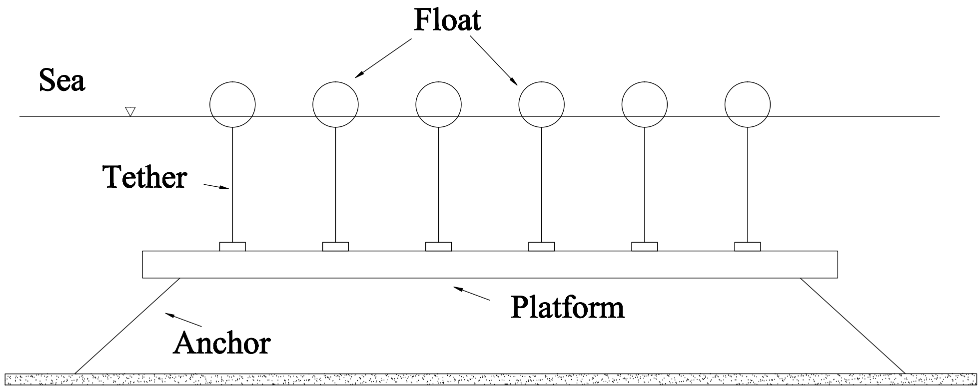

Figure 1.13: Tethered Floating Breakwater

This system functions more or less like and inverted pendulum, whose natural period of oscillation, T_0, is proportional to the square root of the mooring line length [8]. When excited by a wave whose period is near T_0, it tends to oscillate out of phase with the incident wave, so the velocity of water particles relative to the floats may become rather important [11].

In this study, box type floating breakwaters with screens are investigated at a constant construction water depth (h=14m) with two sets of model investigations as fixed and chain moored floating breakwaters with a model scale of 1/20. Experiments carried out with variable structure width and structure draft under the design waves with periods ranging from T=4sec to T=6.5sec and wave heights ranging from 0.3m to 1.7m. In Chapter 2, the literature survey research is presented. In Chapter 3, physical model studies which include construction of units, wave generation, calibration, data analysis. In Chapter 4, experiments and discussion of results are presented. In the final chapter, Chapter 5, the conclusion of this thesis and future recommendations are stated.

CHAPTER 2

LITERATURE SURVEY

2.1 Introductıon

The literature survey for this thesis was carried out using the Middle East Technical University library system and the Internet. Most of the literature reviewed is described in this section. The history of floating breakwaters goes back in time to 1842. Probably the first paper was published in the Civil Engineers and Architects Journal in 1842 and was titled ”Reeds floating breakwater.” It was discovered in 1905 that ships hulls could be used as floating breakwaters. There was not much interest in America to use the idea, but in Europe it was used several times. Floating breakwaters were primarily used to protect deep water harbors. During the Second World War in 1941, at Lysekil in Sweden, a 120 meter long concrete floating breakwater was built to protect a small harbor. Probably the most famous floating breakwater in history is the Bombardon, which the Royal Navy of England developed to protect the coastline of Normandy. The shape was a crucifix cross-section. The Bombardon was designed to attenuate a 2.5 meter wave. The oldest floating breakwater in use at the moment is most likely in Bergen, Norway. It was built in 1948 and was made of 20m long concrete barges [12]. In previous days, the structural length of a breakwater has been relatively large (120 m). Recent studies have shown that increased structural length will reduce transmitted wave height [13].

There are several types of floating breakwaters, which include box, pontoon, mat, and tethered float (Chapter 1). Box-type breakwaters are usually constructed of reinforced concrete. They generally act as barges, which dissipate energy at the wave surface. Advantages of this type of breakwater are numerous and include a fifty-year design life, simple construction, proven performance, and effectiveness under ”moderate” wave conditions. The only major disadvantage of the box-type breakwater is its relatively high cost in comparison to the other types of floating breakwaters [15].

2.2 Floating breakwater numerical studies

The hydrodynamic problem of floating breakwaters is extremely complex especially in the case of a moving structure. There are several studies dealing with the hydrodynamic problem of floating breakwaters in deep and intermediate water depth [25]. Linear models and analytical solutions, which describe the full hydrodynamic problem, have been developed by Hwang and Tang (1986) [26], Williams and McDougal (1991) [27], Drimer et al. (1992) [28], Bhatta and Rahman (1993)[29], Isaacson and Bhat (1998) [30], Williams et al. (2000) [31] and Kriezi et al. (2001) [33]. A coupled solution for diffraction and body movement is proposed to eliminate the error introduced by the linear approach of the problem (Isaacson [34], 1982a; Gottlieb and Yim, 1995 [35]). A limited number of studies have dealt with the interaction of the floating body with oblique waves (Isaacson and Bhat, 1998 [36]; Sannasiraj et al., 1998 [37]). The current behind the floating structure has also been studied (Isaacson and Cheung, 1993) [38], while overtopping has been studied by Isaacson (1982b) [39]. Different models have been studied which calculate the forces on the mooring system of a floating breakwater (Niwinski et al., 1982 [40] ;Yamamoto, 1982 [41]; Yamamoto et al., 1982 [42]; Nossen et al., 1991 [44]; Isaacson and Bhat, 1994 [45];Yoon et al., 1994) [46].

Inoue et al. (1995) [10], in a numerical study of the behavior of multiple floating breakwater, states that; the multiple floating breakwater system shows the better performance than a single breakwater in most wavelengths. The application of multiple floating breakwater as the protection of offshore structures in coastal engineering should be stressed. He notes that because there exist hydrodynamic interactions between multiple floating bodies, in the vicinity of a critical wavenumber where the fluid between the bodies is resonant, the transmission coefficients undergo rapid changes, ranging from complete transmission to no transmission. Also, the variation of transmission coefficients due to the change of the width of the structure is less than due to the changes of the clearance between structures. In the design stage of multiple floating breakwater, suitable adjustment of the clearance may provide better performance than that of the width.

2.3 Floating breakwater model studies

A lot of research has been done on the hydrodynamic behavior of floating breakwaters. The main focus of all these studies has always been to obtain transmission coefficients that are as small as possible. The transmission coefficient is the ratio between the wave height at the leeward (harbor) side of the floating breakwater relative to the wave height of the incident wave. In order to obtain satisfactory results, many designs were model-tested. Although the tested models do vary in design, the common research topics can be split into the influence of the structural design and the structural dynamics on the wave attenuating capacity of the structure. The major aspects of the structural design that have been tested:

- Shape
- Width of the floating section of the structure
- Draft of the structure
- Mass of the structure
- Permeability of the structure

All these structural factors influence the (hydro)dynamic behavior of the floating breakwater. In some of the model tests, the vertical, horizontal and rotational oscillations were treated separately in order to understand the individual influence of the design parameters on the different motions [1].

In their reports, Tolba [49] and Silander [16] proved that a heave motion floating breakwater will perform better when it is not affected in its vertical degree of freedom. Sway motion on the other hand has a negative contribution on the attenuating capacity of the floating breakwater. Silander [16] proved that a free-motion floating breakwater performs better at a certain frequency range when the structural width is optimal.

The draft and the mass of the structure are related to one another when the structural width is kept constant. Increasing the draft with a screen has a positive effect on the wave transmission as Tolba [49] concludes in his report.

The experimental studies are rather limited, performed in small-scale facilities, and only for regular wave forcing [25]. Sutko and Haden (1974)[47] presented a series of small-scale experiments. Fugazza and Natale (1988) [48] studied the phenomenon numerically and experimentally. They investigated the influence of the stiffness of the horizontal part of the mooring system. An experimental study of the phenomenon for a breakwater in a floating mode was presented by Williams (1988), in which the efficiency and the response of the structure was studied. Tolba (1998) [49] and Isaacson and Bhat (1998) [50] studied experimentally pile-restrained floating breakwaters and, in particular, the influence of the heave motion on the efficiency of the structure. Christian (2000) [51] studied a $1/15$ scale, prefabricated form of floating breakwaters, and investigated the efficiency of the structure and the horizontal forces acting on it in a laboratory model.

Syed et al. (2008) [9], in an experimental study on laboratory investigations on multiple pontoon breakwaters, states that the introduction of array of hollow vertical cylinders to the sea side of the floating breakwater, the W/L ratio required to restrict wave transmission by %50 is decreased from 0.44 to 0.38. Also, the array of hollow vertical cylinders effectively reduces the wave reflection at the sea side of the breakwater by approximately %60 thereby reducing the forces in the mooring lines by about %20.

Koutandos et al. (2005) [25], in an experimental study of floating breakwaters under regular and irregular wave forcing, states that; for the fixed floating breakwater, the efficiency of the structure can be considered satisfactory for B/L (B (m) is the width of the structure and L (m) is the wavelength.) greater than 0.25 and d/h (d (m) is the draft height and h (m) is the water depth) ranging between 1/5 to 1/3. He also states that the fixed floating breakwater operates in a highly reflective manner with values of the reflection coefficient ranging between 0.4 (longest wave period) and 0.9 (shortest wave period). In his study, it is concluded that the attached plates (screens) at the front of the floating breakwater considerably enhances the efficiency of the structure.

In his PhD. thesis, Silander (1999) [16] carried out several experiments with different floating breakwater models in the Hydraulic Laboratory at the Helsinki University of Technology. Over 20 different floating breakwater cross sections, which were in use at that time, were investigated thoroughly in a wave flume. In his study, the effects of permeability, width, continuity, wave angle and cross-section are studied. According to his experiments on fixed and moving breakwaters, a fixed breakwater usually attenuates better than a moving breakwater, even in irregular waves. When the limit of horizontal motion of the breakwater in regular waves is less than 0.3 multiplied by incident wave height, the moving breakwater can have the same transmission coefficient as a fixed breakwater. A fixed breakwater will normally create the lower limit for the transmission coefficient. It was determined that by connecting vertical barriers to the floating breakwater, the wave attenuation ability can be improved remarkably. Catamarans were found to be more efficient at wave attenuation than the box type breakwaters.

According to his experiments on the effect of wave angle, he states that an increased wave angle compared to perpendicularly approaching wave reduced the transmission coefficient. The actual transmission coefficient will thus be less than it is for perpendicularly approaching waves. He also mentions that permeable barriers can be used to improve transmission performance as the structure will become more stable. For short crested waves or when the breakwater is long in relation to the local wave length, as a system with solid and permeable vertical barriers may perform as well as a system with only solid vertical faces. A permeability ratio higher than 0.2 usually results into a significant increase in the transmission coefficient and it should be avoided.

Sorensen (1991) [17] claimed that it was impossible to achieve a K_t value as low as 0.3 if the L/B value was not between 0.8 - 3. However catamarans achieved this performance (L is wave length and B width of the structure).The reduction in wave force is realized to be considerable when the length of the structure exceeds six wave lengths [14].

It is indicated that B (m), the width of a structure, L (m), the wave length, L_{CR} (m) , the wave crest length, L_S (m) , the length of the structure, D (m) , the draft and h (m) the water depth have a large effect on wave transmission [18]. The effect of wave steepness, short crested waves and anchor system should not be neglected in research.

Williams and McDougal (1996) [32] conducted a two-dimensional analysis of a floating breakwater with a rectangular cross-section. Since they assumed beam waves and an infinitive structural length, the motions of the floating breakwater were described to be two-dimensional in the xz-plane. The mooring lines were schematized as linear springs. Besides the two-dimensional representation of the model, Williams and McDougal assumed regular, small amplitude waves with constant periods. When considering the irregular oblique nature of ocean waves, the assumptions done in this study can be invalid. However, the results give a good representation on the effectiveness of a floating breakwater in different wave conditions. The most important conclusions of this study are: - The breakwater is most effective near the surge natural frequency - The performance of the structure is optimal when the diffracted and radiated waves are of the same magnitude, but with a phase difference.

Similar results were obtained by Yamamoto and Yoshida (1979) [43] as they conducted experimental tests for two kinds of floating breakwater types in order to validate theory-based calculations. The first type was a three-circle cylinder with a cross-section of three adjacent circles. The second type had a rectangular cross-section. As was the case in the study performed by Williams and McDougal, Yamamoto and Yoshida assumed linear spring stiffness for the mooring lines and beam incident waves. The test results yielded a good agreement with the theoretical models. Yamamoto and Yoshida concluded that even zero transmission coefficients could be obtained at either very low or high frequencies. The best performance was gained for waves with frequencies near the natural frequency of the structure.

Cox (1989) [52] mentions that the wave attenuation characteristics of floating breakwaters were first investigated from an analytical standpoint by approximation which consisted of idealized forms of wave barriers. A rigid structure of finite width, B, height, D, and draft d, fixed near the surface of a water body at depth, h, was analyzed by Macagno (1953) [53]. Cox (1989 also mentions that Wiegel (1959) [54] investigated Macagno's conceptual model with a consideration of the wave power transmission. Cox (1989) generalized power transmission theory developed by Wiegel. These analytical approaches will be investigated in detail in the coming chapters (see Page 48).

In the present thesis the performance of box type floating breakwaters (FBs) with screens under regular waves approaching perpendicularly to the units is examined experimentally in a wave flume. The influence of wave characteristics and certain geometric characteristics, such as the width and draft of the structure, on its efficiency is examined. Three different width in combination with three different screen height, a total of nine different cases, of FBs are examined. Different values of wave steepness have been used in model tests. Model tests shows clearly that wave transmission depends on the incident wave steepness and the shape of the structure. For this study, the wave steepness range was selected as H/L, 0.015-0.045, where H is wave height.

Although a lot of theoretical and practical research has been done, no practical solution has been found for the general problem of creating a floating breakwater, able to attenuate waves of a wide frequency range. The floating breakwaters that have been built in real situations were designed to serve at specific locations with specific wave conditions [1].

CHAPTER 3

PHYSICAL MODEL STUDY

3.1 Introduction

Physical modeling of coastal structures is a challenging task that includes both scale effects and laboratory effects. Scale effects result from the use of incorrectly scaled parameters such as fluid density and viscosity. Other dissimilarities may result from physical constraints on a model due to space limitations or necessary simplification of prototype input conditions. Hydraulic models can be classified as either design models or process models. The design model is mainly used to simulate an actual prototype situation. The process model is used to study a physical process in detail. Designs developed using physical models are commonly designed based on a large number of experiments. For the typical hydraulic models, scaling of viscosity and gravity simultaneously is not practical. Gravity forces and the related effects are considered to be more important than viscous forces in this physical model study. This means that the Froude number, F_r, is represented correctly. As usual for maritime engineering the Froude's similitude was adopted in this study; therefore, once set the most suitable geometric scale which is strictly connected to the dimensions of both the prototype and the experimental equipment, to be equal to:

$$I_r = \frac{I_m}{I_p} = \frac{1}{20} \;\; (scale) \tag{3.1}$$

Where I_m and I_p are respectively the lengths referred to the model and the prototype; the following reduction scales obtained for: ”t” time, ”T” wave periods, ”V” volumes,

”W” weights and then adopted in the experimental study.

$$t_r = \frac{t_m}{t_p} = \frac{1}{\sqrt{20}} = \frac{1}{4.47} \tag{3.2}$$

$$T_r = \frac{T_m}{T_p} = \frac{1}{\sqrt{20}} = \frac{1}{4.47} \tag{3.3}$$

$$V_r = \frac{V_m}{V_p} = \frac{1}{20^3} = \frac{1}{8000} \tag{3.4}$$

$$W_r = \frac{W_m}{W_p} = \frac{1}{8000} \tag{3.5}$$

3.2 Model set-up

METU, Civil Engineering Department, Coastal and Harbor Engineering Laboratory wave flume in which the 2 dimensional tests were carried out is shown in Figure 3.1. The wave flume is 26.8 m long, 1m deep and 6.1 m wide. The wave flume is equipped with piston type wave-maker (Figure A.8) capable of generating regular and random waves in which two dimensional modeling was undertaken.

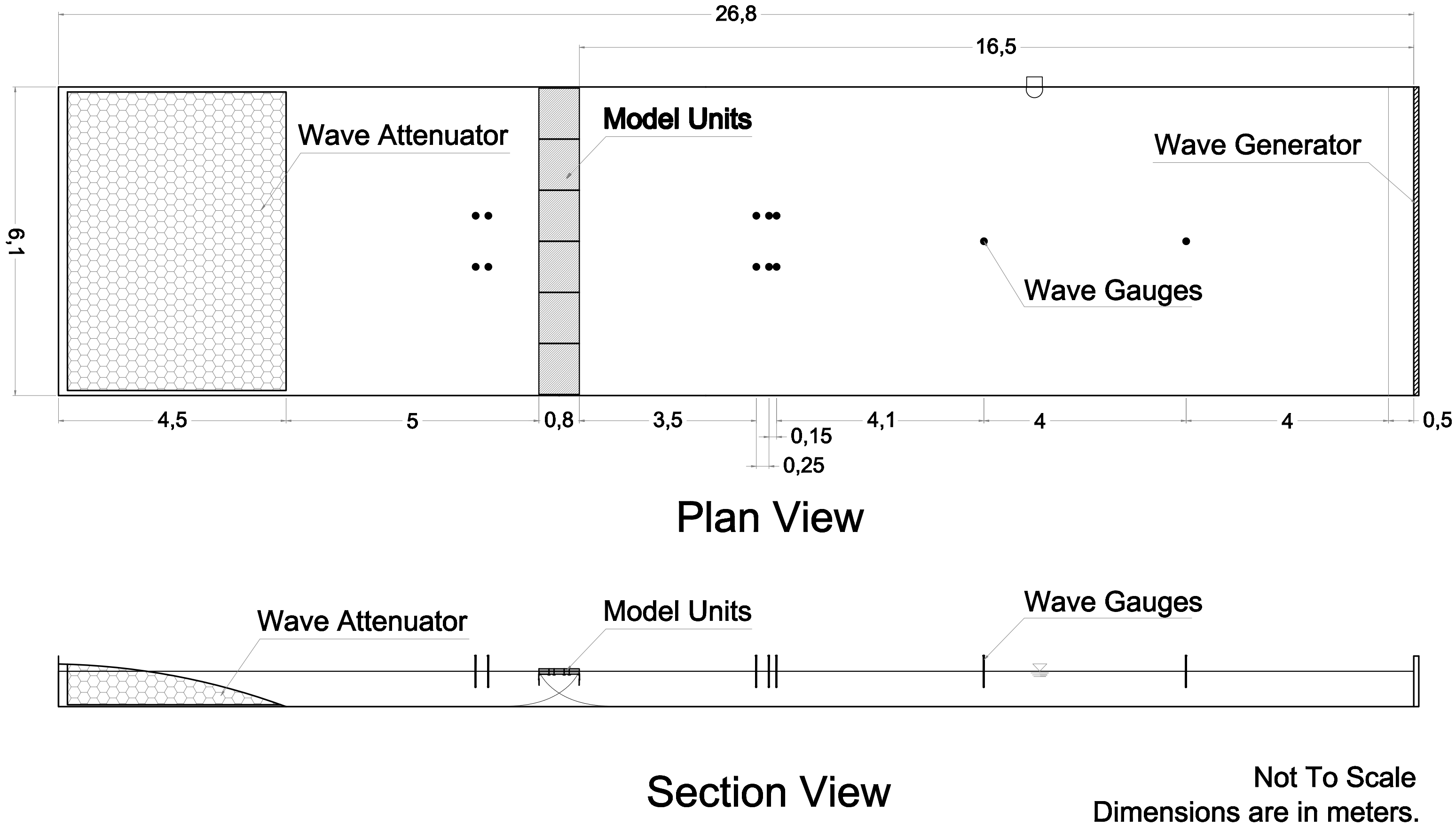

Figure 3.1: The Laboratory Wave Flume

3.2.1 Model Units

Model scale adopted for wave flume tests is 1/20. To determine the model unit dimensions, technical manuals of floating breakwater manufacturers and a research over the internet was conducted. According to this research, prototype floating elements dimensions are selected. The model length was determined based on wave flume width of approximately 6.1 meters minus the clearance from both sides of the units in both sides. Six floating units with L_s = 1 m (L_s, structure length) connected to each other can fit the wave flume with this set-up. Model units can be seen in Figure 3.2.

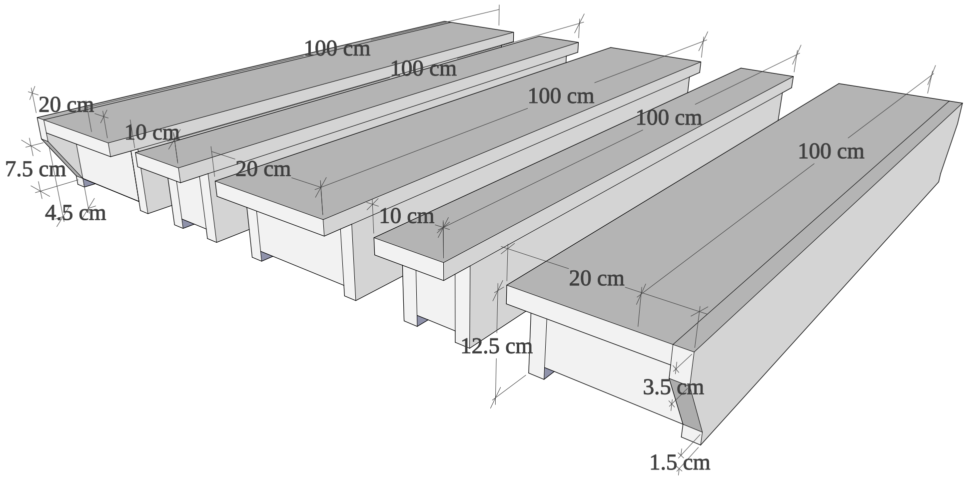

Figure 3.2: Model Units

3.2.1.1 Model Unit Construction

The model units are constructed as closed boxes using 21 mm thick water resistant plywood. As structure width, B (m), has a large effect on wave transmission, model units with varying widths needed to be constructed. For practicality, instead of constructing units with different widths, units are divided and constructed in 5 segments. Three segments having 20 cm width and two segments having 10 cm width are constructed. These 5 segments can be seen in Figure 3.2 and A.9.

These segments can be used in different combinations to form model units with varying widths of 40-50-60-70-80 cm. In this study, model units with widths of 40 cm, 60 cm and 80 cm are used. The core of the breakwater model consists polyethylene foam and aluminium plates (Figure 3.3). The polyethylene foam and the aluminium plates is placed in a way to ensure the center of gravity of the units is fixed. This is important to keep a fixed freeboard of 5 cm. This corresponds to a 1 m freeboard in prototype level, which is widely used by manufacturers around the world.

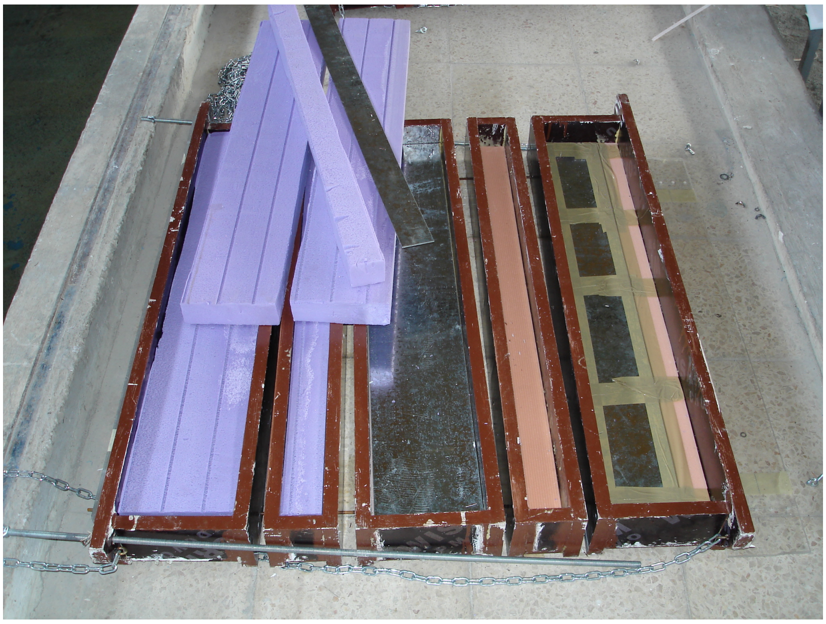

Figure 3.3: Polyethylene foam and aluminium plate filling in the core of segments

To be able to test the model units with varying drafts, d, fibreglass barriers are mounted on each side of the model units. The fiberglass barriers are mounted so that they can be modified to test different draft heights ranging from 7.5 cm to 22.5 cm (Figure 3.4).

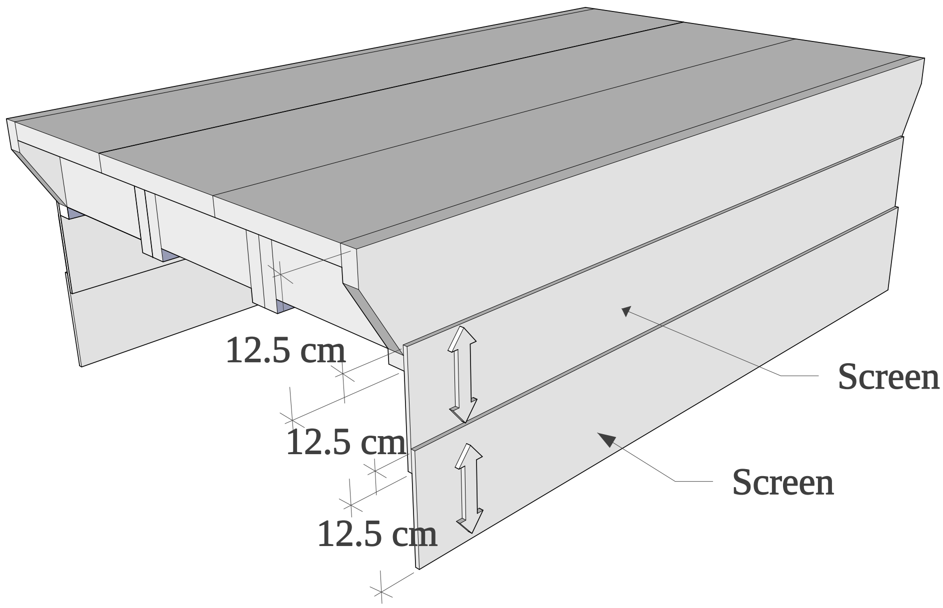

Figure 3.4: Variable fiberglass barriers (draft)

3.2.2 Wave Attenuators

One of the most common laboratory effects that plague physical model experiments is reflection of wave energy from boundaries of from model structures, and dealing with wave reflection ranks right behind the wave generation in importance to high quality laboratory experiments [19]. Unwanted reflections can alter significantly the incident wave field, which in turn may impact test results. Well conducted model studies attempt to minimize wave reflections by placing wave attenuators (absorbers) at reflective boundaries.

3.2.2.1 Passive Absorbers

Traditionally, wave absorption at model boundaries has consisted of placing gentle slopes (less than 1:10), porous material, or screens in front of the boundary to dissipate a large fraction of incident wave energy. These ”passive absorbers” can be designed to be effective over a specified range of wave conditions, but they often require a substantial length to reduce the reflection below %10. Thus, passive absorbers can use up valuable space in a wave flume or basin [20]. A thorough survey of wave absorbers by Ouellet and Datta (1986) [19] indicated that the most popular passive absorber is a constant slope beach constructed of gravel or stones. Although these fixed absorbers prove effective in reducing wave reflection, they are not easily moved, making them less practical for model basins where frequent boundary changes may be needed.

Several experiments are conducted in order to improve the wave attenuation capacity of the wave absorbers. Wave flume was initially equipped with a sloping steel frame wave attenuator. To improve the attenuation performance, steel mesh boxes were constructed filled with plastic wire scrubbers used in dish washing. Plastic wire scrubbers are very effective in dissipating the wave energy, they are flexible and it is a very economical solution. In the first phase of wave attenuator performance improvement experiments, a steal mesh box is placed as shown in Figure 3.5.

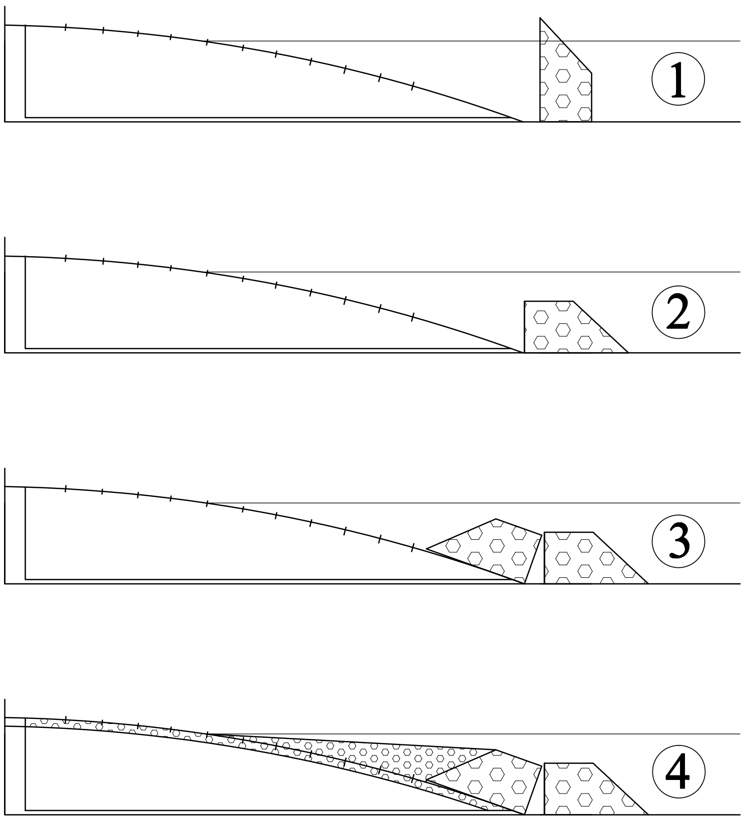

Figure 3.5: Wave Attenuator improving phases

Phase 1 experiments resulted in a rather high reflection in the wave flume. That is caused by the vertically placed steel mesh box acting like a vertical wall. So, in the second phase, steel mesh box was placed horizontally to the wave flume bed. In the third phase,a secondary steel mesh box is placed as shown in Figure 3.5. Although phase 3 experiments results were satisfactory, further improvement is reached by filling the empty spaces formed between the sloping steel frame and secondary steel mesh box. Phase number 4 shown in Figure 3.5 is the final set-up of the wave attenuator system.

3.2.3 Data acquisition

Data acquisition was controlled by the (Danish Hydraulics Institute) DHI - Standard cabinet 101E and the DHI filter cabinet 153/IF along with a PC-computer to collect data from probes. The DHI Instrument System for hydraulic model tests is designed as a modular system consisting of transducers, plug-in conditioning and amplifier modules and a Standard Cabinet with space for up to 8 plug-in modules. The DHI - Standard Cabinet 101E is supplying the modules with power from the built-in +/- 15 Volt power supply through a pcb dashboard. The transducers are connected to sockets on the front panel of the modules. Gain and Zero adjustments potentiometers are mounted on the front panel too. Signal outputs from the modules can be taken from the BNC sockets on the modules. The 8 signal outputs are also available form a common D-connector on the rear panel of the Standard Cabinet. This common D-connector makes data sampling easy when connected to the DHI - 153/IF input filter cabinet. The DHI filter cabinet 153/IF is used for collecting the conditioned signals from a large number of transducers often used in hydraulic model tests, and provide a simpler and easier connection between the transducer/conditioners being the front end part of the data acquisition system and the digital computer with various peripherals, being the back end part of the acquisition system. The DHI filter cabinet is designed for use in combination with PC-AT computers and corresponding 16 channel A/D converter DT2811. The transducers mentioned above are the DHI - Wave Meter 102E wave gauges. The DHI - Wave Meter 102E is based on a conductivity type wave gauge. Thus, the wave gauge comprises two thin, parallel stainless steel electrodes. When immersed in water, the meter measures the conductivity of the instantaneous water volume between the two electrodes, a conductivity that changes proportionally to changes of the water surface elevation, i.e. the wave height, between the electrodes. A set of compensation electrodes, mounted at the bottom end of the wave gauge outbalance the influence of temperature or salinity changes of the water. As for the back end part of the acquisition system, data sampled and filtered by the DHI data acquisition system is collected by software developed by TDG using a PC-AT computer. The software is used the sample the data at a rate of 20 Hz for regular waves for a duration up to 90 seconds. The data is saved as a *.csv file in the PC computer for later use in data analysis. The data saved in the *.csv files shown in Table 3.1 are the raw voltage data recorded from the wave gauges [21].

Table 3.1: Raw Voltage Data Sample

Deney Başlangıcı:10-17-2007 14:19:20 Delta t = 0.01

Kanal1	Kanal2	Kanal3	Kanal4	Kanal5	Kanal6	Kanal7	Kanal8	Kanal9	Kanal10	Kanal11	Kanal12	Kanal13	Kanal14	Kanal15
0.005	0.005	0.005		0.015	-0.029	0.010	0.000			0.000	0.000	0.010	0.005	0.010
0.010	0.010	-0.024		0.010	0.005	0.010	0.000			0.005	0.005	0.010	0.000	-0.005
-0.039	0.005	0.000		0.010	0.000	0.010	0.000			0.005	0.000	0.010	0.005	0.010
0.005	0.005	0.015		0.015	0.005	0.010	0.005			0.000	0.000	0.010	0.000	0.010
0.015	0.005	0.005		0.010	0.000	0.005	0.000			-0.005	0.005	0.010	0.005	0.010
0.010	0.010	0.010		0.015	0.005	0.010	0.000			0.000	0.005	0.010	0.000	0.010
0.010	0.005	0.005		0.010	0.005	0.010	0.000			0.000	0.005	0.010	0.005	0.010
0.010	0.005	0.005		0.010	0.005	0.010	-0.068			0.000	0.000	0.010	0.010	0.010
0.015	0.010	0.005		0.010	0.000	0.010	-0.005			0.000	0.000	0.010	0.005	0.010
0.010	0.010	0.010		0.010	0.000	0.010	-0.015			0.000	0.005	0.010	0.000	-0.010
-0.010	0.005	0.005		0.015	0.005	0.010	0.000			0.000	0.005	0.010	0.000	0.010
.	.	.		.	.	.	.			.	.	.	.	.
.	.	.		.	.	.	.			.	.	.	.	.
.	.	.		.	.	.	.			.	.	.	.	.

3.2.4 Wave Gauge Calibration

”Calibration” of an instrument is the process of determining the relationship between the instrument’s output signal and the value of the physical quantity being measured. The calibration procedure usually results in a mathematical relationship (preferably linear) between the sensor’s output and the physical quantity. Some instruments need to be calibrated whenever environmental conditions change or at the start of each new experiment [20]. In this study, conductivity type wave gauges are used. The main advantage of the conductivity type wave gauges is that the gauge exhibits good linear response and can achieve good resolution. The main disadvantage of the instrument is that frequent calibrations are necessary because the conductivity of water changes with temperature and concentration of dissolved salts. Other disadvantages are the small range of linearity, the high cost of auxiliary equipment, and the distortion in wave shape due to the finite distance separating the wires.

Conductivity type wave gauges feature a linear (or nearly linear) relationship between the sensor output and the elevation of the water level on the gauge. This relationship can be determined by calibrating the gauge either statically or dynamically. In static calibration the wave gauge is vertically raised and lowered in known incremental distances relative to the still water level, and the gauge output at each location is recorded. The calibration relationship is obtained as a mathematical curve fit between the recorded gauge outputs and the corresponding elevations in length units. Ideally, the relationship is linear and a least square linear regression can be applied to obtain the necessary conversion equation [20].

During static calibration it is very important to not disturb the water because even the slightest water level fluctuation will impact the quality of the gauge calibration.

In this study, static gauge calibration method is used, but instead of vertically raising and lowering the gauges in known incremental distances to the still water level, the water level has been changed manually in known increment distances. Initially, all the gauges are tested in a large incremental distance range (20 cm). Water level have been raised to +10 cm above the still water level that is going to be used during all the experiments of this study (h=70 cm.) then lowered to -10 cm of the still water level while recording the outputs of all gauges at every centimeter (20 point calibration). The results of the experiment are presented in Table A.1.

The results are plotted (incremental distance versus raw voltage data from each gauge). As an example, Figure 3.6 shows an ideal wave gauge featuring a linear relationship between the sensor output and the elevation of the water level on the gauge. The linear regression equation gives the R^2=1 value which proves a perfect fit. The slope of the regression equation gives the coefficient of calibration for gauge 6, which equals to 17.12.

Figure 3.7 and Figure 3.8 are other examples featuring nearly linear relationship between the sensor output and the elevation of the water level on the gauge and no relationship between the sensor output and the elevation of the water level on the gauge respectively.

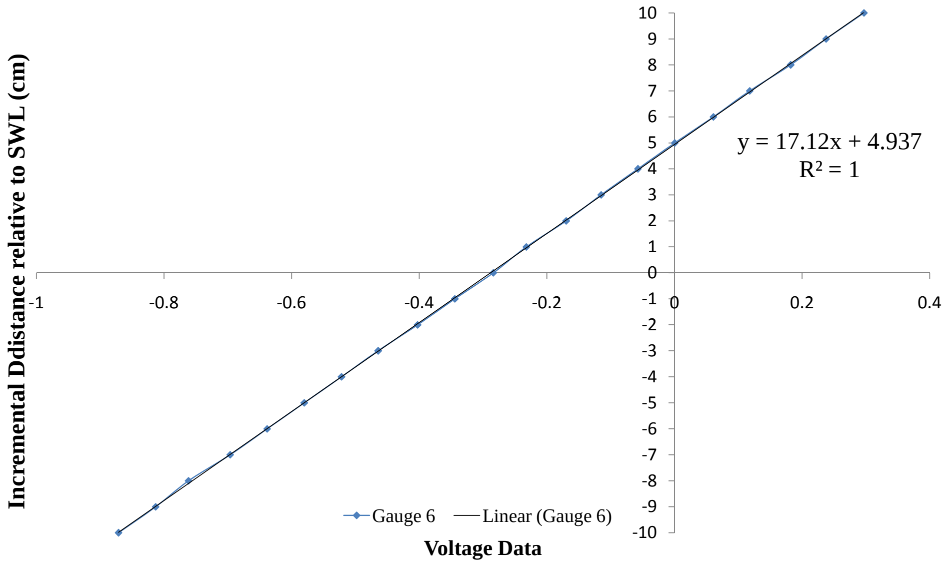

Figure 3.6: Linear regression for Gauge 6 (20 point calibration)

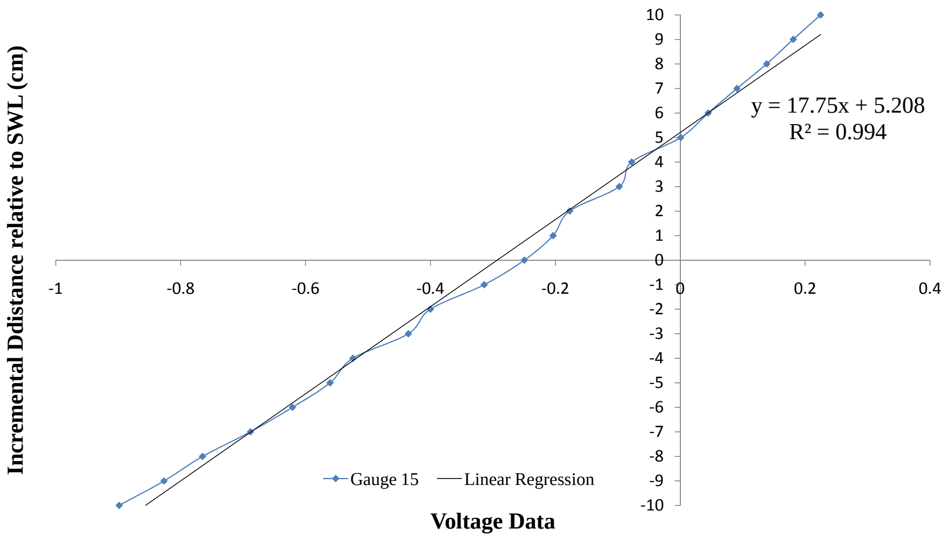

Figure 3.7: Linear regression for Gauge 15 (20 point calibration)

Figure 3.8 shows that wave Gauge 13 is definitely not operating. Figure 3.7 shows that wave gauge 15 is somewhat operational but it is not advised to use this gauge as it may impact the results obtained from this particular gauge. After the elimination of the non operating wave gauges, all gauges are tested in the same incremental distance range (20 cm). Water level have been raised to +10 cm above the still water level (h=70 cm.) then lowered to -10 cm of the still water level while recording the outputs of all gauges at every 5 centimeters (5 point calibration). The results of the experiment are presented in Table A.2.

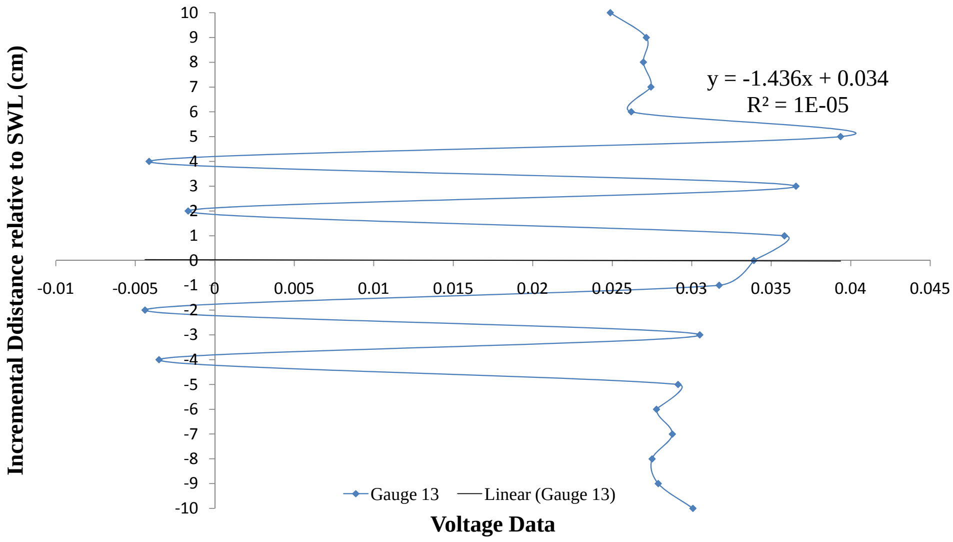

Figure 3.8: Linear regression for Gauge 13 (20 point calibration)

Figure 3.9 for wave gauge 6 shows an ideal wave gauge featuring a linear relationship between the sensor output and the elevation of the water level on the gauge. The linear regression equation gives the R^2=1 value which proves a perfect fit. The perfect linear regression fit for wave gauge 6 for both calibration experiments shows that a 5 point calibration is enough for the calibration of the wave gauges with good linear regression values.

Figure 3.10 shows the linear regression result for wave gauge 15. When compared with the results of the first experiment (20 point calibration), 5 point calibration results in a smoother fit. Although the regression analysis gives the same result (R^2=0.994), the coefficient of calibration differs greatly. In the first calibration experiment, wave gauge 15 has a coefficient of calibration of 17.75 whereas in the second calibration experiment it has a coefficient of calibration of 15.06. It should be noted that the coefficient of calibration is not the same every time a calibration experiment is carried out. But the coefficients of calibration for the same gauge under similar conditions

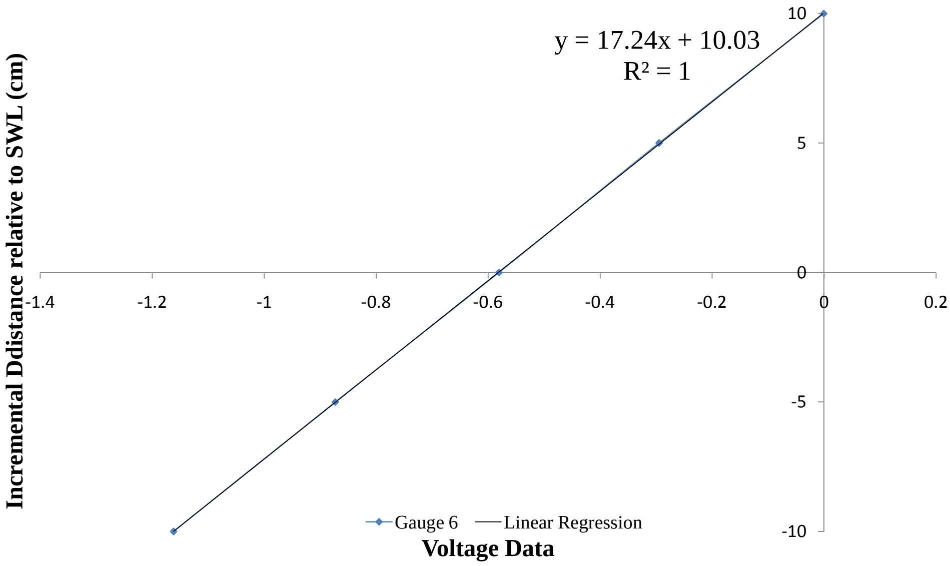

Figure 3.9: Linear regression for Gauge 6 (5 point calibration)

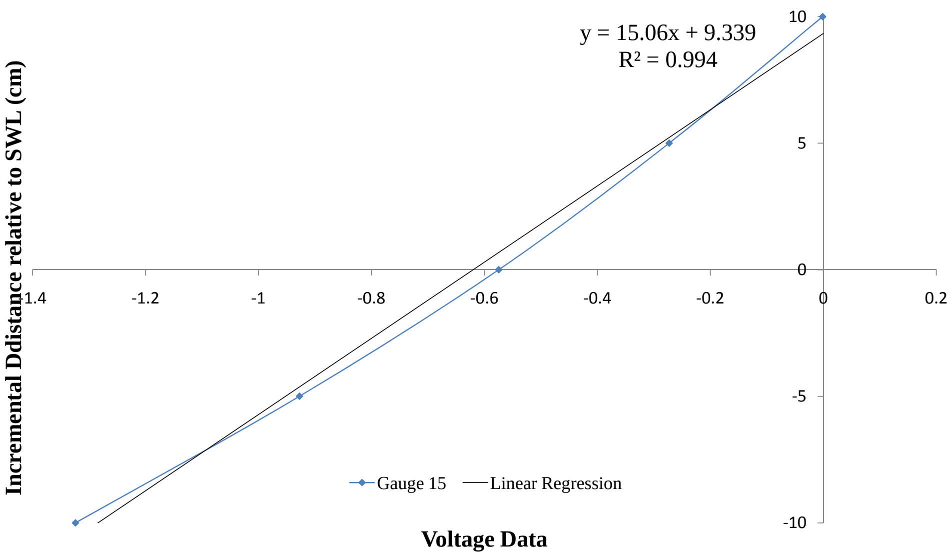

Figure 3.10: Linear regression for Gauge 15 (5 point calibration)

and when the gauges are reset to zero voltage at the same water level, should be close to each other.

The static gauge calibration method is used where the water level changed manually is a time consuming procedure. For further practicality, water level have been raised to +10 cm above the still water level (h=70 cm.) then lowered to -10 cm of the still water level while recording the outputs of all gauges at every 10 centimeters (3 point calibration).The results of the experiment are presented in Table A.3.

Figure 3.11 for wave gauge 6 shows an ideal wave gauge featuring a linear relationship between the sensor output and the elevation of the water level on the gauge. The linear regression equation gives the R^2=1 value which proves a perfect fit. The perfect linear regression fit for wave gauge 6 for all calibration experiments shows that a 3 point calibration is enough for the calibration of the wave gauges with good linear regression values.
According to results of the three different calibration experiments mentioned above, 3 point calibration procedure is used in this study . Calibration procedure is repeated before every experiment. Also, note that the removed wave gauges are replaced with well operating wave gauges. The results for gauge 13 and gauge 15 are the results of replaced, working, wave gauges.

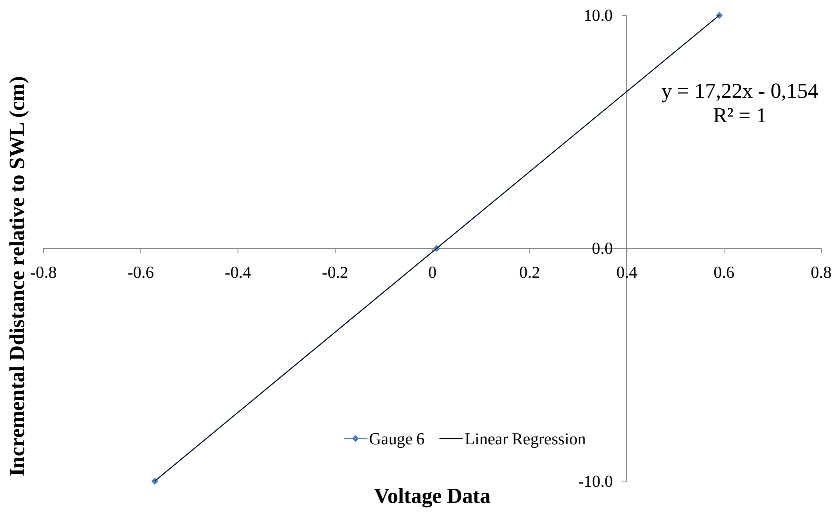

Figure 3.11: Linear regression for Gauge 6 (3 point calibration)

3.2.5 Model Wave Generation

3.2.5.1 Introduction

The use of physical models in coastal engineering would be severely limited if we were unable to create waves in small scale models that exhibited many of the characteristics of waves in nature. Although wind can be used in a small scale tank to generate waves, the tank must be enclosed and of sufficient length for the wind to generate the desired condition. A far more common approach is mechanical wave generation where a movable partition is placed in the wave facility and waves are generated by oscillation of the partition [20].

The earliest wave makers generated uniform waves by moving the wave board in a sinusoidal motion with a given amplitude and period of oscillation. Although this was a very simplified approximation of real-world waves, these simple waves conformed reasonably well to linear wave theory.

Soon the electrical motors driving the wave boards were replaced by hydraulic servo-systems that gave engineers more control over the wave board motion. The wave maker used in this study is a hydraulic servo-system piston type wave maker. The wave maker is controlled via a Stand Alone Controller. The input for this control unit is basically the amplitude of the motion of the wave board and the frequency of this motion. Although the frequency of the motion of the wave maker board can be calculated from the model period of the wave that is going to be generated,

$$f = \frac{1}{T_{\mathrm{m}}} \tag{3.6}$$

where;

f : frequency (Hz)

T_m : Wave period in model scale (sec)

the amplitude of the motion of the wave maker board should be calculated in order to create the desired wave height in the wave flume.

3.2.5.2 Two-Dimensional Governing Equations

Hughes (1993) [20] mentions that a general theory for mechanical wave generation was presented by Havelock (1929) [22]. The motion of an inviscid, irrotational fluid in such a wave flume is described by the two dimensional Laplace equation along with the appropriate boundary conditions. A detailed solution of the two dimensional Laplace equation for the piston type wavemakers can be found in the book "Physical Models and Laboratory Techniques in Coastal Engineering, Advanced Series on Ocean Engineering - Volume 7" by Steven A. Hughes [20].

3.2.5.3 First Order Wave Generation

The equations and boundary conditions to be used in solving the first order wave maker problem for the two dimensional wave board are summarized below.

$$\frac{(\delta^2\phi_1)}{(\delta x^2)} + \frac{(\delta^2\phi_1)}{(\delta z^2)} = 0 \ (in fluid) \tag{3.7}$$

$$\frac{(\delta\phi_1)}{(\delta z)} = 0 \ (at\ z = -h) \tag{3.8}$$

$$\frac{(\delta^2\phi_1)}{(\delta t x^2)} + g\frac{(\delta\phi_1)}{(\delta z)} = 0 \ (at\ z = 0) \tag{3.9}$$

$$\frac{(\delta\phi_1)}{(\delta z)} = f(z)\frac{dX_{01}}{dt} \ (at\ x = 0) \tag{3.10}$$

$$f(z) = (1 + \frac{z}{h + l_v}) \tag{3.11}$$

where;

x : Horizontal coordinate in x direction

y : Horizontal coordinate in y direction

z : Vertical coordinate in z direction

l_v : Vertical distance from bottom to wave board hinge (m)

ϕ : Velocity potential function

h : Water depth (m)

g : Gravitational acceleration (m/s^2)

The solution of the first order wave maker problem, specified by the equations 3.7 to 3.11, is obtained by assuming the velocity potential can be represented by three functions such that;

$$\phi_1(x, z, t) = X(x)Y(y)T(t) \tag{3.12}$$

This allows the Laplace equation to be separated into ordinary differential equations that have known solutions. In the most general sense, the potential function must include all possible solutions, so we sum the solutions that arise when the "separation constant" is real, imaginary and zero. From Dean and Dalrymple (1984) the general velocity potential can be formulated as;

$$\phi_1(x, z, t) = \phi_{k1} + \phi_{k2} + \phi_{k3} \tag{3.13}$$

Substituting the velocity potentials into the equations summarized above (Equations 3.7 to 3.11) and evaluating the results with the given boundary conditions (detailed solutions are in the book "Physical Models and Laboratory Techniques in Coastal Engineering, Advanced Series on Ocean Engineering - Volume 7" by Steven A. Hughes 1993) [20] gives a general first order wave maker solution.

$$\frac{H}{S_0} = \frac{(4 \sinh kh)}{\sinh 2kh + 2kh}[\sinh kh + \frac{(1 - \cosh kh)}{(k(h + l_v))}] \tag{3.14}$$

where;
H : Generated wave Height (m)
h : Water depth (m)
S_0 : Wave board stroke amplitude (m)
l_v : Vertical distance from bottom to wave board hinge (m)
k : Wave number
For the special case when $l_v \to \infty$, the second term in equation 3.14 vanishes, and the wave board motion is that of a piston, i.e. ,

$$\frac{H}{S_0} = \frac{(4 \sinh kh)}{\sinh 2kh + 2kh} \tag{3.15}$$

Equation 3.15 (Dean and Dalrymple 1984) is used to calculate the necessary stroke of the wave maker board to create the desired wave height in the wave flume. Table A.5 shows the necessary wave board stroke amplitudes and frequencies to produce the desired waves.

3.2.6 Data analysis

3.2.6.1 Introduction to Data Analysis

The experimental phase of a study is complete when the data collected over the course of the experiment have been analyzed and converted into a form suitable for its intended use. This does not necessarily mean that all collected data must be analyzed. As often is the case, some data will be from aborted or flawed experiments, and it would be pointless to analyze those data. Types of analysis range from simple to sophisticated, depending on the particular experiment and the needs of the researcher. The most elementary analysis simply involve converting recorded data into a more useful form (e.g., converting digital wave gauge voltages to equivalent water surface elevations expressed in engineering length units). Time series are commonly analyzed using time domain (statistical) techniques or frequency domain (spectral) techniques [20].

3.2.6.2 Analysis of Digital Data

Many of the recent developed wave recorders are equipped with electronic units which convert analog signals of the surface wave profile into digital signals and record them on a real-time basis. These signals are later processed by computers to yield information of the wave heights and periods as well as the spectra. Most conventional wave recorders, however, process information of the wave profile as an analog signal and register it on a strip-chart. These records need to be analyzed manually. Because such conventional wave recorders are still in common use. In this study, digital data has been recorded with the help of electronic equipment. The analysis of the wave record in this study is carried out using MATLAB software. Basically, the raw wave data is analyzed using zero-upcrossing method, maxima and minima of the records have been calculated. Maximum wave height (H_{max}), minimum wave height (H_{min}), mean wave height (H_m) and significant wave heights (H_s) and their corresponding wave periods (T) are calculated using this method. In hydraulic model tests of maritime structures in a wave flume, the first item of measurement is the characteristics of the incident waves, and the second item is the coefficient of reflection of the model structure. In a wave flume with the installation of a model structure to be tested and sometimes in a relatively short wave flume with ineffective wave absorbers, waves reflected by the model travel back to the wave generator and re-reflected there. They propagate toward the structure and are reflected again, and the process is repeated during the recording time. Therefore spectral analysis is used to separate the waves traveling toward the wave generator and the waves traveling toward the structures. These waves are the reflected waves (H_r) and the incident waves (H_i) respectively. The flow chart of wave data analysis is shown in Figure 3.12. Further detail on the wave data analysis will be discussed in the next subsection.

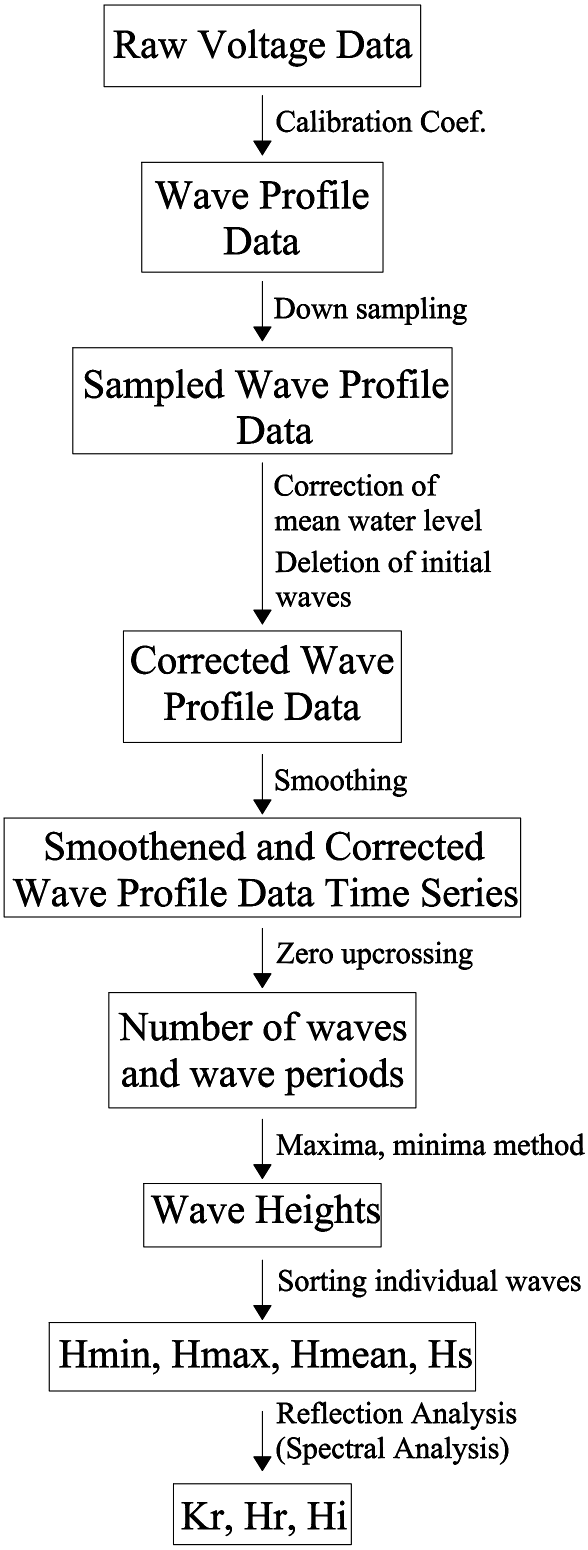

Figure 3.12: The flow chart of the wave data analysis

3.2.6.3 Data analysis methods details

In this subsection, the flow chart of wave analysis (Figure 3.12) will be discussed in details. All the calculations are carried out using MATLAB software.

Raw Voltage Data Raw voltage data stored in the PC computer (section 3.2.3, page 28) is transformed into wave height data using the calibration function found from the 3 point calibration procedure mentioned earlier in the section 3.2.4 (page 33) carried out before every experiment.

Sampling Great care must be taken when selecting the sampling time interval for digitizing sea surface elevations. A common ”rule of thumb” is that an absolute minimum of 10 evenly-space samples must be obtained over one wavelength (time equal to one wave period). Fewer samples may miss the wave crest, particularly for steep waves. For a typical laboratory wave period of 1 sec, wave data would need to be collected at a 10-Hz rate at a minimum; however, most investigators prefer to collect at higher rates (e.g., @0-30 Hz). Provided the instrument system has sufficient capacity, higher collection rates give better delineation of the waves and aliasing of the signal is reduced [23]. In this study the data is sampled at 20 Hz for regular waves.

Correction of mean water level - Deletion of initial waves A simple procedure to determine the mean water level is to use the arithmetic mean of all data points measured from any reference level [24]. This arithmetic mean is subtracted from the time series for every gauge to produce time series with mean level of water is set to zero.
This correction is necessary for the zero upcrossing method. In a wave flume test, few initial waves generated by the wave maker may not have the specific wave height and wave period. This is caused by the wave generator not being able to start its intended wave generation motion instantly. These recorded waves are removed from the time series of every wave gauge.

Smoothing the Time Series Wave records may contain ”glitches” or ”spikes” that arise from problems with the instrument or data acquisition, and it is important to remove these errors in the data before further analysis [20]. Every data point is averaged using the prior two data points and the next two data points and the data point itself to smooth the time series curves. Figure 3.13 shows a snapshot of a time series of one particular wave gauge. Data points marked with the circles are used for the smoothing of the data point in the middle of the marked data points. The resulting new data point is marked with an arrow. This procedure is carried out for all data points to produce the smoothed data series.

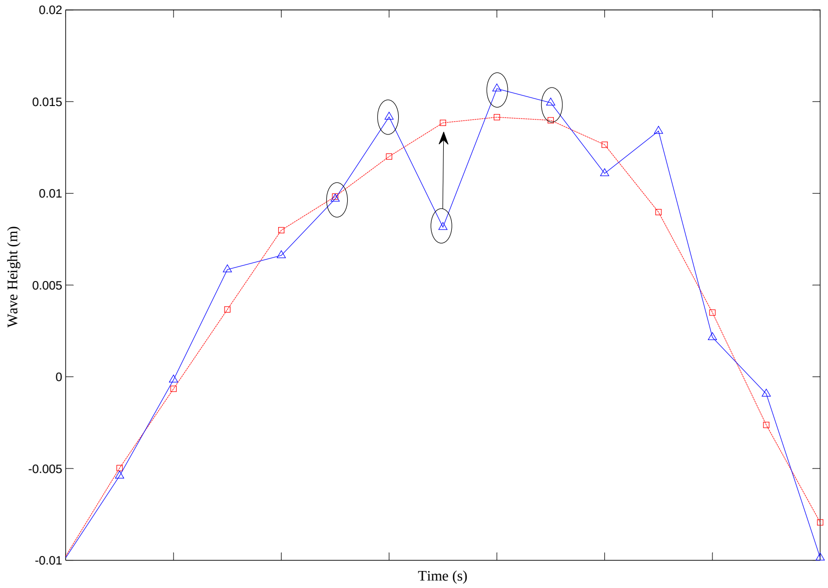

Figure 3.13: An example data point smoothing

Zero upcrossing method - Maxima and Minima method One of the most common time domain analysis that can be used to extract wave characteristics from time series is zero-crossing method. Individual waves are determined by zero upcrossing method. Each wave is defined as the water level elevation variation between two successive up crossings of the time series relative to the zero elevation. Waves defined by the upcrossing method are composed of a wave crest followed by a trough. Wave

height is taken as the total vertical distance between the wave crest (highest elevation of the wave) and wave trough (lowest elevation of the wave).
Zero upcrossing of the wave profile is detected through the following criteria:

$$\eta * \eta_{i+1} < 0 \text{ and } \eta_{i+1} > 0 \tag{3.16}$$

where;
η_i : surface elevation at i-th point of the time series after correction of the mean water level(m)

The time of the zero upcrossing is determined by linear interpolation between sampling times of η_i and η_{i+1}. The time difference from this point to the next zero upcrossing point yields the zero upcrossing wave period.
The conditions defining a maximum in the wave profile are:

$$\eta_{i-1} < \eta_i \ \ and \ \ \eta_i > \eta_{i+1} \tag{3.17}$$

It is suggested that the time and the elevation of the maximum point be estimated by fitting parabolic curve to the three points η_{i-1}, η_i and η_{i+1} in order to eliminate the problem of underestimating the true maximum between two discrete sampling points. The formula for a parabolic fitting is:

$$\eta_{max} = C - \frac{B^2}{4A} \ \ and \ \ t_{max} = t_i - \Delta t \frac{B}{2A} \tag{3.18}$$

where;

$$A = \frac{1}{2}(\eta_{i-1} - 2\eta_i + \eta_{i+1}), \ \ B = \frac{1}{2}(\eta_{i+1} - \eta_{i-1}), \ \ C = \eta_i \tag{3.19}$$

In order to determine the zero upcrossing wave height, the highest point on the surface elevation must be searched for in the time interval between two zero upcrossing points. Once this is found among the sampled points, it is designated as η_i, and then η_{max} is estimated by means of equations 3.18 by use of neighboring data points η_{i-1} and η_{i+1}. The lowest surface elevation η_{min} is obtained by similar process, and the wave height is calculated as the sum of the absolute values of η_{max} and η_{min}. Unless the technique of parabolic fitting is employed, the data sampling interval must be quite narrow to avoid an artificially introduced decrease in wave height derived from digitized data [24]. At this point all the wave heights in a particular time series are obtained. H_{max}, H_{min} and H_s can be derived from these wave heights. For significant wave height, the waves in the time series are counted and selected in descending order of wave height from the highest wave, until one-third of the total number of waves is reached. The means of their heights and periods are calculated (H_s, T_s)

Wave Reflection Analysis (Spectral Analysis) As mentioned earlier in this section, in a wave flume with the installation of a model structure to be tested, waves reflected by the model travel back to the wave generator and re-reflected there. They propagate toward the structure and are reflected again, and the process is repeated during the recording time. Although they appear complicated, the components of these multi-reflection waves having the same frequency can be synthesized into a single train of waves because the components all have the same frequency and the phase differences are fixed. A similar expression is possible for waves traveling toward the wave generator. The synthesized profiles of incident and reflected waves for a specific frequency can be expressed as:

$$\eta_I = a_I \cos(kx - \sigma t + \varepsilon_I) \tag{3.20}$$

$$\eta_R = a_R \cos(kx - \sigma t - \varepsilon_R) \tag{3.21}$$

where;
a_I : Amplitude of incident wave (m)
a_R : Amplitude of reflected wave (m)
η_I : Surface elevations of incident wave (m)
η_R : Surface elevations of reflected wave (m)
k : Wave number of $2\pi/L$
L : Wavelength (m)
σ : Angular frequency of $2\pi/T$
T : Wave period

ε_I : Phase angle of incident wave

ε_R : Phase angle of reflected wave

Further, the surface elevations are recorded at two adjacent stations (wave gauges) of x_1 and $x_2 = x_1 + \Delta\ell$. The observed profiles of composite waves will be;

$$\eta_1 = (\eta_I + \eta_R)_{(x=x_1)} = A_1 \cos\sigma t + B_1 \sin\sigma t \tag{3.22}$$

$$\eta_2 = (\eta_I + \eta_R)_{(x=x_2)} = A_2 \cos\sigma t + B_2 \sin\sigma t \tag{3.23}$$

where;

$$A1 = a_I \cos\phi_I + a_R \cos\phi_R \tag{3.24}$$

$$B1 = a_I \sin\phi_I - a_R \sin\phi_R \tag{3.25}$$

$$A2 = a_I \cos(k\Delta\ell + \phi_I) + a_R \cos(k\Delta\ell + \phi_R) \tag{3.26}$$

$$B2 = a_I \sin(k\Delta\ell + \phi_I) - a_R \sin(k\Delta\ell + \phi_R) \tag{3.27}$$

$\Delta\ell$: Distance between two adjacent wave gauges (m)

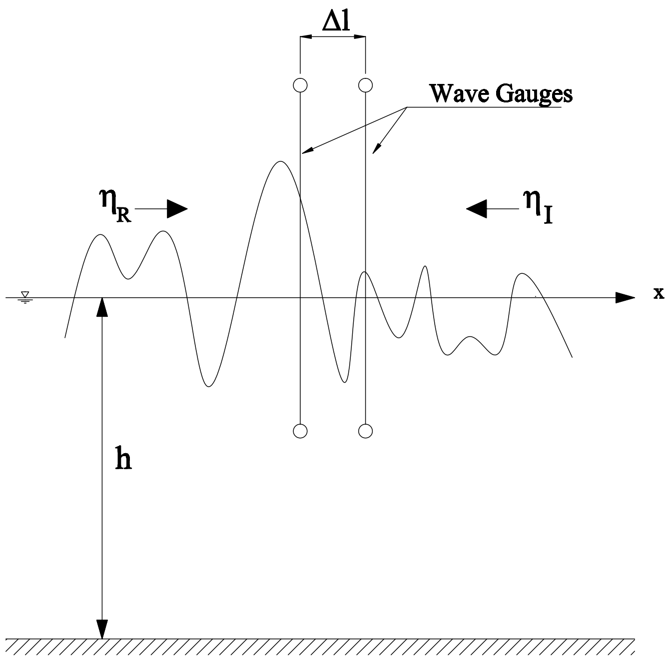

Figure 3.14: Definition sketch for $\Delta\ell$

$$\phi_I = kx_1 + \varepsilon_I \tag{3.28}$$

$$\phi_R = kx_1 + \varepsilon_R \tag{3.29}$$

Equations 3.24, 3.25, 3.26 and 3.27 can be solved to yield the estimate of

$$a_I = \frac{\sqrt{(A_2 - A_1 \cos k\Delta\ell - B_1 \sin k\Delta\ell)^2 + (B_2 + A_1 \sin k\Delta\ell - B_1 \cos k\Delta\ell)^2)}}{2|\sin k\Delta\ell|} \tag{3.30}$$

$$a_I = \frac{\sqrt{(A_2 - A_1 \cos k\Delta\ell + B_1 \sin k\Delta\ell)^2 + (B_2 - A_1 \sin k\Delta\ell - B_1 \cos k\Delta\ell)^2)}}{2|\sin k\Delta\ell|} \tag{3.31}$$

$$\sigma^2 = gk \tanh kh \tag{3.32}$$

Actual wave profiles usually contain some higher harmonics. Use of the Fourier enables to estimate the amplitudes of A_1, B_1, A_2 and B_2 for the fundamental frequency [24]. All the amplitudes of Fourier components are analyzed by the Fast Fourier Transform (FFT) technique. This technique is carried out using the ready to use package provided with the MATLAB software.

Once the amplitudes of Fourier components are calculated, the incident spectral density function $S_i(f)$ and the reflected spectral density function $S_r(f)$ is calculated.

The result of a spectral resolution by this method is schematically shown in Figure 3.15.

It is seen that the spectral estimates diverge in the neighborhood of frequencies satisfying the condition $k\Delta\ell = n\pi$ for n=0,1,2,... . Because the factor $|\sin k\Delta\ell|$ in the denominator on the right side of equations 3.30, 3.31 becomes very small and errors due to noise are greatly amplified. The spectral estimates are effective in the frequency range outside of the neighborhood of such diverging points. The effective frequency range of resolution can be judged with the following guideline [24]:

$$Upperlimit(f_{max}) \quad : \frac{\Delta\ell}{L_{min}} = 0.45 \tag{3.33}$$

$$Lowerlimit(f_{min}) \quad : \frac{\Delta\ell}{L_{max}} = 0.05 \tag{3.34}$$

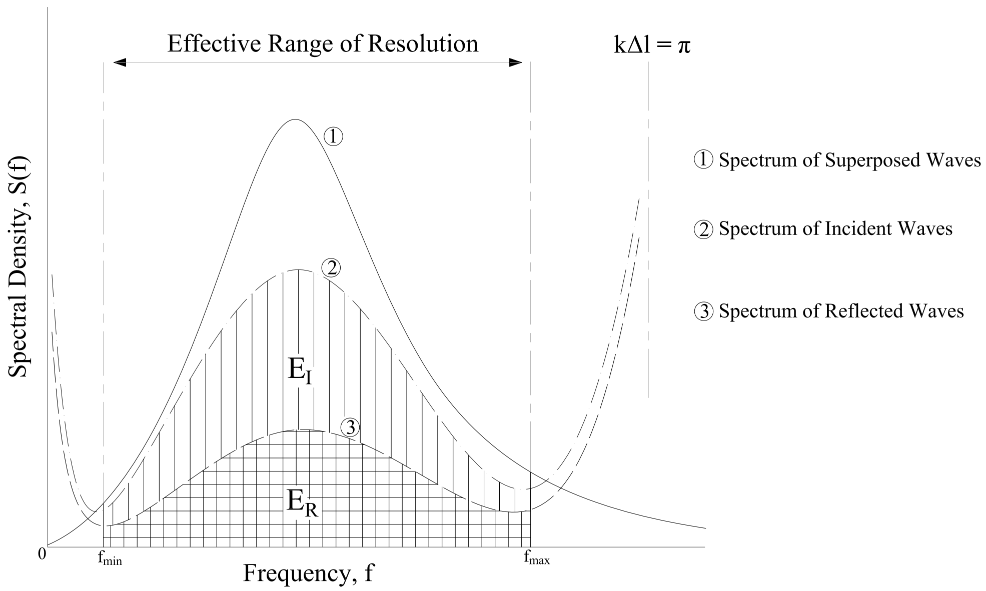

Figure 3.15: Illustration of the spectral resolution of incident and reflected waves

The symbols L_{min} and L_{max} denote wavelengths corresponding to the upper (f_{max}) and lower (f_{min}) limits of the effective frequency range, respectively. When the distance between the two wave gauges has been fixed, the effective frequency range of the resolution of incident and reflected waves can be determined from equations 3.33 and 3.34. Working the other way, when the plan of a hydraulic model test is being prepared, the distance $\Delta\ell$ should be selected such that the major part of the wave energy of the spectrum of the test wave is contained in the effective frequency range f_{min} to f_{max} [24].

Wave gauges in the sea side of the units are positioned in a way to capture the major part of the wave energy of the spectrum of the test waves used in this study. Two linear groups of three wave gauges are placed in a way to set the distance between the adjacent wave gauges is either 15 cm, 25 cm or 40 cm (Figure 3.16).

The motivation behind this is to circumvent the divergence problem at $k\Delta\ell = n\pi$. By employing three gauges, two pairs can be used to eliminate the divergence problem at a particular frequency for which the other pair fails to yield proper resolution. By taking the average of the results of pairs of wave gauges giving a non-diverging estimate at the respective frequencies, a three gauge array can extend the effective

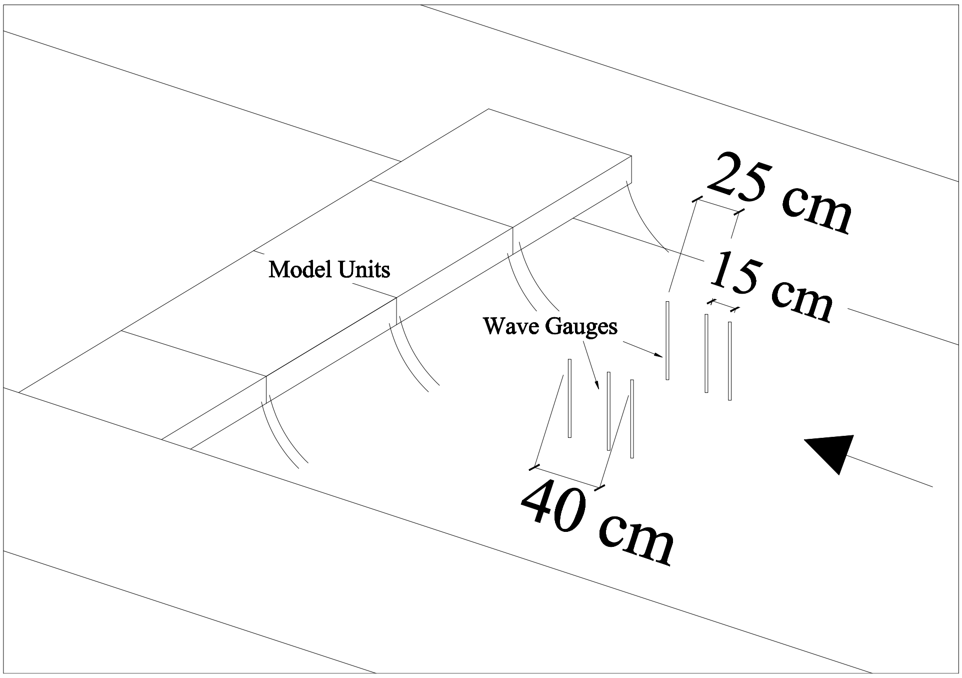

Figure 3.16: Seaward wave gauge set-up

range of wave resolution considerably [24].

For the estimation of the reflection coefficient, the energies of incident and reflected waves, E_I and E_R within the range f_{min} and f_{max} need to be calculated. This is accomplished as:

$$E_I = \int_{f_{min}}^{f_{max}} S_I(f)\, df \tag{3.35}$$

$$E_R = \int_{f_{min}}^{f_{max}} S_R(f)\, df \tag{3.36}$$

Since the energies of the incident and reflected waves must be proportional to the squares of the respective wave heights, the reflection coefficient defined as the ratio of heights can be estimated from:

$$K_r = \sqrt{\frac{E_R}{E_I}} \tag{3.37}$$

This reflection coefficient represents that of the wave group as a whole. The incident wave height H_i and the reflected wave height H_r can be estimated with the above coefficient of reflection K_r and the mean value of wave heights at the two locations, which is denoted by H_s as

$$H_i = \frac{1}{(1 + {K_r}^2)^2} H_s, \quad H_r = \frac{K_r}{(1 + {K_r}^2)^2} H_s \tag{3.38}$$

where;
H_i : Incident wave height (m)
H_r : Reflected wave height (m)
H_s : Significant wave height (m)
K_r : Reflection coefficient

The above technique is applicable to both regular and irregular trains of waves [24].

Wave Transmission Coefficient Transmission of waves past a structure is usually defined in terms of the transmission coefficient K_t. Transmission coefficient is defined as the ratio of incident and transmitted wave. Therefore, K_t equal to 1 corresponds to full transmission and K_t equal to 0 represents no transmission. This relationship can be expressed as;

$$K_t = \frac{H_t}{H_i} \tag{3.39}$$

where;
H_i : Incident wave height (m)
H_t : Transmitted wave height (m)

In this study, the incident wave height (H_i) used to calculate the transmission coefficient (K_t) is taken from a phase called ”wave search” (wave calibration). In the wave search phase, the characteristics of the incident waves in absence of the floating breakwater model units are determined. This phase is required as the calculation of the waves transmission is based on the comparison between the height of the incident wave before installing the floating breakwater units and the height of the transmitted wave, measured after having installed it. The upstream and downstream wave heights in the presence of the breakwater, causing at least a partial reflection of the wave, could affect the incident wave height and invalidate the resulting transmission coefficient. Although, reflection analysis is used to remove the reflection effect from the incident wave height, wave search method is used to be on the safe side.

The results of the wave search phase (based on the characteristics of the reference waves) are shown in Table 3.2.

Table 3.2: Results of the wave search phase

No units			Gauge1	Gauge2	Gauge3	Gauge5	Gauge6	Gauge7	Gauge8	Gauge11	Gauge12	Gauge13	Gauge15	Gauge16	Results below are in model scale			
Period (prototype)	Steepness		1	2	3	4	5	6	7	8	9	10	11	12	$H_{m\,(mean)}$	K_r	H_I	H_R
4.0	0.015	H_m	0.016	0.016	0.014	0.017	0.018	0.016	0.018	0.020	0.018	0.013	0.018	0.019	0.02	0.16	0.02	0.00
4.0	0.025	H_m	0.029	0.027	0.027	0.028	0.029	0.028	0.030	0.033	0.030	0.022	0.031	0.032	0.03	0.11	0.03	0.00
4.0	0.035	H_m	0.038	0.035	0.036	0.035	0.037	0.036	0.040	0.043	0.041	0.028	0.042	0.042	0.04	0.09	0.04	0.00
4.0	0.045	H_m	0.048	0.045	0.045	0.044	0.047	0.045	0.048	0.054	0.054	0.036	0.050	0.050	0.05	0.09	0.04	0.00
4.5	0.015	H_m	0.017	0.018	0.019	0.021	0.020	0.019	0.020	0.023	0.023	0.015	0.021	0.022	0.02	0.14	0.02	0.00
4.5	0.025	H_m	0.032	0.033	0.033	0.032	0.034	0.031	0.035	0.039	0.039	0.026	0.035	0.036	0.03	0.10	0.03	0.00
4.5	0.035	H_m	0.043	0.044	0.044	0.044	0.045	0.042	0.050	0.052	0.054	0.034	0.050	0.049	0.05	0.08	0.04	0.00
4.5	0.045	H_m	0.053	0.055	0.053	0.055	0.056	0.053	0.062	0.065	0.066	0.043	0.062	0.061	0.06	0.08	0.05	0.00
5.0	0.015	H_m	0.024	0.026	0.023	0.022	0.027	0.023	0.025	0.026	0.028	0.020	0.026	0.026	0.02	0.12	0.02	0.00
5.0	0.025	H_m	0.039	0.042	0.039	0.038	0.043	0.037	0.042	0.043	0.046	0.033	0.043	0.042	0.04	0.09	0.04	0.00
5.0	0.035	H_m	0.056	0.059	0.056	0.053	0.059	0.051	0.059	0.059	0.064	0.046	0.060	0.059	0.06	0.08	0.05	0.00
5.5	0.015	H_m	0.027	0.030	0.028	0.029	0.030	0.029	0.029	0.029	0.032	0.024	0.029	0.028	0.03	0.11	0.03	0.00
5.5	0.025	H_m	0.044	0.048	0.047	0.048	0.049	0.046	0.049	0.049	0.054	0.039	0.047	0.047	0.05	0.09	0.05	0.00
6.0	0.015	H_m	0.033	0.031	0.032	0.032	0.032	0.032	0.035	0.038	0.039	0.026	0.033	0.033	0.03	0.11	0.03	0.00
6.0	0.025	H_m	0.055	0.056	0.053	0.053	0.055	0.054	0.059	0.063	0.066	0.046	0.057	0.056	0.06	0.09	0.05	0.00
6.5	0.015	H_m	0.038	0.036	0.040	0.037	0.034	0.035	0.038	0.034	0.041	0.031	0.036	0.034	0.04	0.13	0.04	0.00
6.5	0.025	H_m	0.065	0.061	0.068	0.066	0.060	0.063	0.063	0.059	0.067	0.052	0.060	0.058	0.06	0.10	0.06	0.01

As mentioned earlier in the literature survey chapter, the wave attenuation characteristics of floating breakwaters were first investigated from an analytical standpoint by approximation which consisted of idealized forms of wave screens. A rigid structure of finite width, B, height, D, and draft d, fixed near the surface of a water body at depth, h, was analyzed by Macagno (1953) [53]. He assumed that water did not overtop the screen, as if the dimension (D-d) were very large. An expression for the coefficient of transmission, K_t, defined as the ratio of the wave height in the lee of the structure, H_t, to the incident wave height, H_i, was developed as;

$$K_t = 1/\sqrt{1 + \left(\frac{\pi B \sinh(2\pi D h/L)}{L \cosh(2\pi(h-d)/L)}\right)^2} \tag{3.40}$$

where;
K_t : Transmission coefficient
B : Width of the structure (m)
D : Height of the structure (m)
d : Height of the draft (m)
h : Water depth (m)
L : Wavelength (m)

Wiegel (1959) [54] investigated this conceptual model with a consideration of the wave power transmission (the time rate of energy propagation), and he determined that the ratio of the transmitted wave power, P_t, to the incident wave power, P_i, is;

$$\frac{P_t}{P_i} = \left(\frac{4\pi(h-d)/L}{\sinh 4\pi h/L} + \frac{\sinh 4\pi(h-d)/L}{\sinh 4\pi/L}\right) / \left(1 + \frac{4\pi/L}{\sinh 4\pi h/L}\right) \tag{3.41}$$

The transmission coefficient, K_t, is the square root of P_t/P_i. Experiments performed by Wiegel (1959) demonstrated a consistent trend of decreasing transmission coefficient with the increasing screen draft but increasing transmission with the wave period (T) or wave length (L).

Cox (1989) [52] found the effect of blockage on transmission in Macagno's Theory to be understated, particularly when comparing results with Wiegel's Theory for smaller

B/L values. Therefore Cox generalized the power transmission theory developed by Wiegel to be applicable to finite width and depth structures by merging the thin plate Wiegel theory with the long wave finite width screen theory of Dean (1975). This latter theory argues that the velocity profile of a wave passing under a screen becomes uniform, similar to a shallow water wave. The resulting expression, which has been verified with experimental results on broad, deep draft designs is;

$$K_t = \sqrt{P_t/P_i}\left(\left(2\sqrt{1+(\frac{2\pi B}{L})^2}\right)/\left(\frac{2+(2\pi B)^2}{L}\right)\right) \tag{3.42}$$

The transmission coefficients found during the experiments of this thesis are compared with Macagno Theory [53], Wiegel Theory [54] and the Cox Theory [52]. The results of this comparison will be presented in Chapter 4.

CHAPTER 4

EXPERIMENTS and RESULTS

4.1 Model Waves

During the experiments with the floating breakwater units, model wave generation is carried out using a piston type wave maker controlled via a Stand Alone Controller. The inputs for this control unit are basically the amplitude of the motion of the wave board and the frequency of this motion. The frequency was calculated using Equation 3.6 and Equation 3.15 (Dean and Dalrymple 1984) is used to calculate the necessary stroke of the wave maker board to create the desired wave height in the wave flume. Table A.5 shows the necessary wave board stroke amplitudes and frequencies to produce the desired waves. During the experiments, waves with prototype wave periods ranging from 4 to 6.5 sec and with steepness ranging between 0.015 - 0.045 are used. Wave characteristics used in this study are summarized in Table 4.1. In Table 4.1 prototype and model values of wave periods (T), wave length in deep water (L_0) and at depth h=14m (L) and wave height in deep water (H_0) and at depth h=14m (H) are given.

The waves produced by the wave maker using the Equation 3.15 (Dean and Dalrymple 1984) are verified by plotting the experiment results versus theoretical curve produced using the Dean and Dalrymple's formula. It can be seen that the plotted results are in agreement with the theoretical curve (Figure 4.1) and Dean and Dalrymple's equation is within the limits of the experimental results. Floating breakwater unit dimension definitions are given in Figure 4.2.

Table 4.1: Prototype and model wave characteristics

Steepness	$T_{(p)}$ (sec)	$T_{(m)}$ (sec)	$L_{o(p)}$ (m)	$L_{o(m)}$ (m)	$L_{(p)}$ (m)	$L_{(m)}$ (m)	$H_{o(p)}$ (m)	$H_{o(m)}$ (m)	$H_{(p)}$ (m)	$H_{(m)}$ (m)
0.015	4.0	0.894	24.960	1.248	24.960	1.248	0.374	0.019	0.372	0.019
0.025	4.0	0.894	24.960	1.248	24.960	1.248	0.624	0.031	0.621	0.031
0.035	4.0	0.894	24.960	1.248	24.960	1.248	0.874	0.044	0.869	0.043
0.045	4.0	0.894	24.960	1.248	24.960	1.248	1.123	0.056	1.117	0.056
0.015	4.5	1.006	31.590	1.580	31.358	1.568	0.474	0.024	0.466	0.023
0.025	4.5	1.006	31.590	1.580	31.358	1.568	0.790	0.039	0.777	0.039
0.035	4.5	1.006	31.590	1.580	31.358	1.568	1.106	0.055	1.088	0.054
0.045	4.5	1.006	31.590	1.580	31.358	1.568	1.422	0.071	1.398	0.070
0.015	5.0	1.118	39.000	1.950	38.252	1.913	0.585	0.029	0.565	0.028
0.025	5.0	1.118	39.000	1.950	38.252	1.913	0.975	0.049	0.942	0.047
0.035	5.0	1.118	39.000	1.950	38.252	1.913	1.365	0.068	1.319	0.066
0.015	5.5	1.230	47.190	2.360	45.340	2.267	0.708	0.035	0.671	0.034
0.025	5.5	1.230	47.190	2.360	45.340	2.267	1.180	0.059	1.118	0.056
0.015	6.0	1.342	56.160	2.808	52.432	2.622	0.842	0.042	0.785	0.039
0.025	6.0	1.342	56.160	2.808	52.432	2.622	1.404	0.070	1.309	0.065
0.015	6.5	1.453	65.910	3.296	59.442	2.972	0.989	0.049	0.911	0.046
0.025	6.5	1.453	65.910	3.296	59.442	2.972	1.648	0.082	1.518	0.076

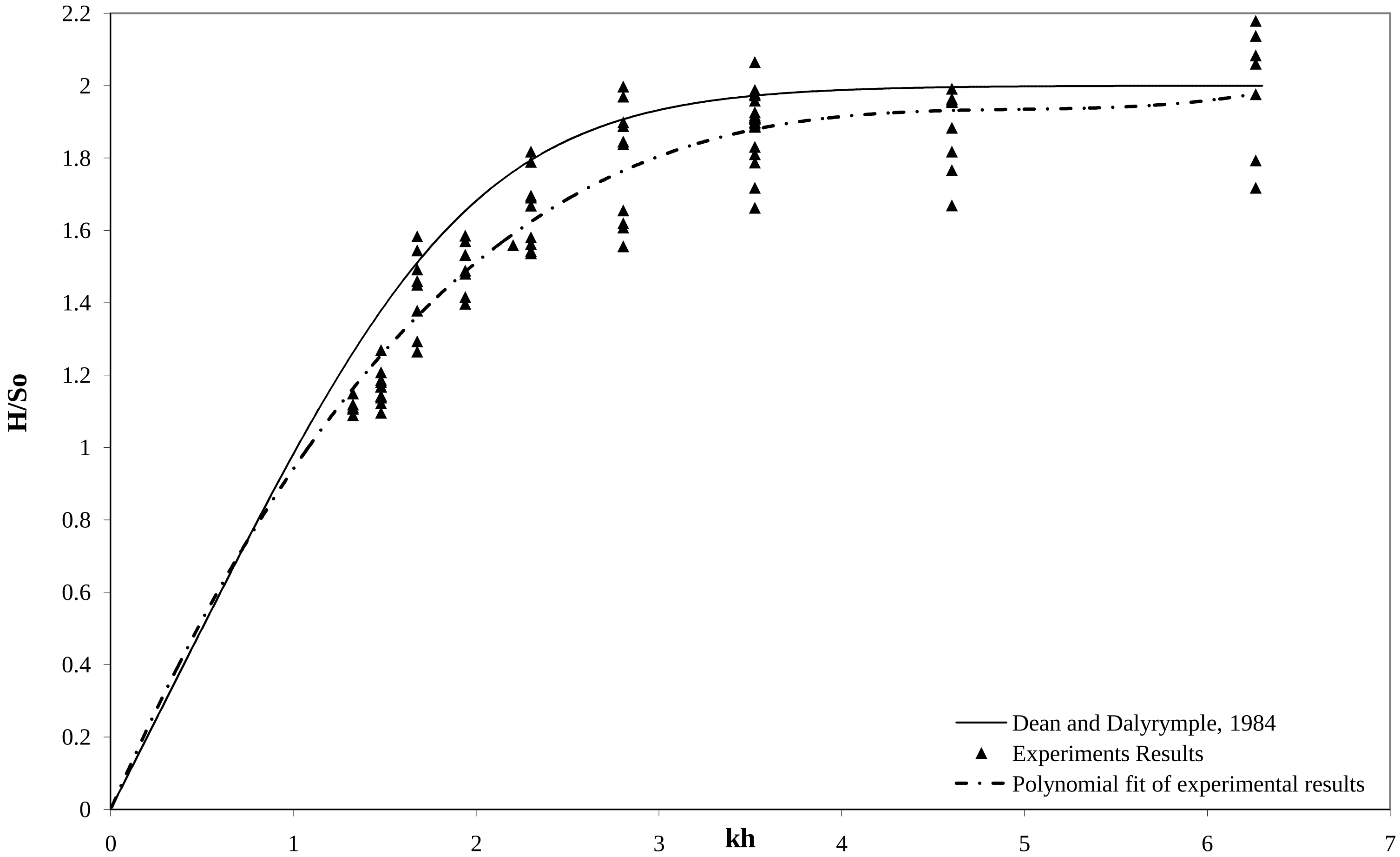

Figure 4.1: Experiments results vs theoretical curve

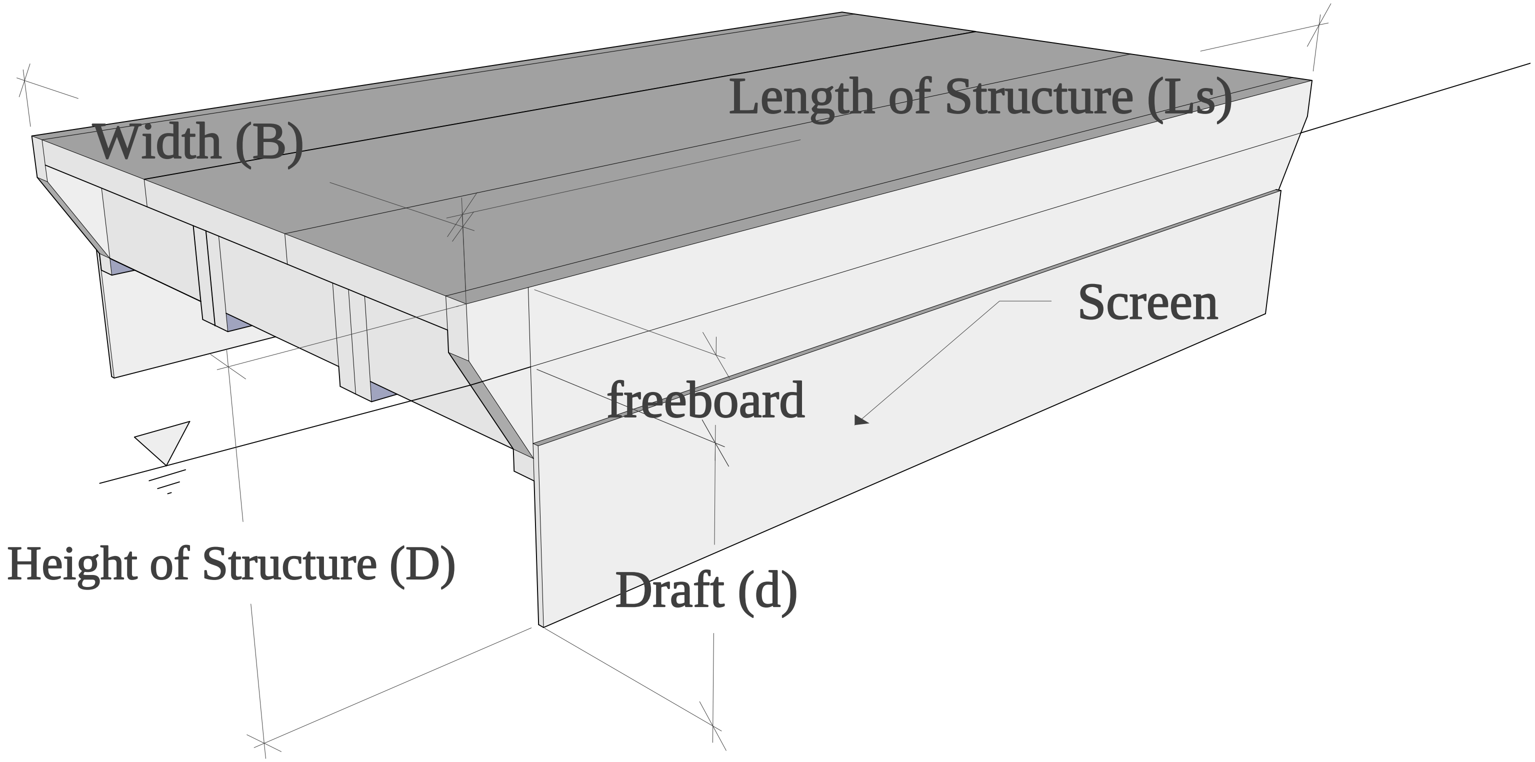

Figure 4.2: Unit dimension definitions

4.2 Model Cases

Model experiments were carried out for six floating breakwater units with structure lengths (L_s=20m) placed in the wave flume. Experiments were carried out with regular waves with 90 degrees incidence angle to the breakwater alignment. The units are tied together with rubber bands as shown in Figure 4.3 allowing minimum independent movement of the units. During the experiments it was observed that six units acted almost as a single unit.

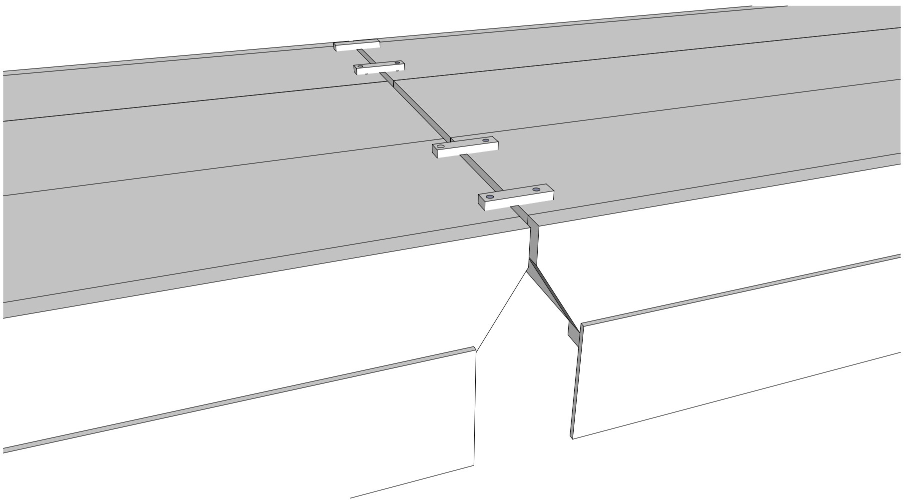

Figure 4.3: Connection of units (rubber band)

In the first series of model tests (Structure types; Case1 to Case9) the units were fixed on steel frames placed on the flume bed as shown in Figure A.9. These series of experiments were aimed to obtain data on transmission and reflection characteristics of the units under incoming waves and to enable to compare the test results with the existing data in literature [25]. Second series of experiments with structure types (Case10 to Case18) were carried out with chain moored units 4.26.

In the experiments three different widths in combination with three different drafts, a total of eighteen different cases are examined. Table 4.2 and 4.3 summarizes the eighteen different cases examined in this study.

Experimental test results in terms of transmission coefficient K_t as measured with the

Table 4.2: Notation of unit characteristics for different model cases

Cases			**Model (cm) Scale 1/20**		**Prototype (m)**	
Fixed	**Chain**	**Notation**	**Width**	**Draft**	**Width**	**Draft**
Case 1	**Case 10**	**B40d7.5**	40	7.5	8	1.5
Case 2	**Case 11**	**B40d17.5**	40	17.5	8	3.5
Case 3	**Case 12**	**B40d27.5**	40	27.5	8	5.5
Case 4	**Case 13**	**B60d7.5**	60	7.5	12	1.5
Case 5	**Case 14**	**B60d17.5**	60	17.5	12	3.5
Case 6	**Case 15**	**B60d27.5**	60	27.5	12	5.5
Case 7	**Case 16**	**B80d7.5**	80	7.5	16	1.5
Case 8	**Case 17**	**B80d17.5**	80	17.5	16	3.5
Case 9	**Case 18**	**B80d27.5**	80	27.5	16	5.5

Table 4.3: Prototype and model values for experiments

Width (prototype) (m)		8			12			16		
Width (model) (cm)		40			60			80		
Draft (prototype) (m)		1.5	3.5	5.5	1.5	3.5	5.5	1.5	3.5	5.5
Draft (model) (cm)		7.5	17.5	27.5	7.5	17.5	27.5	7.5	17.5	27.5
$T_{(m)}$ (sec)	**$T_{(p)}$ (sec)**	**B/L (Approximately)**								
0.89	4	1/3			1/2			2/3		
1.01	4.5	1/4			3/8			1/2		
1.12	5	1/5			1/3			3/7		
1.23	5.5	1/6			1/4			1/3		
1.34	6	1/7			2/9			1/3		
1.45	6.5	1/7			1/5			1/4		

periods ranging from T=4sec to T=6.5sec and wave heights ranging from H=0.3m to H=1.7m. are plotted as transmission coefficient K_t vs H/L (H/L=0.015-0.025-0.035-0.045) and presented in Figure 4.4. With the data presented in Figure 4.4 a decision was reached to use only steepness H/L=0.015 and H/L=0.025 where a complete set of measurement data was available. For steepnesses H/L=0.035 and H/L=0.045 test data was limited due to the difficulties in measurements with this model scale. To see the effect of wave height on the wave transmission, set of graphs are prepared as K_t vs H/L for the tested wave periods T=4sec and T=4.5sec and for all tested widths where data for all steepnesses is available (Figure A.1). However with the available test data, at this stage it is not possible to reach a conclusive result on the effect of wave height on the wave transmission. Based on this conclusion, test results are presented only for steepnesses H/L=0.015 and H/L=0.025 for K_t and K_r using dimensionless variables B/L and h/L.

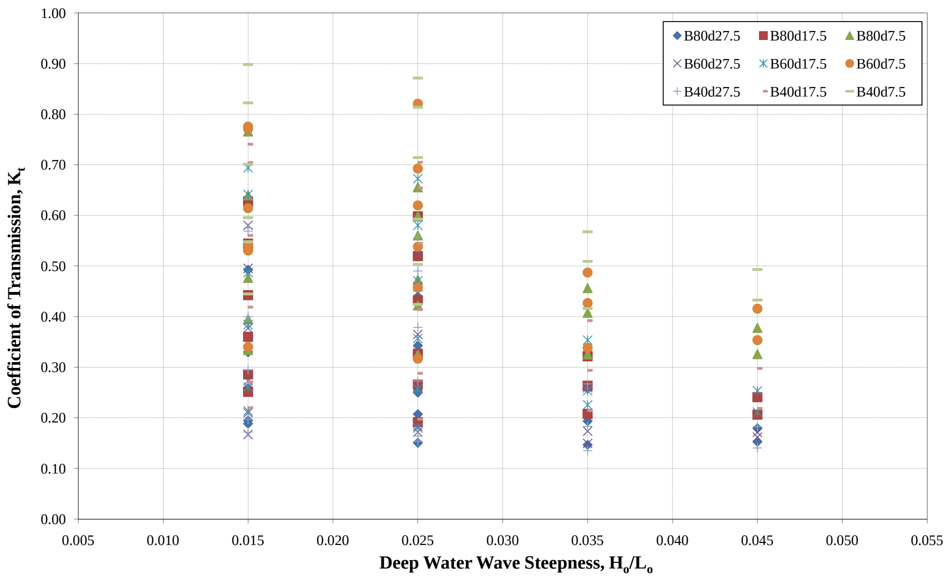

Figure 4.4: K_t vs H/L for all experiments

4.2.1 Case 1 - Case 2 - Case 3 (Width(B)=8 m)

Case 1 (B40d7.5) had fixed mooring and no barriers. It corresponds to a box type floating breakwater. The freeboard of the structure is 5 cm. Height of the structure, D, is 12.5 cm. The draft of the structure, d, is 7.5 cm (1.5m). The width of the structure, B, is 40cm (8m). Structure length, L_s, is 100 cm (20m)(See upper left Figure 4.5). **Case 2** (B40d17.5) had fixed mooring and vertical barriers on both sides of the structure. The freeboard of the structure is 5 cm. Height of the structure, D, is 22.5 cm. The draft of the structure, d, is 17.5 cm (3.5m). The width of the structure, B, is 40cm (8m). Structure length, L_s, is 100 cm (20m) (See upper right Figure 4.5). **Case 3** (B40d27.5) had fixed mooring and vertical barriers on both sides of the structure. The freeboard of the structure is 5 cm. Height of the structure, D, is 32.5 cm. The draft of the structure, d, is 27.5 cm (5.5m). The width of the structure, B, is 40cm (8m). Structure length, L_s, is 100 cm (20m) (See bottom Figure 4.5).

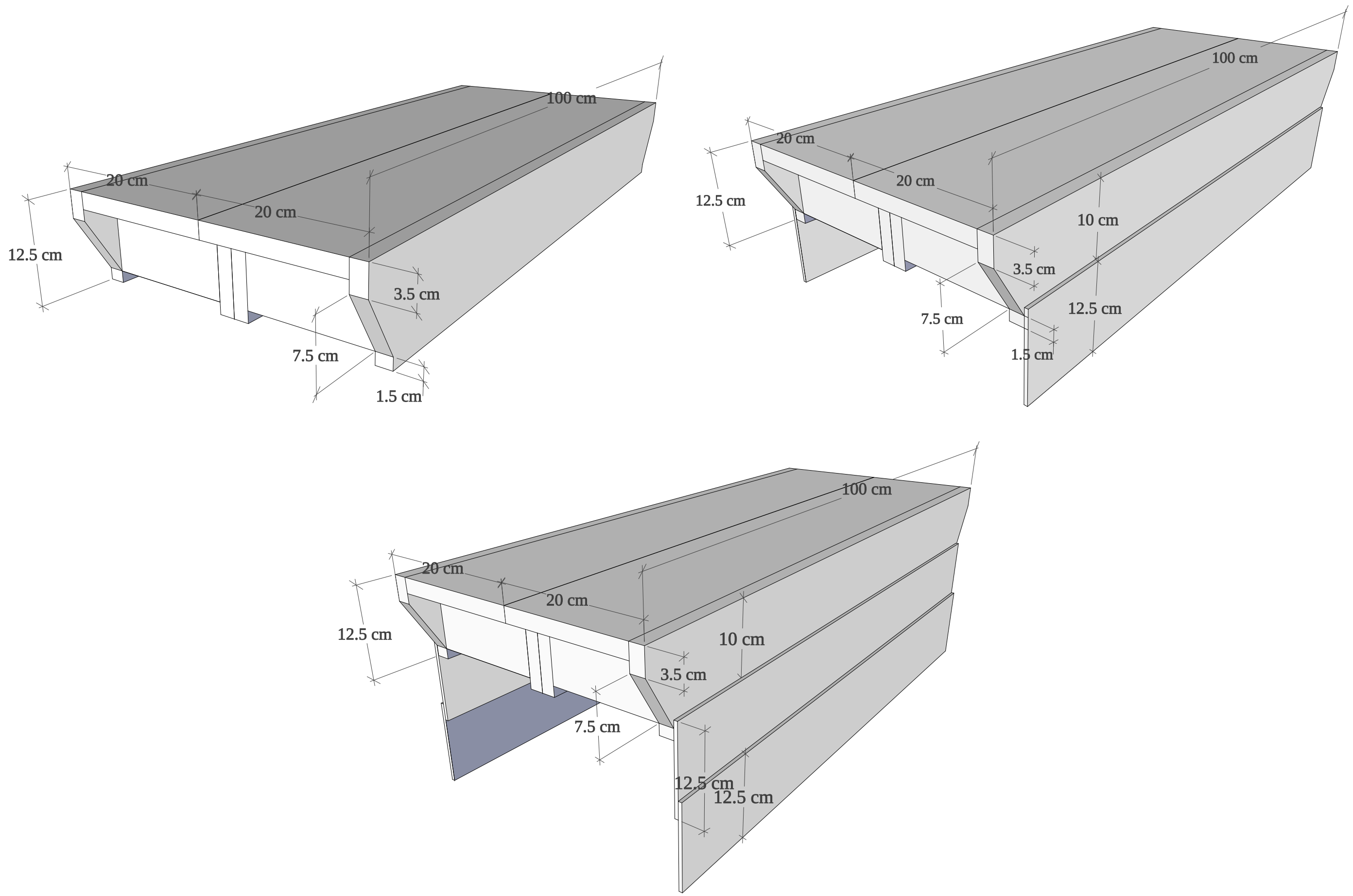

Figure 4.5: Case 1 B40d7.5 - Case 2 B40d17.5 - Case 3 B40d27.5

Experimental results for Case1 - Case2 - Case3 For structure width B=8 m (B=40 cm (model)), Figures 4.6 and 4.7 present the effects of variable drafts on transmitted wave height, H_t, and reflected wave height, H_r, for wave period ranging between T=4-6.5 seconds (B/L=0.135-0.312). In Figure 4.6 and 4.7, wave steepnesses are H/L=0.015 and H/L=0.025 respectively. In both Figures 4.6 and 4.7, with the increasing incoming wave height, H_i, and periods, T, transmitted wave heights, H_t, increase for all drafts where the transmitted wave height, H_t, gets the minimum and maximum values for the maximum and minimum drafts respectively. In both Figures 4.6 and 4.7, with the increasing incoming wave height, H_i, and periods, T, reflected wave heights, H_r, decrease in a similar fluctuating pattern for all drafts where reflected wave heights, H_r, gets minimum and maximum values for the minimum and maximum drafts respectively. Therefore, as the draft increases, transmitted wave height, H_t, decreases and reflected wave height, H_r, increases.

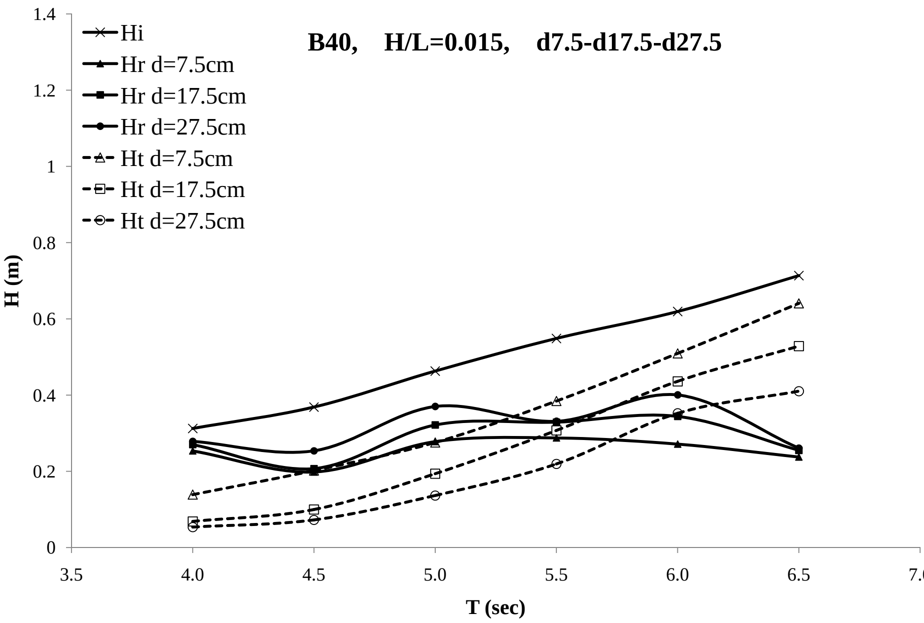

Figure 4.6: Effects of draft change on H_r and H_t (width(B)= 40cm, H/L=0.015)

In order to compare the test results obtained for wave steepnesses H/L=0.015 and H/L=0.025 given in Figures 4.6 and 4.7 respectively, transmission coefficient, ($K_t = H_t/H_i$) and reflection coefficient, ($K_r = H_r/H_i$) are computed and plotted against B/L where L is the wave length at the construction depth (h=14m) and B is the structure

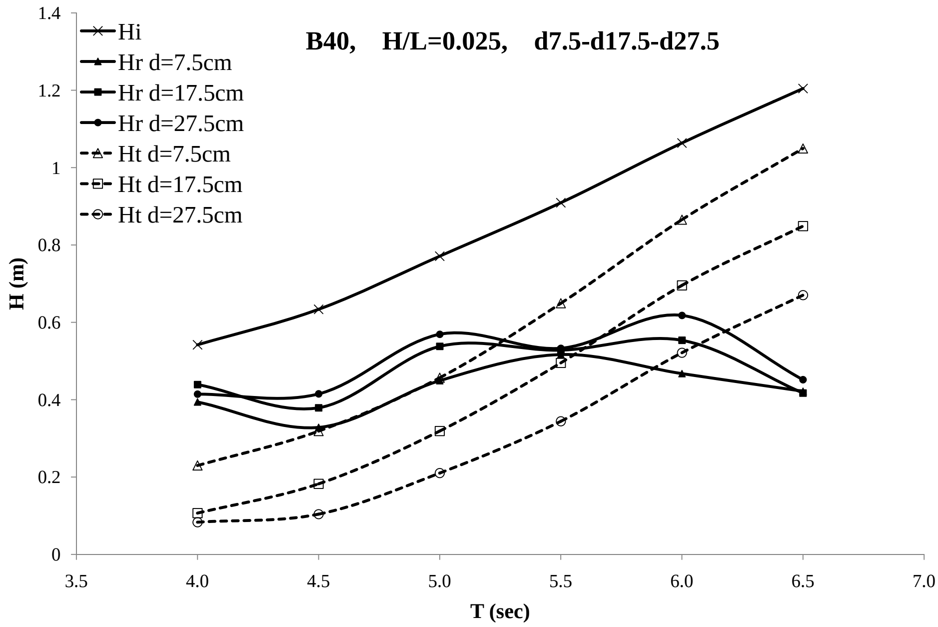

Figure 4.7: Effects of draft change on H_r and H_t (width(B)= 40cm, H/L=0.025)

width. The transmission coefficient, K_t, and the reflection coefficient, K_r, are presented in Figures 4.8 and 4.9 for B/L ranging between 0.135-0.312 and for the wave steepnesses H/L=0.015 and H/L=0.025 respectively.

As it is seen for Figures 4.8 and 4.9, K_t and K_r curves have a similar pattern for both the wave steepnesses H/L=0.015 and H/L=0.025. With the increasing B/L ratio, K_t decreases having maximum and minimum values for the minimum and maximum drafts respectively. Accordingly with the increasing B/L ratio, K_r values get larger having maximum and minimum values for the maximum and minimum drafts respectively. It can be seen from these figures that the increased wave steepness from 0.015 to 0.025 tested in the experiments does not have significant effect in the transmission (K_t) and reflection (K_r) coefficients. Considering both of the wave steepnesses, for B/L=0.321 (T=4 sec) K_t has the maximum value (K_t=0.44) for minimum draft (d=1.5m (d=7.5 cm)) and minimum value (K_t=0.15) for maximum draft (d=5.5m (d=27.5 cm)). Similarly for B/L=0.135 (T=6.5 sec) K_t is maximum (K_t=0.9) for minimum draft (d=1.5m (d=7.5 cm)) and K_t is minimum (K_t=0.57) for maximum draft (d=5.5m (d=27.5 cm)). As for the reflection coefficients, for the given wave steepnesses, for B/L=0.321 (T=4 sec) K_r has the maximum value (K_r=0.74) for maximum draft (d=5.5m (d=27.5 cm)) and minimum value (K_r=0.65) for minimum draft (d=1.5m (d=7.5 cm)). Similarly for B/L=0.135 (T=6.5 sec) K_r is maximum (K_r=0.56) for maximum draft (d=5.5m (d=27.5 cm)) and K_r is minimum (K_r=0.39) for minimum draft (d=1.5m (d=7.5 cm)). Therefore, it can be stated that both wave period and draft very effectively control the wave transmission and wave reflection. Test results both for K_t and K_r are presented in Table A.15 and A.16 in pages 113 and 114 respectively.

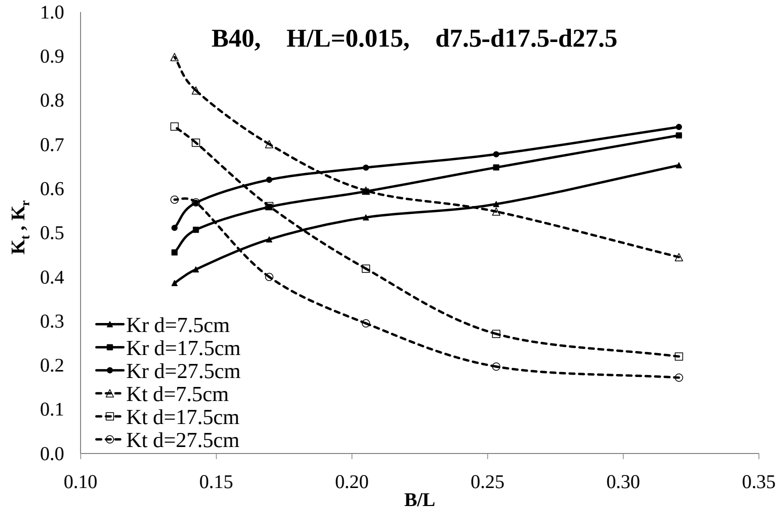

Figure 4.8: Effects of draft change on K_r and K_t (width(B)= 40cm, H/L=0.015)

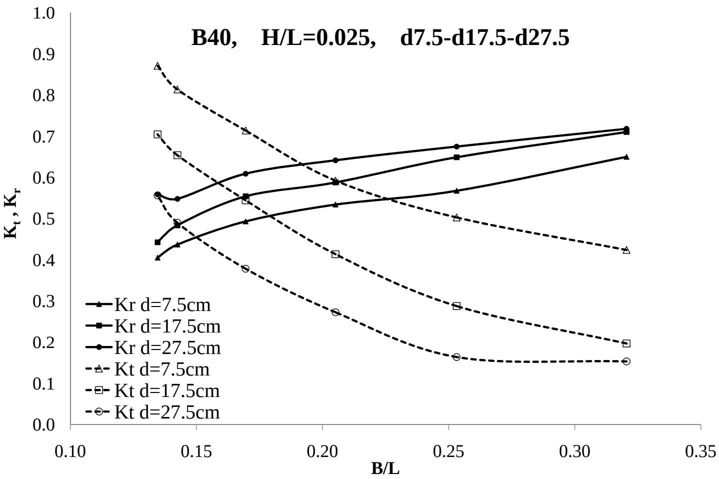

Figure 4.9: Effects of draft change on K_r and K_t (width(B)= 40cm, H/L=0.025)

4.2.2 Case 4 - Case 5 - Case 6 (Width(B)=12 m)

Case 4 (B60d7.5) had fixed mooring and no barriers. It corresponds to a box type floating breakwater. The freeboard of the structure is 5 cm. Height of the structure, D, is 12.5 cm. The draft of the structure, d, is 7.5 cm(1.5m). The width of the structure, B, is 60cm(12m). Structure length, L_s, is 100 cm (20m) (See upper left Figure 4.10). **Case 5** (B60d17.5) had fixed mooring and vertical barriers on both sides of the structure. The freeboard of the structure is 5 cm. Height of the structure, D, is 22.5 cm. The draft of the structure, d, is 17.5 cm (3.5m). The width of the structure, B, is 60cm (12m). Structure length, L_s, is 100 cm (20m) (See upper right Figure 4.10). **Case 6** (B60d27.5) had fixed mooring and vertical barriers on both sides of the structure. The freeboard of the structure is 5 cm. Height of the structure, D, is 32.5 cm. The draft of the structure, d, is 27.5 cm (5.5m). The width of the structure, B, is 60cm (12m). Structure length, L_s, is 100 cm (20m) (See bottom Figure 4.10).

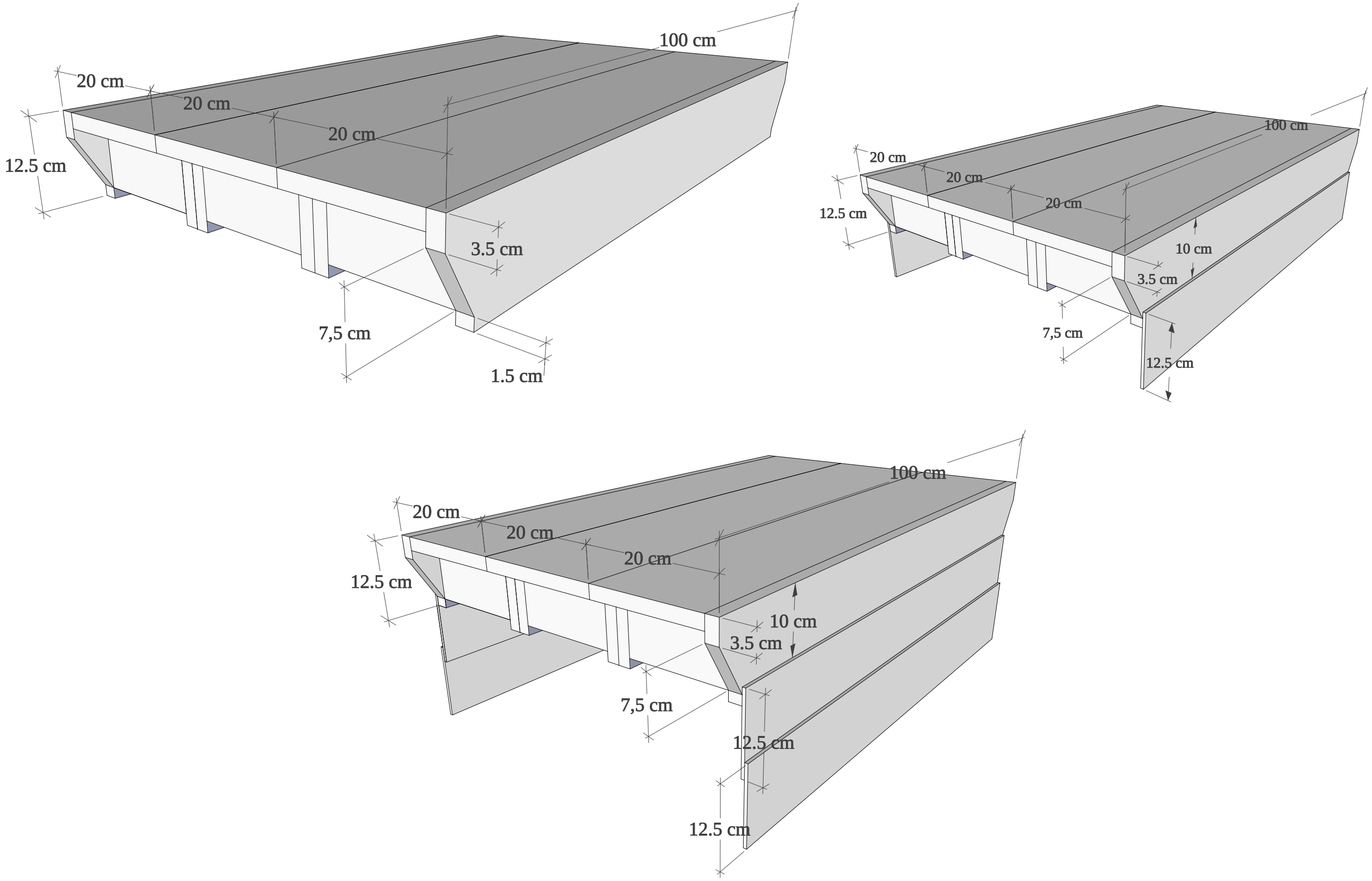

Figure 4.10: Case 4 B60d7.5 - Case 5 B60d17.5 - Case 6 B60d27.5

Experimental results for Case4 - Case5 - Case6 For structure width B=12 m (B=60 cm (model)), Figures 4.11 and 4.12 present the effects of variable drafts on transmitted wave height, H_t, and reflected wave height, H_r, for wave period ranging between T=4-6.5 seconds (B/L=0.202-0.481). In Figure 4.11 and 4.12, wave steepnesses are H/L=0.015 and H/L=0.025 respectively. In both Figures 4.11 and 4.12, with the increasing incoming wave height, H_i, and periods, T, transmitted wave heights, H_t, increase for all drafts where the transmitted wave height, H_t, gets the minimum and maximum values for the maximum and minimum drafts respectively. In both Figures 4.11 and 4.12, with the increasing incoming wave height, H_i, and periods, T, reflected wave heights, H_r, decrease in a similar fluctuating pattern for all drafts where reflected wave heights, H_r, gets minimum and maximum values for the minimum and maximum drafts respectively. Therefore, as the draft increases, transmitted wave height, H_t, decreases and reflected wave height, H_r, increases.

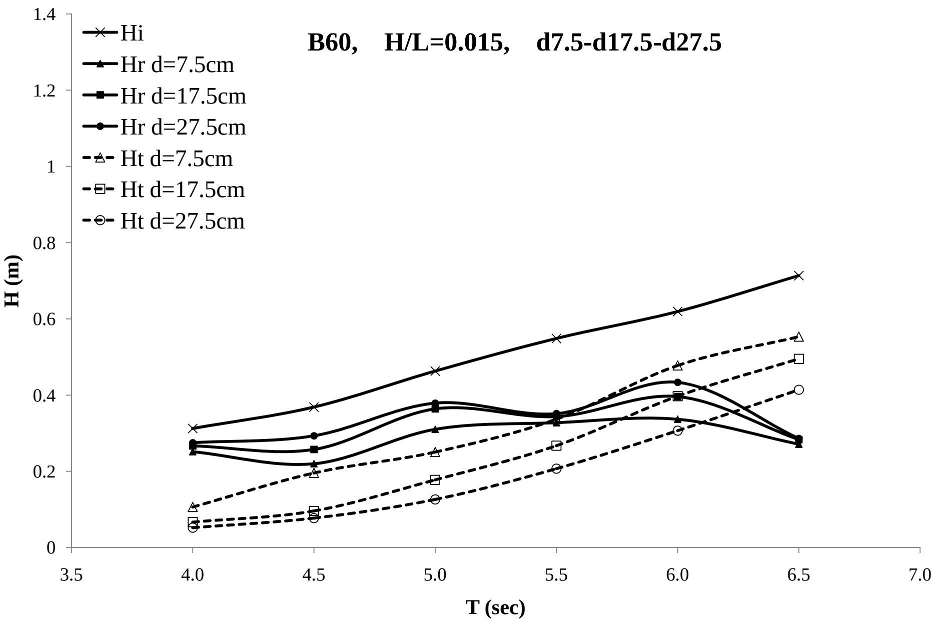

Figure 4.11: Effects of draft change on H_r and H_t (width(B)= 60cm, H/L=0.015)

In order to compare the test results obtained for wave steepnesses H/L=0.015 and H/L=0.025 given in Figures 4.11 and 4.12 respectively, transmission coefficient, (K_t $=H_t/H_i$) and reflection coefficient, (K_r=H_r/H_i) are computed and plotted against B/L where L is the wave length at the construction depth (h=14m) and B is the struc-

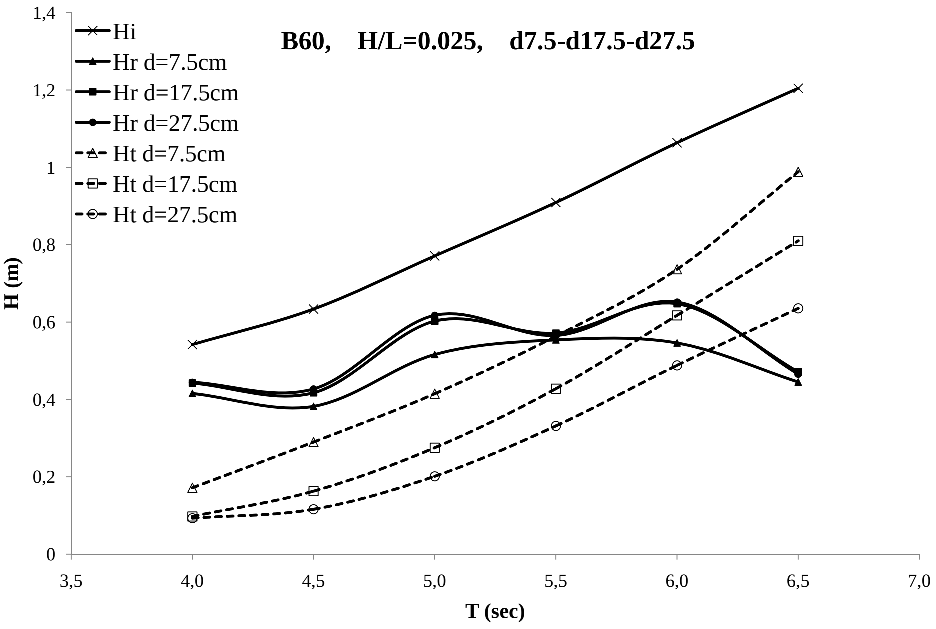

Figure 4.12: Effects of draft change on H_r and H_t (width(B)= 60cm, H/L=0.025)

ture width. The transmission coefficient, K_t, and the reflection coefficient, K_r, are presented in Figures 4.13 and 4.14 for B/L ranging between 0.202-0.481 and for the wave steepnesses H/L=0.015 and H/L=0.025 respectively.

As it is seen for Figures 4.13 and 4.14, K_t and K_r curves have a similar pattern for both the wave steepnesses H/L=0.015 and H/L=0.045. With the increasing B/L ratio, K_t decreases having maximum and minimum values for the minimum and maximum drafts respectively. Accordingly with the increasing B/L ratio, K_r values get larger having maximum and minimum values for the maximum and minimum drafts respectively. It can be seen from these figures that the increased wave steepness (from 0.015 to 0.025) tested in the experiments does not have significant effect in the transmission (K_t) and reflection (K_r) coefficients. Considering both of the wave steepnesses, for B/L=0.481 (T=4 sec) K_t has the maximum value (K_t=0.34) for minimum draft (d=1.5m (d=7.5 cm)) and minimum value (K_t=0.17) for maximum draft (d=5.5m (d=27.5 cm)). Similarly for B/L=0.202 (T=6.5 sec). K_t is maximum (K_t=0.78) for minimum draft (d=1.5m (d=7.5 cm)) and K_t is minimum (K_t=0.58) for maximum draft (d=5.5m (d=27.5 cm)). As for the reflection coefficients, for the given wave steepnesses, for B/L=0.481 (T=4 sec) K_r has the maximum value (K_r=0.74) for maximum draft (d=5.5m (d=27.5 cm)) and minimum value (K_r=0.67) for minimum draft (d=1.5m (d=7.5 cm)). Similarly for B/L=0.202 (T=6.5 sec) K_r is maximum (K_r=0.58) for maximum draft (d=5.5m (d=27.5 cm)) and K_r is minimum (K_r=0.47) for minimum draft (d=1.5m (d=7.5 cm)). Therefore, it can be stated that both wave period and draft control the wave transmission and wave reflection. Test results both for K_t and K_r are presented in Table A.15 and A.16 in pages 113 and 114 respectively.

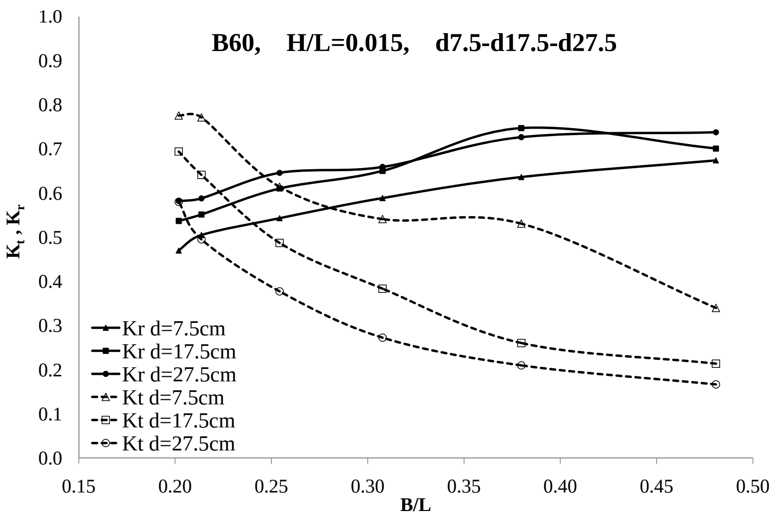

Figure 4.13: Effects of draft change on K_r and K_t (width(B)= 60cm, H/L=0.015)

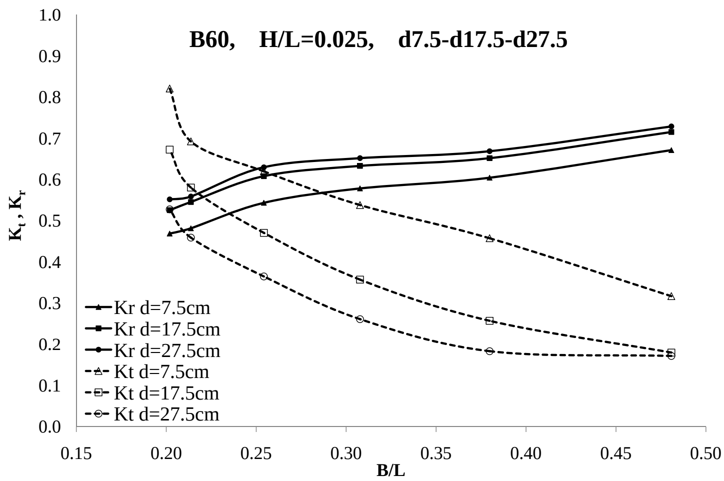

Figure 4.14: Effects of draft change on K_r and K_t (width(B)= 60cm, H/L=0.025)

4.2.3 Case 7 - Case 8 - Case 9 (Width(B)=16 m)

Case 7 (B80d7.5) had fixed mooring and no barriers. It corresponds to a box type floating breakwater. The freeboard of the structure is 5 cm. Height of the structure, D, is 12.5 cm. The draft of the structure, d, is 7.5 cm (1.5m). The width of the structure, B, is 80cm (16m). Structure length, L_s, is 100 cm (20m) (See upper left Figure 4.15). **Case 8** (B80d17.5) had fixed mooring and vertical barriers on both sides of the structure. The freeboard of the structure is 5 cm. Height of the structure, D, is 22.5 cm. The draft of the structure, d, is 17.5 cm (3.5m). The width of the structure, B, is 80cm (16m). Structure length, L_s, is 100 cm (20m) (See upper right Figure 4.15). **Case 9** (B80d27.5) had fixed mooring and vertical barriers on both sides of the structure. The freeboard of the structure is 5 cm. Height of the structure, D, is 32.5 cm. The draft of the structure, d, is 27.5 cm (5.5m). The width of the structure, B, is 80cm (16m). Structure length, L_s, is 100 cm (20m) (See bottom Figure 4.15).

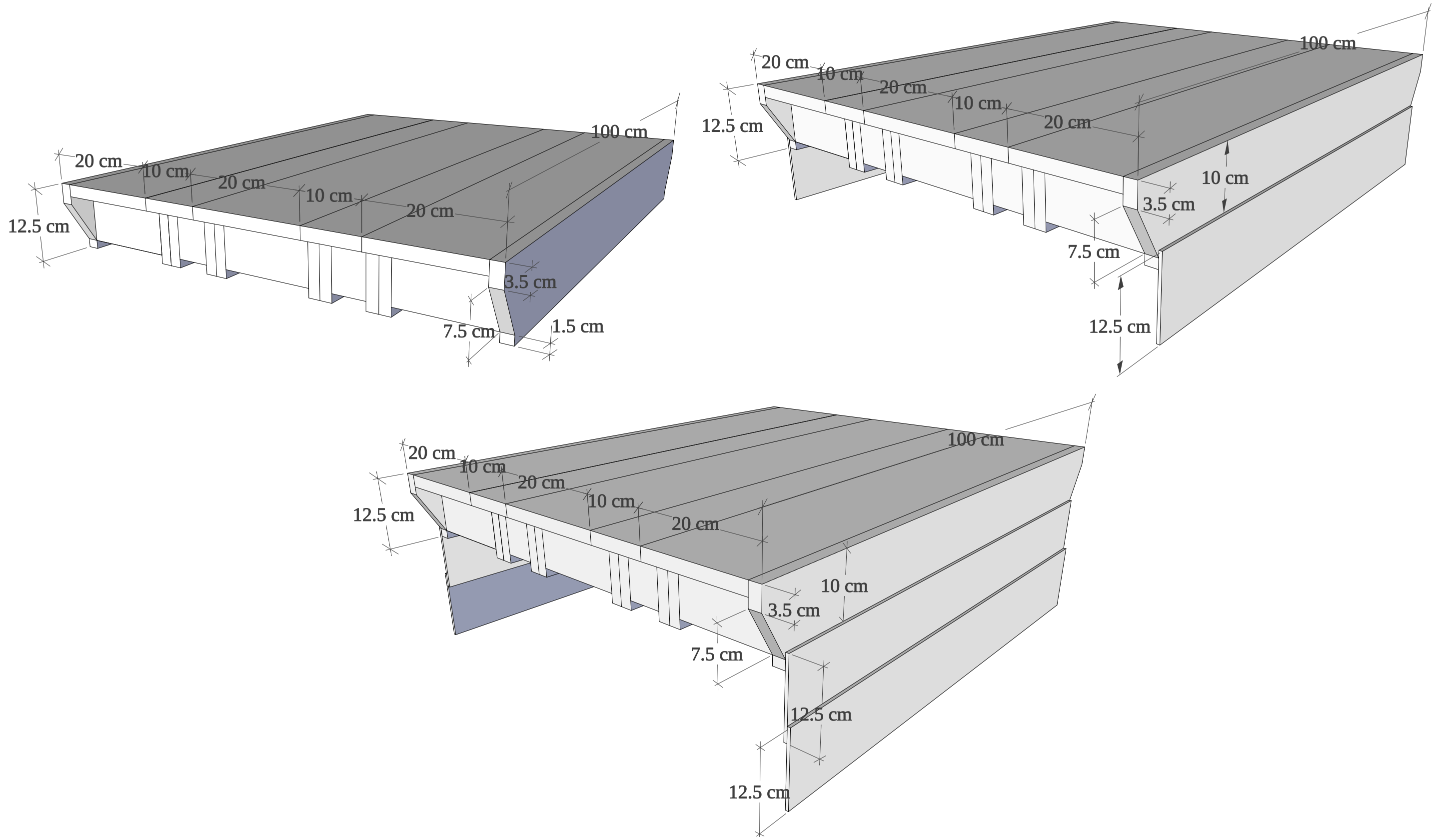

Figure 4.15: Case 7 B80d7.5 - Case 8 B80d17.5 - Case 9 B80d27.5

Experimental results for Case7 - Case8 - Case9 For width of the structure B=16 m (B=80 cm (model)), Figures 4.16 and 4.17 present the effects of variable drafts on transmitted wave height, H_t, and the reflected wave height, H_r, are given for wave period ranging between T=4-6.5 seconds (B/L=0.269-0.641). In Figure 4.16 and 4.17, wave steepnesses are H/L=0.015 and H/L=0.025 respectively. In both Figures 4.16 and 4.17, with the increasing incoming wave height, H_i, and periods, T, transmitted wave heights, H_t, increase for all drafts where the transmitted wave height, H_t, gets the minimum and maximum values for the maximum and minimum drafts respectively. Therefore, as the draft increases, transmitted wave height, H_t, decreases. In both Figures 4.16 and 4.17, with the increasing incoming wave height, H_i, and periods, T, reflected wave heights, H_r, fluctuating pattern is similar for all drafts where reflected wave heights, H_r, gets minimum and maximum values for the minimum and maximum drafts respectively. Therefore, as the draft increases, reflected wave height, H_r, increases for T<6sec. At T=6.5 sec, however, H_r values are measured almost the same.

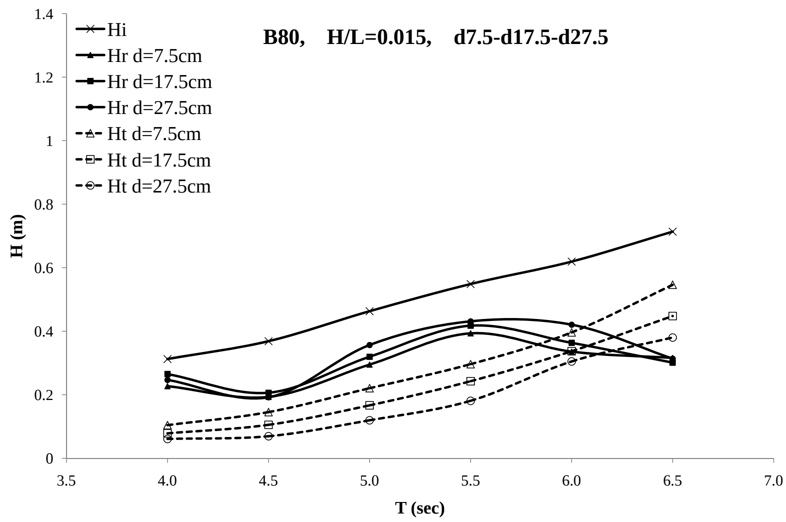

Figure 4.16: Effects of draft change on H_r and H_t (width(B)= 80cm, H/L=0.015)

In order to compare the test results obtained for wave steepnesses H/L=0.015 and H/L=0.025 given in Figures 4.16 and 4.17 respectively, transmission coefficient, ($K_t = H_t/H_i$) and reflection coefficient, ($K_r = H_r/H_i$) are computed and plotted against B/L where L is the wave length at the construction depth (h=14m) and B is the struc-

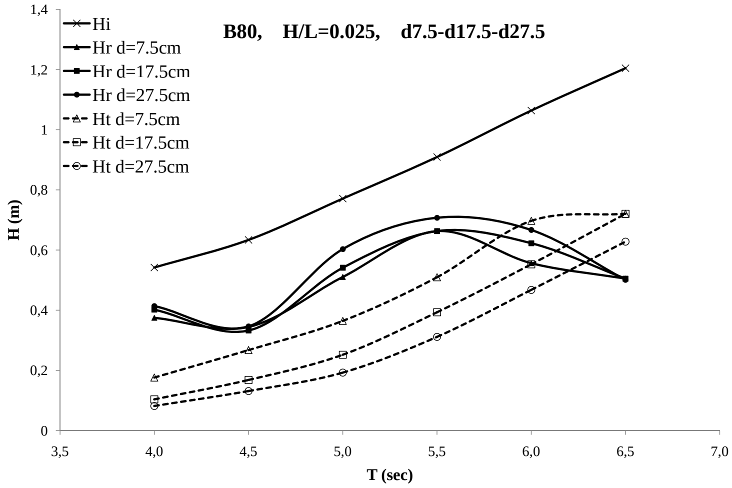

Figure 4.17: Effects of draft change on H_r and H_t (width(B)= 80cm, H/L=0.025)

ture width. The transmission coefficient, K_t, and the reflection coefficient, K_r, are presented in Figures 4.18 and 4.19 for B/L ranging between 0.269-0.641 and for the wave steepnesses H/L=0.015 and H/L=0.025 respectively.

As it is seen for Figures 4.18 and 4.19, K_t and K_r curves have a similar pattern for both the wave steepnesses H/L=0.015 and H/L=0.045. With the increasing B/L ratio, K_t decreases having maximum and minimum values for the minimum and maximum drafts respectively. Accordingly with the increasing B/L ratio, K_r values get larger having maximum and minimum values for the maximum and minimum drafts respectively. It can be seen from these figures that the increased wave steepnesses (from 0.015 to 0.025) tested in the experiments does not have significant effect in the transmission (K_t) and reflection (K_r) coefficients. Considering both of the wave steepnesses, for B/L=0.641 (T=4 sec) K_t has the maximum value (K_t=0.33) for minimum draft (d=1.5m (d=7.5 cm)) and minimum value (K_t=0.15) for maximum draft (d=5.5m (d=27.5 cm)). Similarly for B/L=0.269 (T=6.5 sec). K_t is maximum (K_t=0.77) for minimum draft (d=1.5m (d=7.5 cm)) and K_t is minimum (K_t=0.53) for maximum draft (d=5.5m (d=27.5 cm)). As for the reflection coefficients, for the given wave steepnesses, for B/L=0.641 (T=4 sec) K_r has the maximum value (K_r=0.72) for maximum draft (d=5.5m (d=27.5 cm)) and minimum value (K_r=0.67) for minimum draft (d=1.5m (d=7.5 cm)). Similarly for B/L=0.269 (T=6.5 sec) K_r is maximum (K_r=0.61) for maximum draft (d=5.5m (d=27.5 cm)) and K_r is minimum (K_r=0.53) for minimum draft (d=1.5m (d=7.5 cm)). In Figure 4.19 where the steepness is 0.025, the effect of draft on K_t and K_r cannot be observed at B/L=0.269. However for smaller B/L values, it can be stated that both wave period and draft control the wave transmission and wave reflection. Test results both for K_t and K_r are presented in Table A.15 and A.16 in pages 113 and 114 respectively.

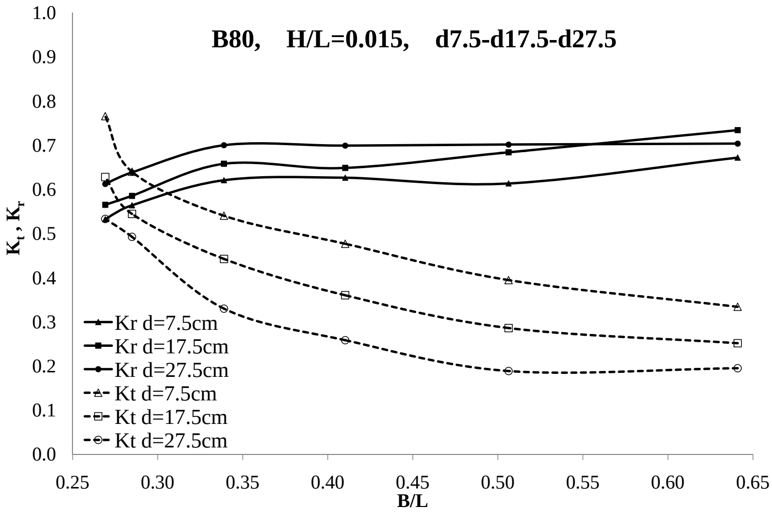

Figure 4.18: Effects of draft change on K_r and K_t (width(B)= 80cm, H/L=0.015)

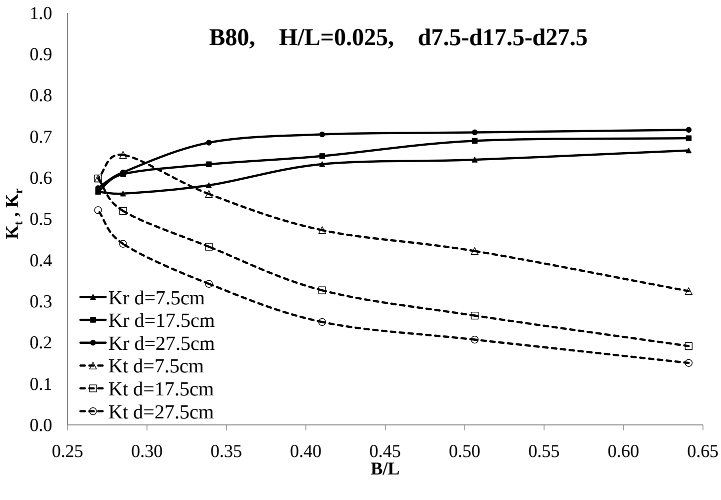

Figure 4.19: Effects of draft change on K_r and K_t (width(B)= 80cm, H/L=0.025)

4.3 Discussion of experimental results for Case1 - Case9

In order to see the effect of structure width, B, on wave transmission and wave reflection, tests results both for wave steepnesses H/L=0.015 and H/L=0.025 are plotted for each draft as K_t vs h/L and K_r vs h/L for the tested B values and presented in Figures 4.20 and 4.21.

As for the wave transmission (Figure 4.20), K_t values for a given draft vary in a similar range both for the wave steepnesses H/L=0.015 and H/L=0.025. Therefore, the effect of steepness is insignificant for the tested wave steepness (0.015 and 0.025) ranges. Figure 4.20 shows the effect of structure draft (d) and the structure width (B) on the wave transmission. For all structures drafts and structure widths, as h/L increase (wave period decreases) K_t values decrease. Considering all B values, for d=1.5m, K_t values range approximately between 0.3 and 0.9, for d=3.5m whereas for d=5.5m, K_t values range approximately between 0.2 and 0.75, for d=5.5m, K_t values range between 0.15 and 0.6. Therefore it can be concluded that as the draft increase K_t values decrease for all h/L ranging between 0.24 and 0.56.

Similarly for draft d=1.5m, minimum K_t values are obtained for maximum structure width B=16m (B80). As the draft increases, for d=3.5m, K_t values are similar for all B values for h/L>0.4. For h/L<0.4, B=16m (B80) gives the smallest K_t value. For draft d=5.5m, for tested structures widths (B), K_t values obtained are almost the same for the tested h/L values. It can be stated that as the draft increases the effect of structure width (B) becomes less significant.

As for the wave reflection 4.21, K_r values for a given draft vary in a similar range both for the wave steepnesses H/L=0.015 and H/L=0.025. Therefore, the effect of steepness is insignificant for the tested wave steepness (0.015 and 0.025) ranges. Figure 4.21 shows the effect of structure draft (d) and the structure width (B) on the wave reflection. Also it is seen that for increasing values of draft (d) from 1.5m to 5.5m, K_r values approximately between 0.4 and 0.7 for all B values.

For B=8m (B40), when d=1.5m, K_r range approximately between 0.39 and 0.65. When d=3.5m, K_r values range approximately between 0.46 and 0.72. When, d=5.5m, K_r values range approximately between 0.51 and 0.74. So it can be stated that for structure width B=8m (B40) K_r values increase slightly with increasing draft (d). However, for B=12m (B60) and B=16m (B80), for all drafts, when h/L>0.56 there is no significant effect of B on K_r coefficients.

It can be stated that for larger h/L values (for small T values) effect of structure width (B) on wave reflection is similar for the tested draft (d) values and has approximately the same value (K_r=0.7) for h/L=0.56.

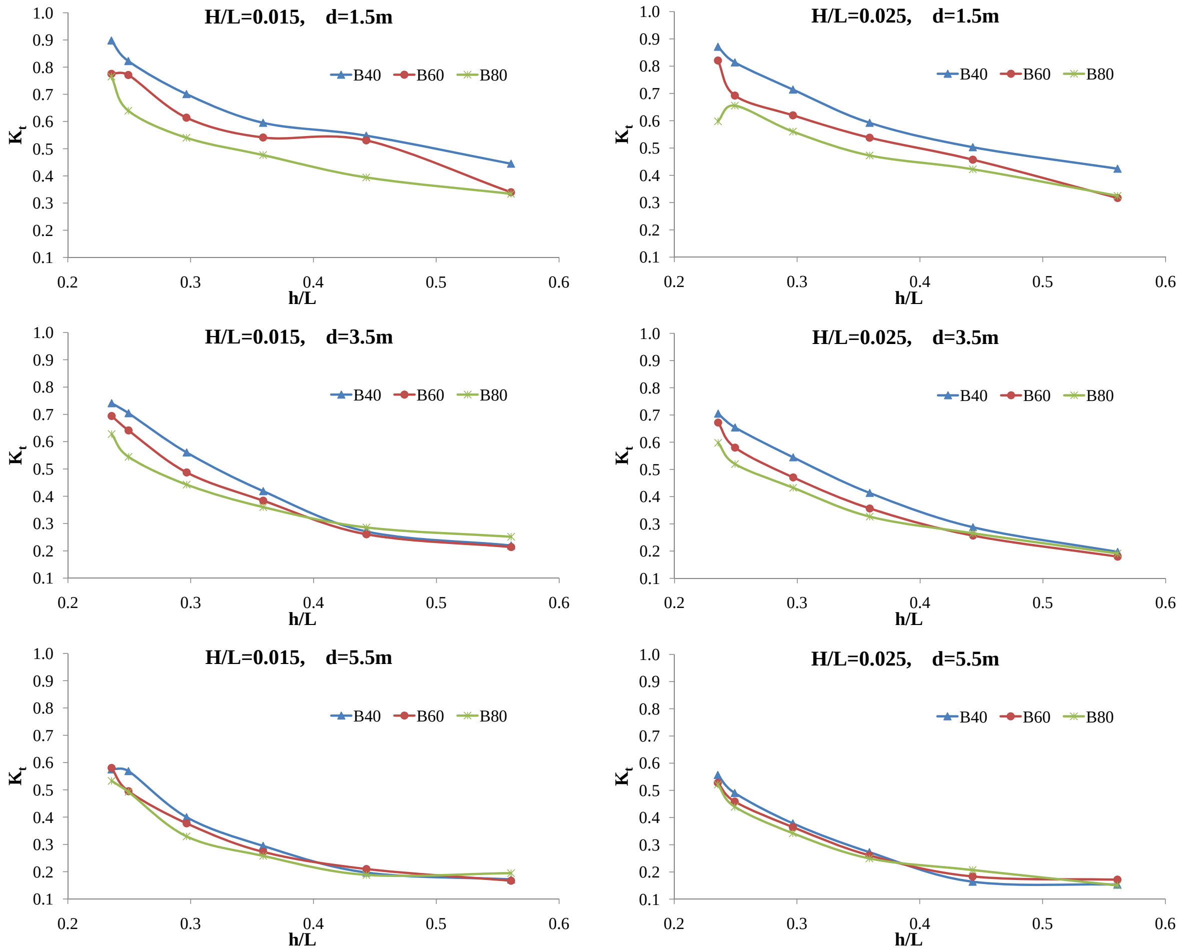

Figure 4.20: K_t vs h/L for H/L=0.015-0.025

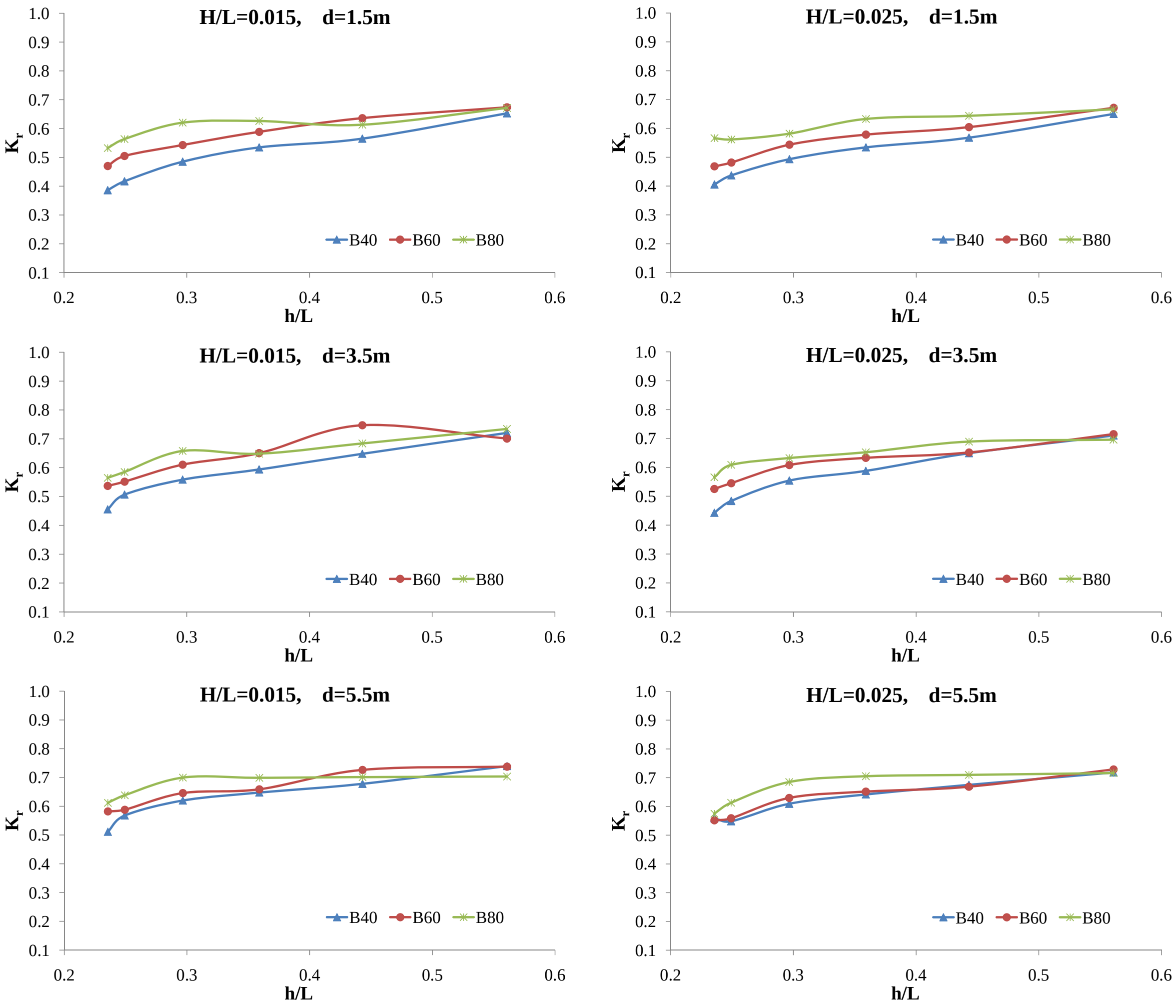

Figure 4.21: K_r vs h/L for H/L=0.015-0.025

To investigate the effect of structure draft, the test results are re-plotted in Figures 4.22 and 4.23 as K_t vs d/h for B=8m, B=12m and B=16m for selected wave periods and the wave steepnesses H/L=0.015 and H/L=0.025 respectively. In these figures test results obtained for periods T=4sec, T=5sec and T=6sec. are presented for convenience in discussions. In Appendix A, results for all periods are presented (Figures A.4 and A.5). As it seen from Figures 4.22 and 4.23, the effect of wave steepness (0.015 and 0.025) on the test results is insignificant. The curves given in Figures 4.22 and 4.23 confirms the discussion carried out previously on structure draft and structure width where; as T increases K_t increases, as draft increase K_t decreases for increasing d/h values. Also, as draft increases (increasing d/h values), the effect of B on K_t decreases. This decrease is more significant for smaller periods.

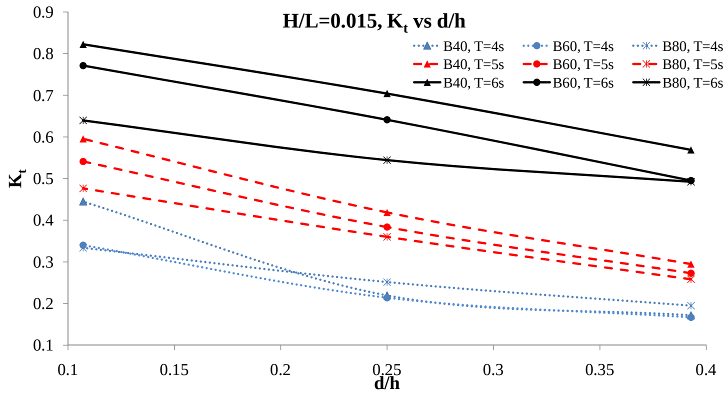

Figure 4.22: K_t vs d/h for H/L=0.015

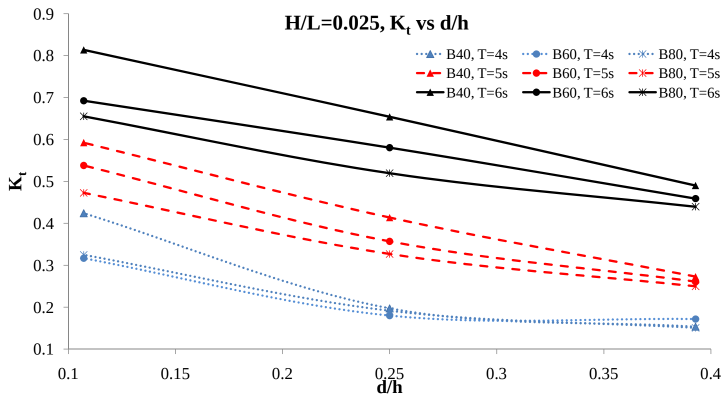

Figure 4.23: K_t vs d/h for H/L=0.025

4.4 Comparison of theoretical and experimental results

A comparative study is carried out using the transmission coefficients found during the experiments with Macagno (1953) [53],and the Cox (1989) [52]. Among the two theories mentioned, Macagno's Theory is a suitable for the case of this study because Macagno's theory takes both the height of the structure (freeboard + draft) and the draft into account while calculating a theoretical transmission coefficient (Equation 4.1).

$$K_t = 1/\sqrt{1 + \left(\frac{\pi B \sinh(2\pi Dh/L)}{L \cosh(2\pi(h-d)/L)}\right)^2} \tag{4.1}$$

where;

K_t : Transmission coefficient

B : Width of the structure (m)

D : Height of the structure (m)

d : Draft (m)

h : Water depth at the construction depth (m)

L : Wavelength at the construction depth(m)

Cox's Theory (Equation 4.2) takes into account the width of the structure and the draft of the structure is taken into consideration in P_t and P_i (Wiegel, 1959 [54]).

$$K_t = \sqrt{P_t/P_i}\left(\left(2\sqrt{1+\left(\frac{2\pi B}{L}\right)^2}\right) / \left(\frac{2+(2\pi B)^2}{L}\right)\right) \tag{4.2}$$

where;

K_t : Transmission coefficient

B : Width of the structure (m)

P_t : Transmitted wave power (Wiegel, 1959; Eq.3.41)

P_i : Incident wave power (Wiegel, 1959; Eq.3.41)

L : Wavelength at the construction depth(m)

Theoretical curves for K_t for each width and draft tested in the experiments are computed from Equations 4.1 and 4.2 presented in Figure 4.24. It is not possible to make a comparative statement on K_t value theoretically computed using Macagno and Cox equations for B/L<0.5. For B/L>0.5 theoretical curves result almost similar values.

Transmission coefficient data points gathered from the experiments are also plotted on these theoretical curves in Figure 4.25. Transmission coefficient data points gathered from the experiments are also plotted separately on Macagno's theoretical curve and Cox's theoretical curve in Figure A.2 and A.3 respectively given in Appendix A.

As it is seen from Figure 4.25 for B/L<0.305 experimental results are more in agreement with Cox's theoretical results when compared to Macagno's theoretical values. Experimental results are systematically below the theoretical values. Between B/L values 0.305 and 0.51 experimental results are in agreement with Cox's and Macagno's theoretical values. Within this range Macagno and Cox's theoretical values are in agreement. Test results have a scattered pattern around the theoretical curves of Macagno and Cox, again being systemically below the theoretical values. For B/L>0.51, Macagno and Cox are in good agreement whereas experimental results are systematically below the curves. In conclusion, experimental test results can be stated as being in agreement within the tested B/L range. Experimental test results are all below the theoretical curves with an acceptable range from the theoretical value (1%-20%).

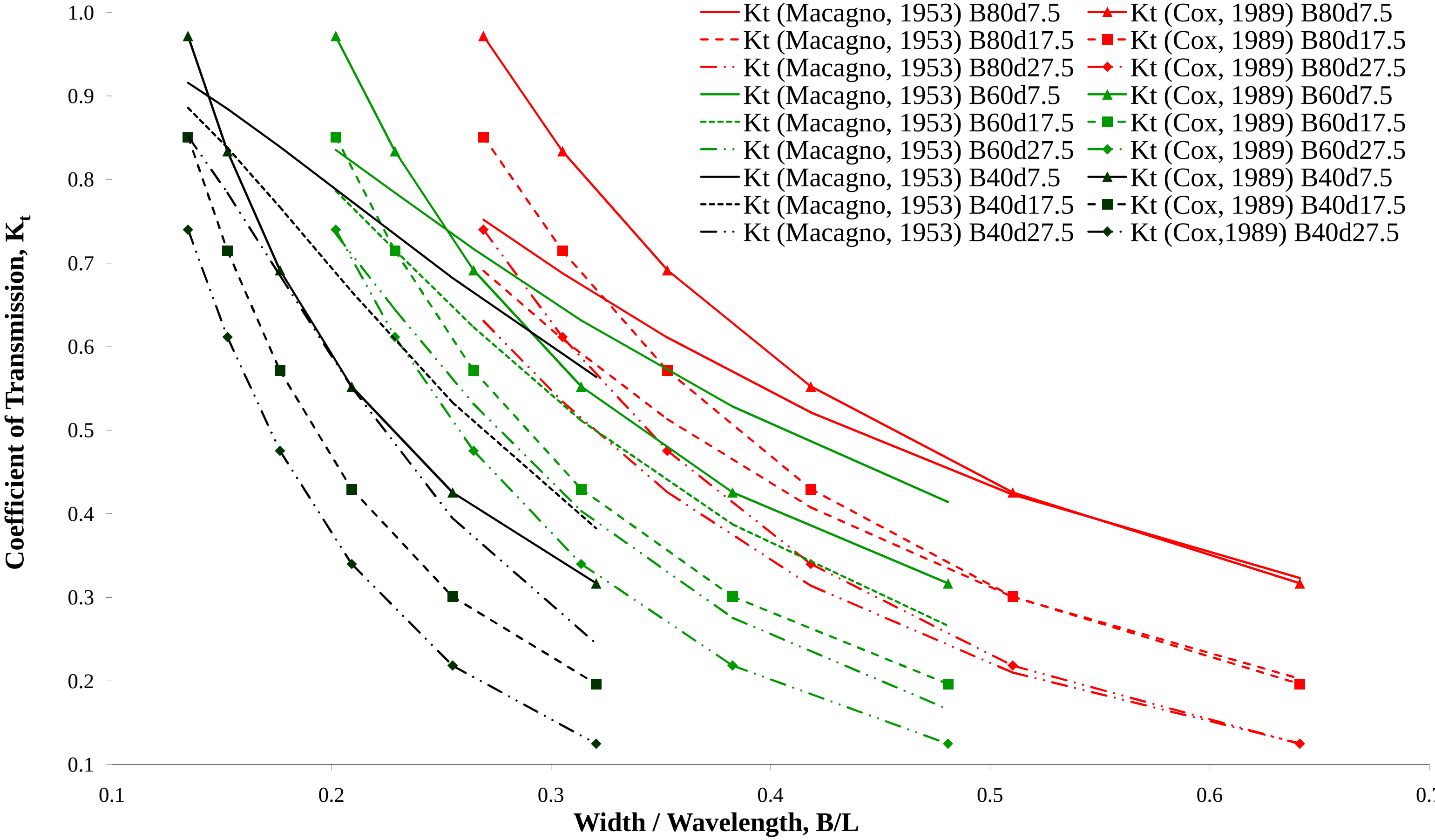

Figure 4.24: Theoretical Macagno and Cox's K_t vs B/L curves

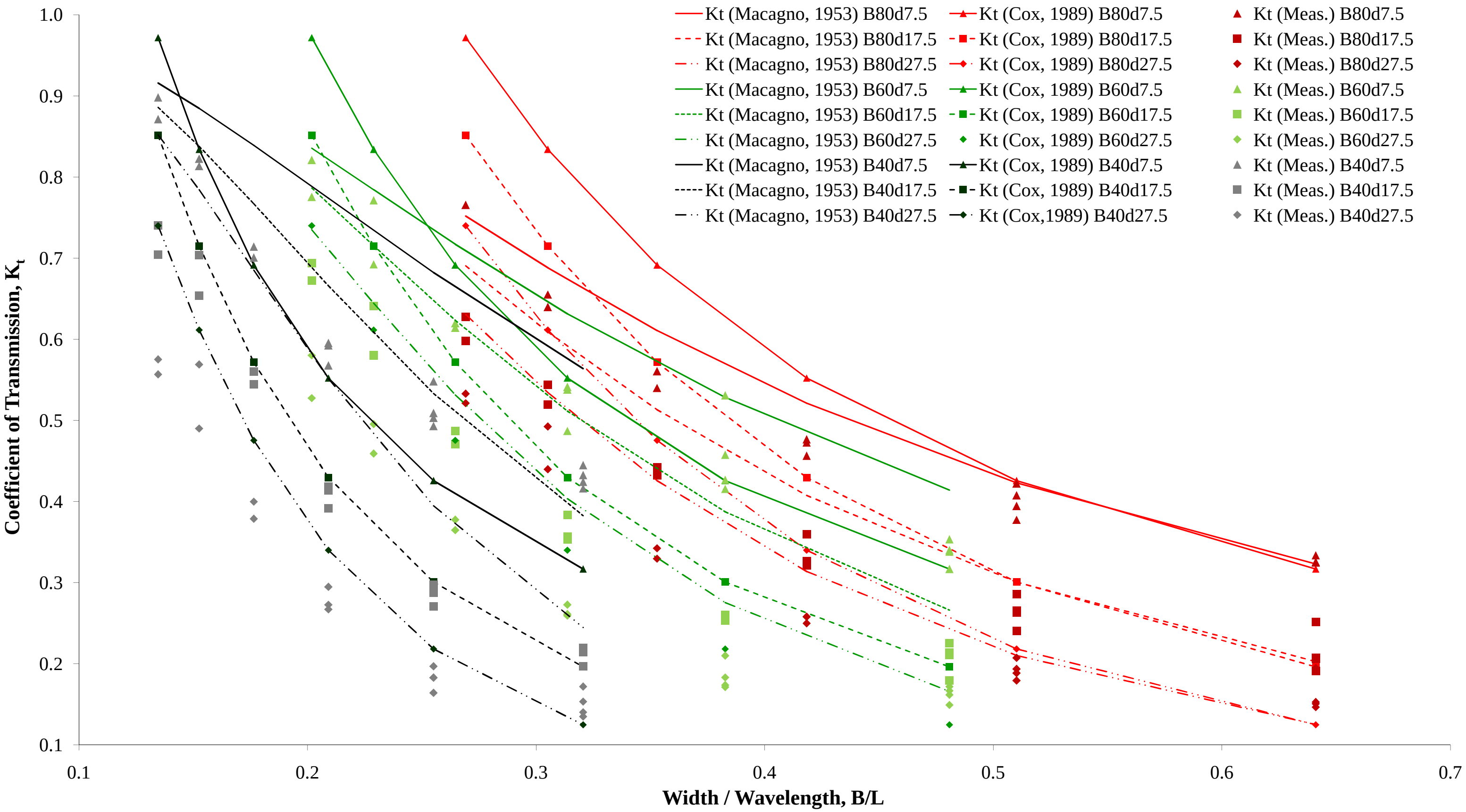

Figure 4.25: Experimental K_t comparison with Macagno and Cox's Theory

4.5 Tests with chain moored floating breakwaters

A series of model tests were carried out with the floating units moored to the wave flume bed with chains. For the chain moored floating units, the important movements are sway, heave and roll motions as shown in Figure 4.26.

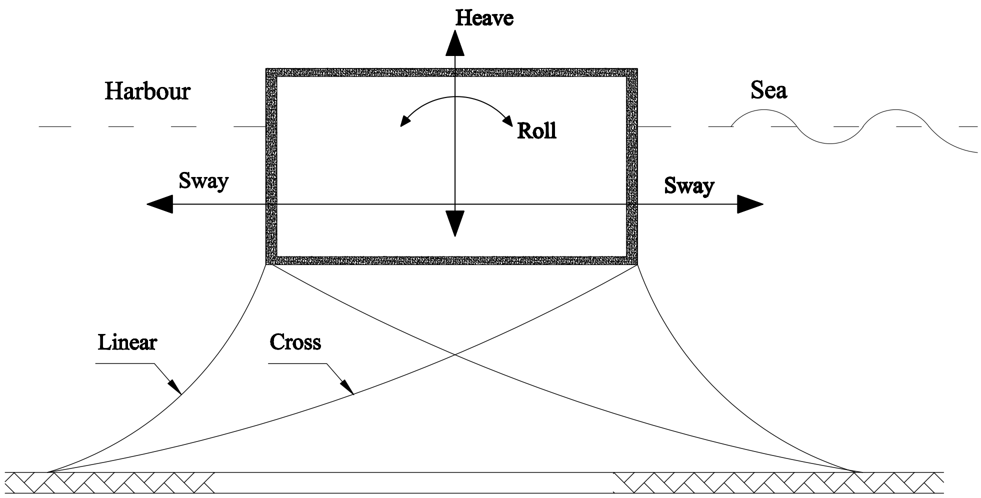

Figure 4.26: Sway, heave and roll motions

Sway is the horizontal motion that the structure will perform after the impact of the incoming wave. Sway will generate a wave that is radiated to the harbor side as well as the sea side of the floating breakwater. Heave is the vertical motion that the structure will perform after the impact of the incoming wave. The wave generated by the heave motion of the floating breakwater radiates to the harbor side with a phase difference compared to the incoming wave. This phase difference depends on the structural dimensions, the wave frequency and the mooring stiffness. Roll occurs when the resultant of the hydrodynamic forces is not in line with the center of rotation of the floating unit. In other words; roll is the hydrodynamic reaction on the wave exciting moments. The horizontal and vertical wave exciting forces times the relevant lever arms produce these moments. The roll motion itself creates a standing wave on the ocean side of the floating breakwater with a phase difference compared to the incoming wave. This phase difference depends on the structural dimensions, the wave frequency and the mooring stiffness. In the laboratory experiments, floating breakwaters are moored with chains to the wave flume bed. The chains maybe cross or linear connected from each corner of the floating unit to the sea bed.(Figure 4.26) In designing the mooring chains, chain weight is selected to meet the horizontal hydrodynamic forces applied to the floating unit. In practice, chain length is selected to create a 1/3 slope for each structure width tested (loose chain). Also, for the chain length selection, the sway motion limit (0.5m) is to be taken into consideration (tight chain) as shown in Figure 4.27.

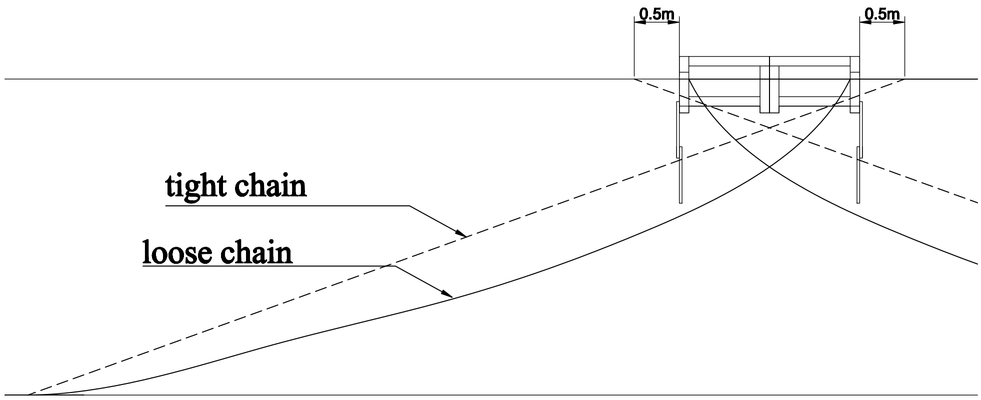

Figure 4.27: Chain mooring

4.6 Presentation and discussion of experimental results for Case10 - Case 18

Experimental results obtained for Case10 to Case18 are presented in Tables A.17 to A.25. For chain moored floating breakwaters (Case10 - Case18) test results are presented as K_t vs d/h for variable widths (B) both for H/L=0.015 and H/L=0.025 separately for wave periods T=4-4.5-5sec. and wave periods T=5.5-6-6.5sec in Figure 4.28, Figure 4.29, Figure 4.30 and in Figure 4.31 respectively.

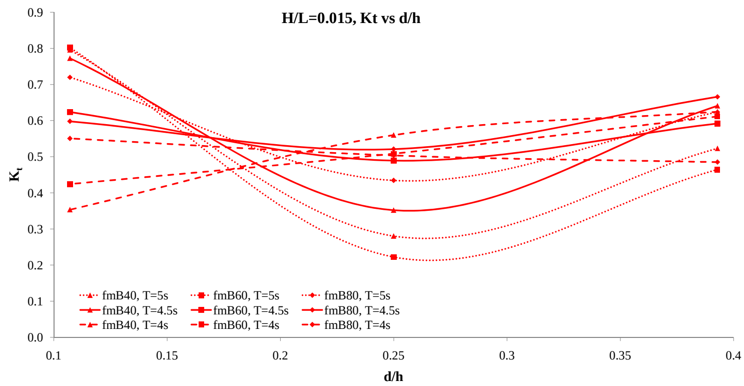

Figure 4.28: K_t vs d/h for H/L=0.015, T=4-4.5-5sec.(chain moored)

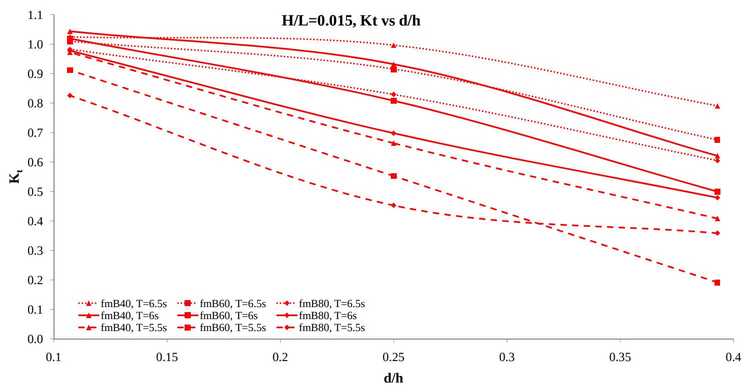

Figure 4.29: K_t vs d/h for H/L=0.015, T=5.5-6-6.5sec. (chain moored)

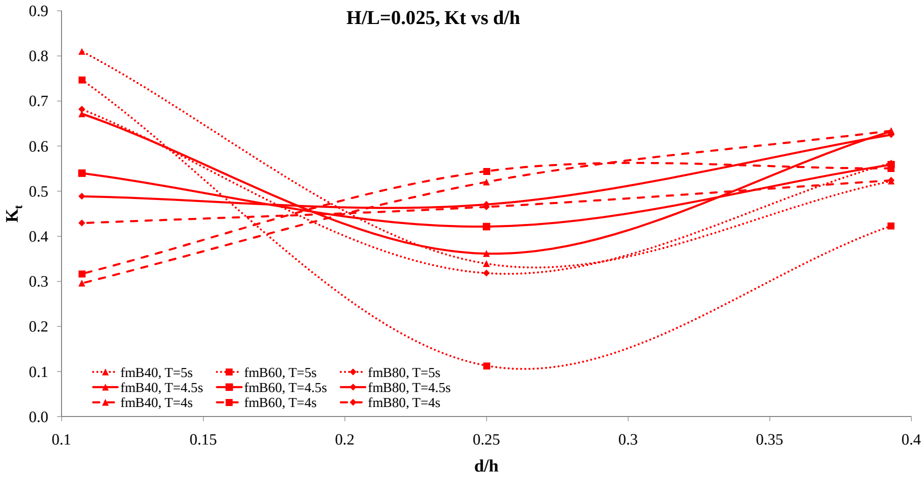

Figure 4.30: K_t vs d/h for H/L=0.025, T=4-4.5-5sec.(chain moored)

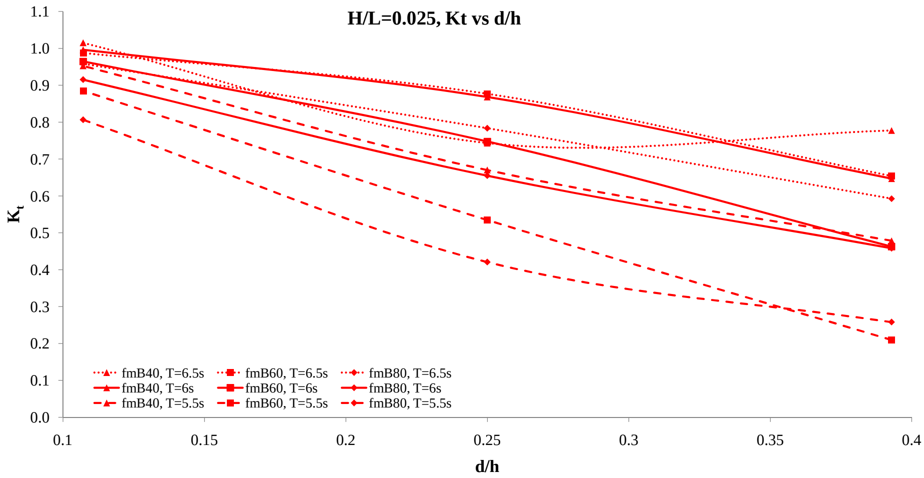

Figure 4.31: K_t vs d/h for H/L=0.025, T=5.5-6-6.5sec. (chain moored)

Comparison of the graphs of H/L=0.015 and H/L=0.025 corresponding to the same wave period ranges shows that the effect of wave steepness (for 0.015 and 0.025)is not significant on the results. Graphs presenting the results of wave periods T=4-4.5-5sec (Figures 4.28 and Figure 4.30) do not show a clear trend of d/h and B values on K_t coefficients. For periods T=4.5-5sec minimum K_t values are observed ranging between 0.22-0.32 corresponds to d/h=0.26. In order to find an explanation to this behavior natural period (T_n) of the floating unit for B=12m (B60) was measured for all drafts as T_n=3.88sec. for d=1.5m, T_n=3.95sec. for d=3.5m, T_n=4.7sec. for d=5.5m. Since these periods are not coinciding with tested wave periods T=4.5-5sec. no further discussion could be carried out. Therefore, it is well understood that series of experiments to be carried out as future studies for the system of floating units acting together which may help to explain the results obtained for T=4.5-5sec.
For wave periods T=5.5-6-6.5sec, the K_t values presented in Figures 4.29 and 4.31 decrease with the increasing d/h values. For d/h=0.11, K_t values range between 0.85-1.05 showing that floating breakwater is not effective on wave transmission. Whereas, for d/h=0.39, K_t values range between 0.35-0.83, disregarding the K_t value obtained as 0.22 for B=12m (B80). It can be stated that increased draft decreases the K_t values. In general, larger structure width (B) values give smaller K_t values except for T=5.5sec for B=16m (B80) and for T=6.5sec. B=8m (B40).

In order to compare the test results of the fixed floating breakwater (Case1 to Case9) with chain moored floating breakwaters (Case10 to Case18) K_t values vs d/h are plotted for the test periods T=5.5-6-6.5sec for variable widths for selected wave steepness H/L=0.015, and presented in Figures 4.32, 4.33 and 4.34. As it is seen from Figures 4.32, 4.33 and 4.34 K_t values obtained for chain moored floating breakwaters are larger than the K_t values of fixed cases consistently. This difference can be attributed to the movement of the chain moored floating units which increases the transmitted wave height.

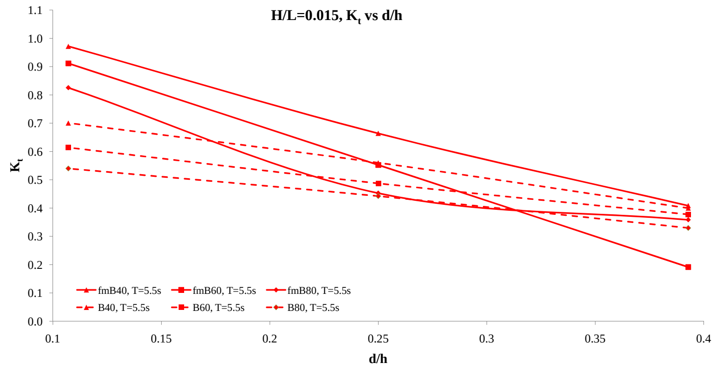

Figure 4.32: K_t vs d/h for H/L=0.015, T=5.5 sec. (fixed and chain moored)

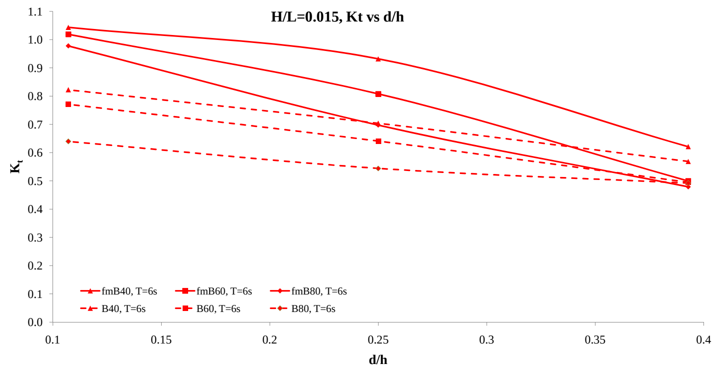

Figure 4.33: K_t vs d/h for H/L=0.015, T=6sec. (fixed and chain moored)

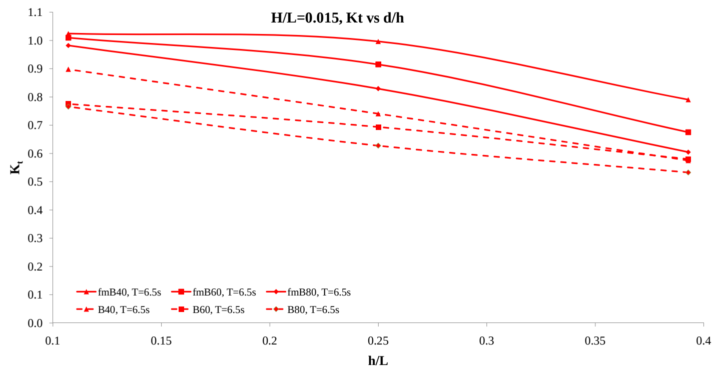

Figure 4.34: K_t vs d/h for H/L=0.015, T=6.5sec. fixed and chain moored)

CHAPTER 5

CONCLUSIONS and FUTURE RECOMMENDATIONS

In the present thesis, the performance of box type floating breakwaters with screens were examined experimentally under regular waves in a wave flume. The experiments were conducted in the Coastal and Harbor Engineering Laboratory wave flume, Civil Engineering Department, Middle East Technical University, Ankara. Experimental studies were carried out in three stages;

1. Calibration
2. Construction of floating model units
3. Experiments
   with fixed units
   with chain moored units

The influence of incident wave characteristics and certain geometric characteristics, such as the width and draft of the structure, on the efficiency of the floating units is examined in the wave steepness range H/L=0.015-0.045. Three different widths of the structure in combination with three different screen (draft) height, a total of eighteen different cases, of floating breakwaters as fixed (Case1 - Case9) and chain moored (Case10 - Case 18) are examined. Results related to transmission and reflection of the incident regular waves on the structure are presented in terms of dimensionless variables d/h and B/L for tested steepness ranges to show the effect of draft (d) and width (B) of the structure on transmission coefficient K_t and reflection coefficient K_r. Based on the experiments carried out for the given test ranges the following conclusions can be derived:

- For Case1 - Case 9
  - The experimental results of transmission coefficients have been compared with Macagno (1959) and Cox (1989) theoretical theories and the agreement is well especially with Cox (1989) theory.
  - For all structures drafts and structure widths, as h/L increase (wave period and wave height decreases) K_t values decrease.
  - As the draft increases the effect of structure width (B) becomes less significant.
  - It is seen that for increasing values of draft (d) from 1.5m to 5.5m, K_r values increase approximately between 0.4 and 0.7 for all B values.
  - As draft increases (increasing d/h values), the effect of B on K_t decreases. This decrease is more significant for smaller periods.
  - Increasing width of the structure causes an increase in reflection and a decrease in transmission resulting in reduced transmitted wave H_t and a higher reflected wave H_r.
  - Steepness increase from 0.015 to 0.025, does not significantly affect the transmission coefficient, K_t.
- For Case10 - Case 18
  - A fixed floating breakwater usually attenuates the waves better than a moored breakwater.
  - K_t values obtained for chain moored floating breakwaters are larger than the K_t values of fixed cases consistently.
  - Steepness increase from 0.015 to 0.025, does not significantly affect the transmission coefficient, K_t, and the reflection coefficient, K_r.
  - The results of wave periods T=4-4.5-5sec do not show a clear trend of d/h and B values on K_t coefficients.
  - For periods T=4.5-5sec minimum K_t values are observed ranging between 0.22-0.32 corresponds to d/h=0.26. Since the natural periods of the units tested are not coinciding with tested wave periods T=4.5-5sec. no further discussion could be carried out.

- For wave periods T=5.5-6-6.5sec, the K_t values decrease with the increasing d/h values.
- For small structure draft (d/h=0.11), K_t values range between 0.85-1.05 showing that floating breakwater is not effective on wave transmission for longer periods T larger than 6sec.
- For larger structure draft (d/h=0.39), K_t values range between 0.35-0.83, disregarding the K_t value obtained as 0.22 for B=12m (B80), it can be stated that increased draft decreases the K_t values.
- In general, larger structure width (B) values give smaller K_t values except for T=5.5sec for B=16m (B80) and for T=6.5sec. B=8m (B40).

Under the light of conclusions drawn from the series of tests carried experimentally on floating breakwaters the following recommendations can be made for future studies;

- Model experiments has to be carried out under irregular waves also.
- Wider range of wave periods and wave heights resulting in wider steepness ranges should be investigated.
- Further insight about the effects of mooring lines on the performance of floating breakwaters can be reached by conducting experiments with different mooring types with different chain weight and lengths.
- Natural periods of the floating units connected together has to be tested to make further discussions on the effectiveness of chain moored floating breakwaters.
- Overtopping observations can be made in order to investigate the effects of overtopping on the transmission and reflection from the floating structures.
- Finally, measuring force data from mooring lines and displacement data of the structure would add more depth to an experimental study carried out for investigating the performance of a floating breakwaters. Force measuring experiments has to be carried out on larger scale model units.

Using floating breakwaters economically might be feasible since construction cost is comparatively cheaper than the other type of breakwaters. However, effectiveness of floating breakwaters depends on wave climate and depth of construction. In the design of the floating breakwaters (Structure length, width and draft), mooring characteristics (Length, weight and strength of mooring lines) the effectiveness of the floating breakwater units must be experimentally tested under the given design conditions before finalizing the design.

REFERENCES

[1] Fousert, M.W. 2006. ”Floating Breakwaters. Theoretical study of a dynamic wave attenuating system”, M.Sc thesis, Delft University of Technology.

[2] Ruol, P. and Martinelli, L. 2007. Wave flume investigation on different mooring systems for floating breakwaters. Proc. Coastal Structure ’07, Venice

[3] Sogreah. 1978. Brise-lames floattant oscillant (Rapport d’Etude, Juillet).

[4] Carver, R.D. 1979. ”Floating breakwater wave attenuation tests for East Bay Marina, Olympia Harbor, Washington”, WES Technical Report HL-79-13, USA, WES.

[5] Gaithwaite, J. 1988. ”P.I.A.N.C - Bulletin No.63 Practical Aspects of Floating Breakwater Design”

[6] Hales, L.Z. 1981. ”Floating Breakwaters - State of the Art”, (CERC, Technical Report 81-1).

[7] Jones, D.B. 1978. ”An assesment of transportable breakwatrs with reference to container off loading and transfer system (COTS)”, (Technical Note no W1529 - USNCEL).

[8] Seymour, R.J. and Isaacs, J.D. 1974. ”Tethered float breakwaters”, Proceedings of Floating Breakwater Conference, University of Rhode Island, Kingston, RI.

[9] Syed, S. A. and Mani, J. S. 2008. ”Laboratory investigations on multiple pontoon floating breakwaters”, Proceedings of 7th International Conf. on Coastal and Port Eng. in Developing Countries, PIANC-COPEDEC VII, Dubai, UAE, Paper No.48

[10] Inoue, Y. and Zhang, X. 1996. ”Numerical study of the behavior of multiple floating breakwater”, Journal of the Kansai Society of Naval Architects, Japan, No.227(19970325) pp. 145-153

[11] Seymour, R.J. and Hanes, D.M. 1979. ”Performance analysis of tethered float breakwater”, Journal of Waterway, Port, Coastal, and Ocean Division.

[12] Western Canada Hydraulic Laboratories Ltd. 1981. ”Development of a Manual for the Design of a Floating Breakwater”, Department of Fisheries and Oceans.

[13] Georgiadis, C. and Hartz, B. J. 1983. ”Theory and Experiment for Response of Long Floating Structures”, Fourth International Symposium on Offshore Engineering.

[14] PIANC. 1994. ”Floating Breakwaters. A practical Guide for Design and Construction”, Report of Working Group no. 13 of the Permanent Technical Committee 2. 1-52 p. ISBN 2-97223-052-1

[15] McCartney, B. 1985. ”Floating breakwater design.” Journal of Waterway, Port, Coastal, and Ocean Engineering, Vol. 111, pp. 304-318.

[16] Silander, J. 1999. ”Floating Breakwaters and Environment”, PhD thesis, Helsinki University of Technology, Helsinki, Finland. 1999

[17] Sorensen, R M. 1991. ”Floating Breakwater for Small Recreational Harbors”, Journal of the Waterways, Harbors and Coastal Engineering Division. Discussion. July/Aug/ Vol. 117. No. 4, pp. 427 - 428

[18] ASCE Manuals and Reports on Engineering Practice. 1994. Planning and design - guidelines for Small Craft Harbors. No 50, pp-119-133. ISBN 0-7844-0033-4.

[19] Ouellet, Y., and Datta, I. 1996. ”A survey of wave absorbers”, Journal of Hydraulic Research, Vol 24, No. 4, pp 265-280.

[20] Hughes, S. A. 1993. Physical Models and Laboratory Techniques in Coastal Engineering, Advanced Series on Ocean Engineering - Volume 7, p.440.

[21] Danish Hydraulics Institute Power Pack and Servo Actuator, Technical Manual. 1991

[22] Havelock, T. H. 1929. ”Forced Surface wave on Water”, Philosophical Magazine, Series 7, Vol 8, pp. 569-576.

[23] Mansard, E. P. and Funke, E. R. 1988. ”Physical Experiments in Laboratories: Contrast of Methodologies and Results,” unpublished lecture notes for the Short Course on Planning and Designing Maritime Structures held prior to the 21st International Coastal Engineering Conference in Malaga, Spain.

[24] Goda, Y., 1985: Random Sea and Design of Maritime Structures. University of Tokyo Press, 323 pp.

[25] Koutandos, E., Prinos, P. and Gironella, X. 2005. ”Floating breakwaters under regular and irregular wave forcing : reflection and transmission characteristics”, Journal of Hydraulic Research, vol. 43, no2, pp. 174-188

[26] Hwang, C. and Tang, F.L.W. 1986. ”Studies on Rectangular Surface Barrier Against Short Waves”. Proceedings of 20th International Conference of Coastal Engineering. ASCE. 1915-1928

[27] Williams, A.N. and McDougal, W.G. 1991. ”Flexible Floating Breakwater”. Journal of Waterway, Port, Coastal, and Ocean Engineering. ASCE 117(5), 429-450.

[28] Drimer, N., Agnon,Y. and Stiassnie, M. 1992. ”A Simplified Analytical Model for a Floating Breakwater in Water of Finite Depth”. Appl. Ocean Res. 14, 33-41.

[29] Bhatta, D.D. and Rahman, M. 1993. ”Computational Methods and Experimental Measurements to a Floating Cylinder in Waves”. Proceedings of the Computational Modeling of Free and Moving Boundary Problems, pp. 395-402.

[30] Isaacson, M. and Bhat, S. 1998. ”Wave Propagation Past a Pile-restrained Floating Breakwater”. Int. J. Offshore Polar Engng. 8, 265-269.

[31] Williams, A.N., Lee, H.S. andHuang, Z. 2000. ”Floating Pontoon Breakwater”. Ocean Engng. 27, 221-240.

[32] Williams, A.N. and McDougal, W.G. 1996. ”A dynamic submerged Breakwater”. Journal of Waterway, Port, Coastal and Ocean Engineering. ASCE.

[33] Kriezi, E.E., Karambas, TH.V., Prinos, P. and Koutitas, C. 2001. ”Interaction of Floating Breakwaters with Waves in Shallow Waters”. Proceedings of the International Conference on IAHR 2001, Beijing, China, Vol. E, pp. 69-76.

[34] Isaacson, M. 1982. ”Non-linear Effects on Fixed and Floating Bodies”. J. Fluid Mech. 120, 267-281.

[35] Gottlieb, O. and Yim, S.C.S. 1995. ”Nonlinear Dynamics of a Coupled Surge Heave Small-body Ocean Mooring System”. Ocean Engng. 24(5), 479-495,

[36] Isaacson, M. and Bhat, S. 1998. ”Wave Propagation Past a Pile-restrained Floating Breakwater”. Int. J. Offshore Polar Engng. 8, 265-269.

[37] Sannasiraj, S.A., Sundar, V. and Sundaravadivelu, R. 1998. ”Mooring Forces and Motions Responses of Pontoon-type Floating Breakwaters”. Ocean. Engng. 25(1), 27-48.

[38] Isaacson, M. and Cheung, K.F. 1993. ”Time-Domain Solution for Wave-current Interactions with a Twodimensional Body”. Applied Ocean Res. 15,39-52.

[39] Isaacson, M. 1982. ”Fixed and Floating Axisymmetric Structures inWaves”. J.Waterway Port Coastal Ocean Div. ASCE 108(2), 180-199.

[40] Niwinski, C.T. and Isaacson,M. 1982. ”Non-linearWave Forces on Floating Breakwaters”. Proc. 18th Int. Conf. Coastal Engng. ASCE 2009-2025.

[41] Yamamoto, T. 1982. ”Moored Floating Breakwater Response to Regular and Irregular Waves”. In: Dynamic Analysis of Offshore Structures. Vol. 1, CML Publications, Southampton, pp. 114-123.

[42] Yamamoto, T.,Yoshiba,A. and Ijima, T. 1982. ”Dynamics of Elasticity Moored Floating Objects”. In: Dynamic Analysis of Offshore Structures. Vol. 1. CML Publications, Southampton, pp. 106-113.

[43] Yamamoto, T. and Yoshida, A. 1979. ”Large wave tank tests on taut-moored breakwaters”. Coastal structures ’79, Vol.II, ASCE.

[44] Nossen, J., Grue, J. and Palm, E. 1991. ”Wave Forces on Three-dimensional Floating Bodies with Small Forward Speed”. J. Fluid Mech. 227, 153-160.

[45] Isaacson, M. and Bhat, S. 1994. ”Wave Force on a Horizontal Plate”. Proceedings of the International SYmposium: An Waves-Physical and Numerical Modeling. pp. 1184-1190

[46] Yoon, G.S., Mastubara, Y. and Noda, H. 1994. ”Simplified Calculation Method for the Mooring Force of Marine Unit”. Proceedings of the International Symposium on Waves-Physical and Numerical Modeling. pp. 1277-1286.

[47] Sutko, A.A. and Haden, E.L. 1974. ”The Effect of Surge, Heave and Pitch on the Performance of a Floating Breakwater”. Proceedings of Floating Breakwater Conference, Rhode Island, pp. 41-53.

[48] Fugazza, M. and Natale, L. 1988. ”Energy Losses and Floating Breakwater Response”. J. Waterway Port Coastal Ocean Engng. ASCE 114, 191-205.

[49] Tolba, E.R.A.S. 1998. ”Behavior of Floating Breakwaters UnderWave Action”. PhD. Thesis, Suez Canal University.

[50] Isaacson, M. and Bhat, S. 1998. ”Wave Propagation Past a Pile-restrained Floating Breakwater”. Int. J. Offshore Polar Engng. 8, 265-269.

[51] Christian, C.D. 2000. ”Floating Breakwaters for Small Boat Marina Protection”. Proc. 27th Coastal Engng. Conf. 3, 2268-2277.

[52] Cox, J.C. 1989. ”Breakwater Attenuation Criteria and Specification for Marina Basins. In Marinas: Design and Operation”. Proceedings of the International Conference on Marinas, Southampton, UK. Computational Mechanics Publications, Southampton and Boston, pp. 139-155.

[53] Macagno, E. O. 1953. ”Experimental study of the effects of the passage of a wave beneath an obstacle”. Proceedings of Academie des Sciences, Paris.

[54] Wiegel, R. L. 1959. ”Rigid vertical thin barrier”. University of California.

APPENDIX A

RESULTS TABLES, FIGURES AND PHOTOS

The following tables are the results of the calibration experiments and the data analysis for nine cases described in Chapter 4. The photos of the piston type wave maker and an example photo showing the units in the wave flume is also presented in this appendix.

Table A.1: 20 Point Calibration Results

Inc. Dist	Gauge 1	Gauge 7	Gauge 16	Gauge 8	Gauge 6	Gauge 13	Gauge 15	Gauge 5	Gauge 14	Gauge 3	Gauge 2	Gauge 11
+10 cm	0.300941	0.387876	0.304872	0.303515	0.296899	0.024882	0.224528	0.401651	0.318045	0.776167	0.827171	0.277954
+9 cm	0.242501	0.309363	0.243593	0.241104	0.23758	0.027144	0.180906	0.31992	0.258078	0.61808	0.659457	0.221786
+8 cm	0.187654	0.236303	0.186433	0.183406	0.182173	0.026961	0.1383	0.244234	0.198548	0.470171	0.505101	0.168176
+7 cm	0.125406	0.152084	0.120699	0.116882	0.117935	0.027441	0.090789	0.156668	0.132641	0.304995	0.331822	0.108598
+6 cm	0.069092	0.077604	0.061699	0.056631	0.060866	0.026201	0.044794	0.078308	0.072367	0.156424	0.17458	0.054359
+5 cm	0.005237	0.004691	0.00164	0.00428	0.000378	0.039365	0.00065	0.009103	0.0088	0.011256	0.009186	0.002962
+4 cm	-0.05865	-0.07685	-0.05847	-0.0587	-0.05723	-0.00414	-0.07785	-0.07555	-0.05924	-0.15174	-0.15812	-0.04932
+3 cm	-0.10922	-0.14838	-0.11812	-0.11906	-0.115	0.036561	-0.09774	-0.15002	-0.1111	-0.29163	-0.30065	-0.10759
+2 cm	-0.16964	-0.22793	-0.17587	-0.17795	-0.16967	-0.00167	-0.17705	-0.2325	-0.17627	-0.45149	-0.47306	-0.15575
+1 cm	-0.22693	-0.30746	-0.24137	-0.2309	-0.23214	0.035832	-0.20376	-0.31648	-0.23539	-0.59916	-0.63267	-0.22056
SWL	-0.27769	-0.37949	-0.29705	-0.28824	-0.28392	0.03391	-0.24977	-0.3933	-0.28813	-0.74639	-0.77722	-0.27206
-1 cm	-0.33656	-0.45997	-0.35862	-0.35486	-0.34412	0.03173	-0.31406	-0.47874	-0.35078	-0.9022	-0.94581	-0.32899
-2 cm	-0.40156	-0.53758	-0.41755	-0.42438	-0.40253	-0.00439	-0.40005	-0.55459	-0.42003	-1.06444	-1.11533	-0.37818
-3 cm	-0.45591	-0.62121	-0.48475	-0.48642	-0.46423	0.030511	-0.43538	-0.64445	-0.47652	-1.21742	-1.27656	-0.4445
-4 cm	-0.52055	-0.69738	-0.54261	-0.55135	-0.52169	-0.00351	-0.5243	-0.72046	-0.54442	-1.38035	-1.44774	-0.49147
-5 cm	-0.57228	-0.78044	-0.60798	-0.61469	-0.58007	0.029141	-0.56092	-0.8079	-0.59949	-1.53463	-1.60637	-0.55684
-6 cm	-0.62753	-0.85893	-0.6669	-0.67653	-0.63841	0.027787	-0.62096	-0.88925	-0.65824	-1.68447	-1.76265	-0.61215
-7 cm	-0.68552	-0.9381	-0.72882	-0.73823	-0.69629	0.028781	-0.68831	-0.97102	-0.72	-1.84236	-1.92691	-0.6668
-8 cm	-0.75107	-1.02568	-0.79792	-0.80888	-0.76153	0.027506	-0.76493	-1.06203	-0.78839	-2.00948	-2.10706	-0.72891
-9 cm	-0.80278	-1.09681	-0.85209	-0.86412	-0.81308	0.027892	-0.82676	-1.13653	-0.84247	-2.14736	-2.25116	-0.77802
-10 cm	-0.86028	-1.1769	-0.91223	-0.92611	-0.87129	0.030076	-0.89858	-1.21803	-0.9051	-2.30107	-2.41692	-0.83313

Table A.2: 5 Point Calibration Results

Inc. Dist	Gauge 1	Gauge 2	Gauge 3	Gauge 5	Gauge 6	Gauge 7	Gauge 8	Gauge 11	Gauge 13	Gauge 14	Gauge 15
+10 cm	0.002993	0.005223	-0.00023	0.006562	-0.00062	0.004718	-0.00323	-0.00343	0.003836	-0.00128	0.002179
+5 cm	-0.28868	-0.81494	-0.7761	-0.38514	-0.29464	-0.37534	-0.30883	-0.27957	-0.30393	-0.27302	-0.30523
SWL	-0.57413	-1.61465	-1.52905	-0.76735	-0.58049	-0.75087	-0.61078	-0.55066	-0.60423	-0.57452	-0.60704
-5 cm	-0.86873	-2.42883	-2.29107	-1.15635	-0.87288	-1.13457	-0.92101	-0.82753	-0.91236	-0.92721	-0.91535
-10 cm	-1.15438	-3.23014	-3.038	-1.54362	-1.1616	-1.51506	-1.22616	-1.09844	-1.21484	-1.32406	-1.22122

Table A.3: 3 Point Calibration Results

Inc. Dist	Gauge 1	Gauge 2	Gauge 3	Gauge 5	Gauge 6	Gauge 7	Gauge 8	Gauge 11	Gauge 13	Gauge 14	Gauge 15
+10 cm	1.315538	0.868446	0.693276	0.714356	0.589952	0.662362	0.617436	0.571487	0.609681	0.611561	0.617056
SWL	0.000891	0.004649	0.002479	-0.00156	0.008497	0.005583	-0.0059	-0.00177	-0.00183	0.001461	-0.00128
-10 cm	-1.31569	-0.85909	-0.68128	-0.72308	-0.57147	-0.65844	-0.63014	-0.57309	-0.61039	-0.61332	-0.61455

Table A.4: Wave board stroke and frequencies to produce desired wave heights

Steepness	T_p (sec)	T_m (sec)	$L_{o(m)}$ (m)	$L_{(m)}$ (m)	$H_{o(p)}$ (m)	$H_{o(m)}$ (m)	K_s	$H_{(m)}$ (m)	k (2π/L)	H/h	kh	**S_0 (cm)**	**f (Hz)**
0.015	4.0	0.894	1.248	1.248	0.374	0.019	0.995	0.019	5.035	0.03	3.524	**9.442**	**1.118**
0.025	4.0	0.894	1.248	1.248	0.624	0.031	0.995	0.031	5.035	0.04	3.524	**15.736**	**1.118**
0.035	4.0	0.894	1.248	1.248	0.874	0.044	0.995	0.043	5.035	0.06	3.524	**22.031**	**1.118**
0.045	4.0	0.894	1.248	1.248	1.123	0.056	0.995	0.056	5.035	0.08	3.524	**28.325**	**1.118**
0.015	4.5	1.006	1.580	1.568	0.474	0.024	0.984	0.023	4.007	0.03	2.805	**12.221**	**0.994**
0.025	4.5	1.006	1.580	1.568	0.790	0.039	0.984	0.039	4.007	0.06	2.805	**20.368**	**0.994**
0.035	4.5	1.006	1.580	1.568	1.106	0.055	0.984	0.054	4.007	0.08	2.805	**28.515**	**0.994**
0.045	4.5	1.006	1.580	1.568	1.422	0.071	0.984	0.070	4.007	0.10	2.805	**36.662**	**0.994**
0.015	5.0	1.118	1.950	1.913	0.585	0.029	0.966	0.028	3.285	0.04	2.300	**15.755**	**0.894**
0.025	5.0	1.118	1.950	1.913	0.975	0.049	0.966	0.047	3.285	0.07	2.300	**26.259**	**0.894**
0.035	5.0	1.118	1.950	1.913	1.365	0.068	0.966	0.066	3.285	0.09	2.300	**36.763**	**0.894**
0.015	5.5	1.230	2.360	2.267	0.708	0.035	0.948	0.034	2.772	0.05	1.940	**20.279**	**0.813**
0.025	5.5	1.230	2.360	2.267	1.180	0.059	0.948	0.056	2.772	0.08	1.940	**33.799**	**0.813**
0.015	6.0	1.342	2.808	2.622	0.842	0.042	0.932	0.039	2.397	0.06	1.678	**25.982**	**0.745**
0.025	6.0	1.342	2.808	2.622	1.404	0.070	0.932	0.065	2.397	0.09	1.678	**43.304**	**0.745**
0.015	6.5	1.453	3.296	2.972	0.989	0.049	0.921	0.046	2.114	0.07	1.480	**33.025**	**0.688**
0.025	6.5	1.453	3.296	2.972	1.648	0.082	0.921	0.076	2.114	0.11	1.480	**55.042**	**0.688**

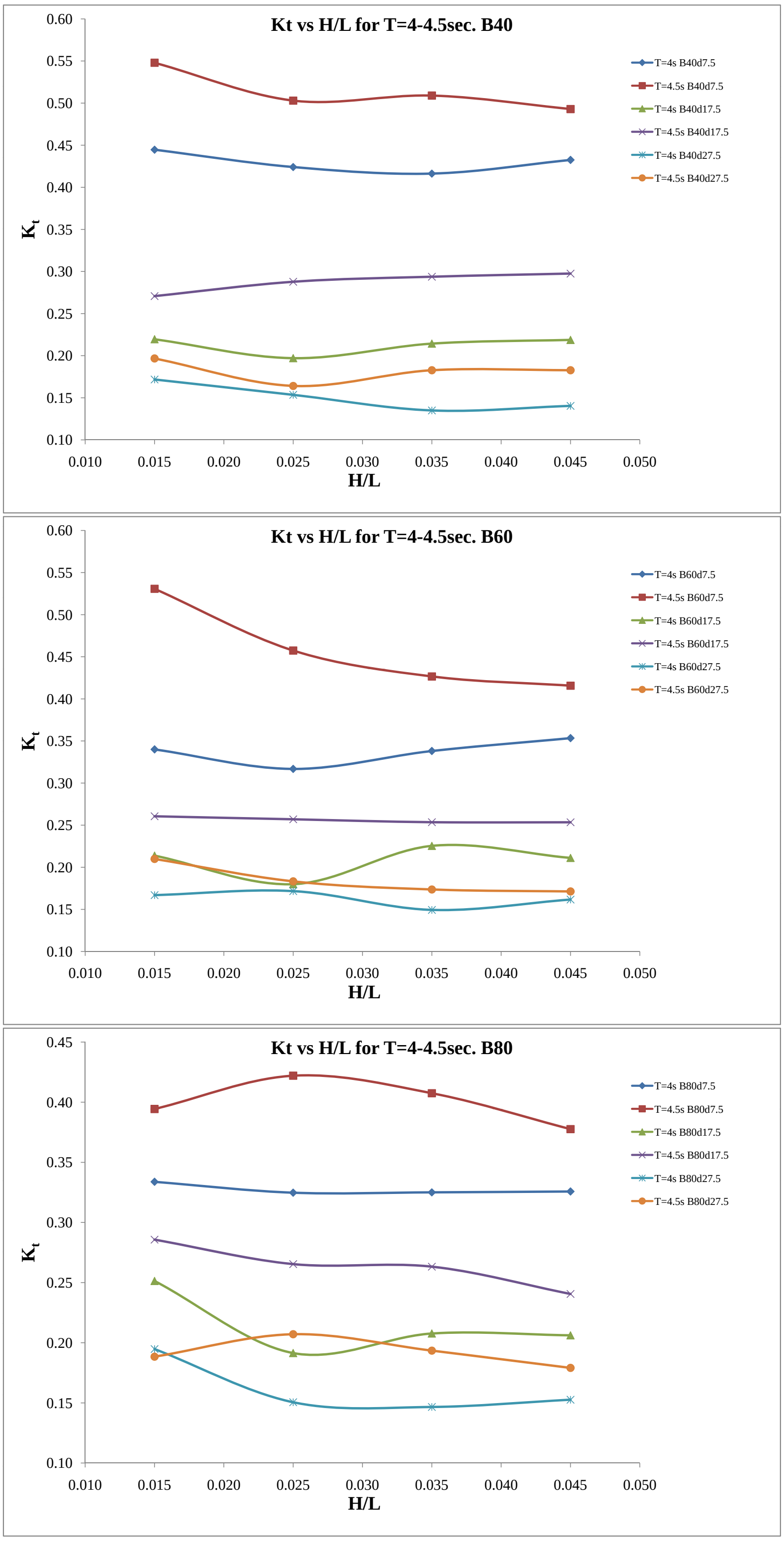

Figure A.1: K_t vs H/L for B=8-12-16m, T=4-4.5s

Table A.5: Wave board stroke and frequencies to produce desired wave heights

Steepness	T_p (sec)	T_m (sec)	$L_{o(m)}$ (m)	$L_{(m)}$ (m)	$H_{o(p)}$ (m)	$H_{o(m)}$ (m)	K_s	$H_{(m)}$ (m)	k (2π/L)	H/h	kh	S_0 (cm)	f (Hz)
0.015	4.0	0.894	1.248	1.248	0.374	0.019	0.995	0.019	5.035	0.03	3.524	**9.442**	**1.118**
0.025	4.0	0.894	1.248	1.248	0.624	0.031	0.995	0.031	5.035	0.04	3.524	**15.736**	**1.118**
0.035	4.0	0.894	1.248	1.248	0.874	0.044	0.995	0.043	5.035	0.06	3.524	**22.031**	**1.118**
0.045	4.0	0.894	1.248	1.248	1.123	0.056	0.995	0.056	5.035	0.08	3.524	**28.325**	**1.118**
0.015	4.5	1.006	1.580	1.568	0.474	0.024	0.984	0.023	4.007	0.03	2.805	**12.221**	**0.994**
0.025	4.5	1.006	1.580	1.568	0.790	0.039	0.984	0.039	4.007	0.06	2.805	**20.368**	**0.994**
0.035	4.5	1.006	1.580	1.568	1.106	0.055	0.984	0.054	4.007	0.08	2.805	**28.515**	**0.994**
0.045	4.5	1.006	1.580	1.568	1.422	0.071	0.984	0.070	4.007	0.10	2.805	**36.662**	**0.994**
0.015	5.0	1.118	1.950	1.913	0.585	0.029	0.966	0.028	3.285	0.04	2.300	**15.755**	**0.894**
0.025	5.0	1.118	1.950	1.913	0.975	0.049	0.966	0.047	3.285	0.07	2.300	**26.259**	**0.894**
0.035	5.0	1.118	1.950	1.913	1.365	0.068	0.966	0.066	3.285	0.09	2.300	**36.763**	**0.894**
0.015	5.5	1.230	2.360	2.267	0.708	0.035	0.948	0.034	2.772	0.05	1.940	**20.279**	**0.813**
0.025	5.5	1.230	2.360	2.267	1.180	0.059	0.948	0.056	2.772	0.08	1.940	**33.799**	**0.813**
0.015	6.0	1.342	2.808	2.622	0.842	0.042	0.932	0.039	2.397	0.06	1.678	**25.982**	**0.745**
0.025	6.0	1.342	2.808	2.622	1.404	0.070	0.932	0.065	2.397	0.09	1.678	**43.304**	**0.745**
0.015	6.5	1.453	3.296	2.972	0.989	0.049	0.921	0.046	2.114	0.07	1.480	**33.025**	**0.688**
0.025	6.5	1.453	3.296	2.972	1.648	0.082	0.921	0.076	2.114	0.11	1.480	**55.042**	**0.688**

Table A.6: Data Analysis Results for case 1 B40d7.5

B40d7.5			Gauge1	Gauge2	Gauge3	Gauge5	Gauge6	Gauge7	Gauge8	Gauge11	Gauge12	Gauge13	Gauge15	Gauge16	Results below are in model scale					
Period (prototype)	Steepness		1	2	3	4	5	6	7	8	9	10	11	12	$H_{m\ (mean)}$	K_r	H_I	H_R	K_t	H_t
4.0	0.015	H_m	0.006	0.025	0.007	0.008	0.012	0.007	0.021	0.022	0.020	0.016	0.026	0.015	0.02	0.65	0.02	0.01	0.44	0.01
4.0	0.025	H_m	0.010	0.038	0.011	0.012	0.020	0.012	0.032	0.035	0.033	0.026	0.039	0.023	0.02	0.65	0.03	0.02	0.42	0.01
4.0	0.035	H_m	0.014	0.054	0.014	0.016	0.027	0.016	0.045	0.048	0.045	0.036	0.054	0.030	0.03	0.64	0.04	0.03	0.42	0.01
4.0	0.045	H_m	0.017	0.068	0.018	0.020	0.035	0.020	0.056	0.062	0.057	0.045	0.066	0.037	0.04	0.63	0.05	0.03	0.43	0.02
4.5	0.015	H_m	0.010	0.028	0.011	0.009	0.032	0.010	0.013	0.012	0.027	0.019	0.028	0.032	0.02	0.56	0.02	0.01	0.55	0.01
4.5	0.025	H_m	0.017	0.045	0.018	0.015	0.050	0.015	0.023	0.019	0.043	0.030	0.047	0.051	0.03	0.57	0.03	0.02	0.50	0.02
4.5	0.035	H_m	0.023	0.065	0.024	0.020	0.070	0.020	0.034	0.029	0.060	0.044	0.067	0.071	0.04	0.56	0.04	0.02	0.51	0.02
4.5	0.045	H_m	0.027	0.082	0.029	0.025	0.085	0.024	0.048	0.039	0.075	0.054	0.085	0.085	0.05	0.55	0.06	0.03	0.49	0.03
5.0	0.015	H_m	0.015	0.033	0.015	0.013	0.033	0.013	0.026	0.024	0.029	0.021	0.035	0.034	0.02	0.53	0.03	0.01	0.60	0.01
5.0	0.025	H_m	0.024	0.058	0.024	0.022	0.056	0.022	0.039	0.039	0.049	0.034	0.059	0.056	0.04	0.53	0.04	0.02	0.59	0.02
5.0	0.035	H_m	0.032	0.083	0.033	0.031	0.078	0.030	0.057	0.055	0.068	0.049	0.084	0.078	0.06	0.52	0.06	0.03	0.57	0.03
5.5	0.015	H_m	0.018	0.028	0.019	0.019	0.021	0.019	0.037	0.038	0.034	0.018	0.028	0.020	0.03	0.48	0.03	0.01	0.70	0.02
5.5	0.025	H_m	0.032	0.051	0.032	0.034	0.036	0.033	0.066	0.067	0.058	0.031	0.050	0.034	0.04	0.49	0.05	0.03	0.71	0.03
6.0	0.015	H_m	0.027	0.042	0.026	0.026	0.046	0.027	0.029	0.031	0.036	0.020	0.040	0.045	0.03	0.42	0.03	0.01	0.82	0.03
6.0	0.025	H_m	0.044	0.069	0.043	0.044	0.077	0.045	0.047	0.051	0.060	0.035	0.066	0.074	0.06	0.44	0.05	0.02	0.81	0.04
6.5	0.015	H_m	0.031	0.028	0.031	0.033	0.031	0.031	0.039	0.039	0.040	0.030	0.029	0.030	0.03	0.39	0.03	0.01	0.90	0.03
6.5	0.025	H_m	0.052	0.047	0.053	0.052	0.051	0.051	0.067	0.064	0.066	0.047	0.048	0.051	0.05	0.41	0.05	0.02	0.87	0.05

Table A.7: Data Analysis Results for case 3 B40d17.5

B40d17.5			Gauge1	Gauge2	Gauge3	Gauge5	Gauge6	Gauge7	Gauge8	Gauge11	Gauge12	Gauge13	Gauge15	Gauge16	Results below are in model scale					
Period (prototype)	Steepness		1	2	3	4	5	6	7	8	9	10	11	12	$H_{m\ (mean)}$	K_r	H_I	H_R	K_t	H_t
4.0	0.015	H_m	0.004	0.023	0.004	0.004	0.010	0.004	0.022	0.024	0.020	0.016	0.025	0.011	0.01	0.72	0.02	0.01	0.22	0.00
4.0	0.025	H_m	0.005	0.037	0.006	0.006	0.016	0.006	0.039	0.039	0.032	0.028	0.039	0.017	0.02	0.71	0.03	0.02	0.20	0.01
4.0	0.035	H_m	0.007	0.051	0.008	0.008	0.020	0.008	0.052	0.053	0.043	0.037	0.053	0.023	0.03	0.70	0.04	0.03	0.21	0.01
4.0	0.045	H_m	0.009	0.065	0.009	0.010	0.025	0.010	0.065	0.069	0.055	0.046	0.064	0.029	0.04	0.70	0.05	0.04	0.22	0.01
4.5	0.015	H_m	0.004	0.028	0.005	0.006	0.027	0.005	0.010	0.015	0.025	0.016	0.025	0.026	0.02	0.65	0.02	0.01	0.27	0.00
4.5	0.025	H_m	0.008	0.046	0.009	0.009	0.045	0.009	0.022	0.026	0.040	0.030	0.046	0.047	0.03	0.65	0.03	0.02	0.29	0.01
4.5	0.035	H_m	0.011	0.070	0.013	0.013	0.067	0.013	0.034	0.035	0.059	0.045	0.071	0.069	0.04	0.62	0.04	0.03	0.29	0.01
4.5	0.045	H_m	0.015	0.088	0.017	0.016	0.086	0.015	0.050	0.044	0.073	0.057	0.093	0.087	0.05	0.61	0.06	0.03	0.30	0.02
5.0	0.015	H_m	0.010	0.036	0.010	0.009	0.033	0.010	0.028	0.027	0.029	0.023	0.037	0.033	0.02	0.59	0.03	0.02	0.42	0.01
5.0	0.025	H_m	0.016	0.061	0.017	0.015	0.054	0.016	0.047	0.045	0.047	0.036	0.062	0.053	0.04	0.59	0.05	0.03	0.41	0.02
5.0	0.035	H_m	0.022	0.083	0.022	0.021	0.076	0.021	0.066	0.065	0.065	0.052	0.086	0.075	0.05	0.57	0.06	0.04	0.39	0.02
5.5	0.015	H_m	0.015	0.027	0.015	0.015	0.020	0.015	0.041	0.040	0.035	0.018	0.027	0.018	0.02	0.56	0.03	0.02	0.56	0.02
5.5	0.025	H_m	0.025	0.044	0.025	0.025	0.031	0.024	0.066	0.065	0.057	0.027	0.044	0.029	0.04	0.55	0.05	0.03	0.54	0.02
6.0	0.015	H_m	0.022	0.045	0.022	0.022	0.047	0.023	0.032	0.033	0.036	0.022	0.044	0.047	0.03	0.51	0.03	0.02	0.70	0.02
6.0	0.025	H_m	0.036	0.074	0.035	0.035	0.080	0.036	0.053	0.056	0.059	0.036	0.072	0.078	0.06	0.48	0.06	0.03	0.65	0.03
6.5	0.015	H_m	0.026	0.026	0.027	0.026	0.032	0.026	0.036	0.035	0.039	0.031	0.026	0.031	0.03	0.46	0.03	0.01	0.74	0.03
6.5	0.025	H_m	0.042	0.044	0.044	0.042	0.054	0.042	0.061	0.058	0.064	0.049	0.044	0.053	0.05	0.44	0.05	0.02	0.70	0.04

Table A.8: Data Analysis Results for case 3 B40d27.5

B40d27.5			Gauge1	Gauge2	Gauge3	Gauge5	Gauge6	Gauge7	Gauge8	Gauge11	Gauge12	Gauge13	Gauge15	Gauge16	Results below are in model scale					
Period (prototype)	Steepness		1	2	3	4	5	6	7	8	9	10	11	12	$H_{m\ (mean)}$	K_r	H_I	H_R	K_t	H_t
4.0	0.015	H_m	0.002	0.021	0.003	0.003	0.009	0.003	0.026	0.024	0.019	0.017	0.024	0.010	0.01	0.74	0.02	0.01	0.17	0.00
4.0	0.025	H_m	0.003	0.033	0.003	0.005	0.012	0.005	0.038	0.038	0.030	0.024	0.036	0.015	0.02	0.72	0.03	0.02	0.15	0.00
4.0	0.035	H_m	0.004	0.047	0.004	0.006	0.017	0.006	0.054	0.054	0.042	0.038	0.049	0.021	0.03	0.72	0.04	0.03	0.13	0.00
4.0	0.045	H_m	0.005	0.060	0.005	0.007	0.023	0.007	0.067	0.069	0.055	0.047	0.061	0.028	0.04	0.71	0.05	0.04	0.14	0.01
4.5	0.015	H_m	0.003	0.029	0.004	0.004	0.029	0.004	0.016	0.015	0.026	0.020	0.030	0.030	0.02	0.68	0.02	0.01	0.20	0.00
4.5	0.025	H_m	0.006	0.047	0.007	0.004	0.046	0.005	0.027	0.025	0.040	0.030	0.050	0.048	0.03	0.68	0.03	0.02	0.16	0.01
4.5	0.035	H_m	0.008	0.069	0.009	0.007	0.066	0.008	0.040	0.036	0.057	0.045	0.072	0.067	0.04	0.66	0.04	0.03	0.18	0.01
4.5	0.045	H_m	0.009	0.091	0.011	0.009	0.085	0.009	0.053	0.048	0.073	0.057	0.096	0.087	0.05	0.65	0.06	0.04	0.18	0.01
5.0	0.015	H_m	0.007	0.038	0.007	0.006	0.034	0.007	0.030	0.032	0.029	0.020	0.038	0.033	0.02	0.65	0.03	0.02	0.29	0.01
5.0	0.025	H_m	0.010	0.059	0.010	0.011	0.052	0.010	0.050	0.048	0.045	0.033	0.062	0.050	0.04	0.64	0.04	0.03	0.27	0.01
5.0	0.035	H_m	0.015	0.088	0.015	0.015	0.076	0.016	0.070	0.072	0.065	0.052	0.090	0.075	0.05	0.62	0.07	0.04	0.27	0.01
5.5	0.015	H_m	0.010	0.024	0.011	0.011	0.016	0.011	0.039	0.040	0.035	0.019	0.024	0.016	0.02	0.62	0.03	0.02	0.40	0.01
5.5	0.025	H_m	0.015	0.038	0.016	0.018	0.029	0.018	0.065	0.063	0.055	0.030	0.039	0.026	0.03	0.61	0.04	0.03	0.38	0.02
6.0	0.015	H_m	0.016	0.048	0.018	0.018	0.049	0.018	0.033	0.036	0.036	0.022	0.046	0.049	0.03	0.57	0.04	0.02	0.57	0.02
6.0	0.025	H_m	0.025	0.077	0.025	0.027	0.081	0.027	0.054	0.057	0.059	0.030	0.072	0.082	0.05	0.55	0.06	0.03	0.49	0.03
6.5	0.015	H_m	0.021	0.025	0.022	0.019	0.031	0.021	0.032	0.031	0.038	0.031	0.025	0.032	0.03	0.51	0.03	0.01	0.57	0.02
6.5	0.025	H_m	0.033	0.038	0.034	0.033	0.054	0.033	0.056	0.053	0.062	0.049	0.038	0.053	0.04	0.56	0.04	0.02	0.56	0.03

Table A.9: Data Analysis Results for case 4 B60d7.5

B60d7.5			Gauge1	Gauge2	Gauge3	Gauge5	Gauge6	Gauge7	Gauge8	Gauge11	Gauge12	Gauge13	Gauge15	Gauge16	Results below are in model scale					
Period (prototype)	Steepness		1	2	3	4	5	6	7	8	9	10	11	12	$H_{m\ (mean)}$	K_r	H_I	H_R	K_t	H_t
4.0	0.015	H_m	0.004	0.023	0.005	0.006	0.011	0.006	0.021	0.022	0.019	0.017	0.025	0.014	0.01	0.67	0.02	0.01	0.34	0.01
4.0	0.025	H_m	0.008	0.039	0.007	0.010	0.019	0.008	0.035	0.038	0.032	0.027	0.041	0.022	0.02	0.67	0.03	0.02	0.32	0.01
4.0	0.035	H_m	0.011	0.053	0.011	0.013	0.023	0.011	0.048	0.052	0.044	0.036	0.053	0.028	0.03	0.66	0.04	0.03	0.34	0.01
4.0	0.045	H_m	0.014	0.068	0.015	0.016	0.033	0.014	0.058	0.065	0.055	0.044	0.064	0.036	0.04	0.63	0.05	0.03	0.35	0.02
4.5	0.015	H_m	0.009	0.030	0.010	0.010	0.032	0.009	0.011	0.013	0.026	0.017	0.028	0.030	0.02	0.64	0.02	0.01	0.53	0.01
4.5	0.025	H_m	0.015	0.052	0.015	0.014	0.055	0.015	0.024	0.023	0.044	0.034	0.050	0.053	0.03	0.60	0.03	0.02	0.46	0.01
4.5	0.035	H_m	0.019	0.068	0.019	0.018	0.069	0.019	0.037	0.029	0.059	0.047	0.071	0.071	0.04	0.59	0.04	0.03	0.43	0.02
4.5	0.045	H_m	0.023	0.086	0.024	0.021	0.088	0.022	0.050	0.043	0.073	0.055	0.091	0.089	0.06	0.59	0.06	0.03	0.42	0.02
5.0	0.015	H_m	0.013	0.035	0.013	0.012	0.034	0.012	0.027	0.024	0.029	0.020	0.037	0.035	0.02	0.59	0.03	0.02	0.54	0.01
5.0	0.025	H_m	0.021	0.059	0.022	0.020	0.056	0.020	0.046	0.043	0.048	0.036	0.063	0.058	0.04	0.58	0.05	0.03	0.54	0.02
5.0	0.035	H_m	0.028	0.084	0.027	0.026	0.078	0.027	0.063	0.062	0.066	0.049	0.087	0.076	0.06	0.55	0.06	0.04	0.49	0.03
5.5	0.015	H_m	0.017	0.028	0.017	0.017	0.020	0.018	0.041	0.040	0.035	0.016	0.029	0.019	0.02	0.54	0.03	0.02	0.61	0.02
5.5	0.025	H_m	0.027	0.048	0.027	0.027	0.033	0.028	0.068	0.067	0.058	0.030	0.049	0.031	0.04	0.54	0.05	0.03	0.62	0.03
6.0	0.015	H_m	0.024	0.044	0.024	0.024	0.048	0.024	0.031	0.032	0.036	0.020	0.042	0.047	0.03	0.50	0.03	0.02	0.77	0.02
6.0	0.025	H_m	0.038	0.074	0.037	0.037	0.081	0.039	0.052	0.055	0.061	0.035	0.073	0.079	0.05	0.48	0.06	0.03	0.69	0.04
6.5	0.015	H_m	0.028	0.027	0.029	0.027	0.032	0.028	0.038	0.037	0.039	0.029	0.026	0.031	0.03	0.47	0.03	0.01	0.78	0.03
6.5	0.,025	H_m	0.046	0.043	0.050	0.049	0.051	0.046	0.062	0.061	0.065	0.048	0.043	0.051	0.05	0.47	0.05	0.02	0.82	0.05

Table A.10: Data Analysis Results for unit case 5 B60d17.5

B60d17.5			Gauge1	Gauge2	Gauge3	Gauge5	Gauge6	Gauge7	Gauge8	Gauge11	Gauge12	Gauge13	Gauge15	Gauge16	Results below are in model scale					
Period (prototype)	Steepness		1	2	3	4	5	6	7	8	9	10	11	12	$H_{m\,(mean)}$	K_r	H_I	H_R	K_t	H_t
4.0	0.015	H_m	0.003	0.022	0.004	0.004	0.010	0.004	0.023	0.024	0.020	0.016	0.024	0.012	0.01	0.70	0.02	0.01	0.21	0.00
4.0	0.025	H_m	0.004	0.035	0.004	0.006	0.015	0.005	0.040	0.041	0.032	0.027	0.038	0.017	0.02	0.72	0.03	0.02	0.18	0.00
4.0	0.035	H_m	0.006	0.049	0.006	0.008	0.019	0.007	0.053	0.055	0.043	0.037	0.050	0.021	0.03	0.70	0.04	0.03	0.23	0.01
4.0	0.045	H_m	0.007	0.066	0.009	0.010	0.024	0.009	0.069	0.073	0.056	0.045	0.065	0.029	0.04	0.71	0.05	0.04	0.21	0.01
4.5	0.015	H_m	0.005	0.027	0.006	0.004	0.027	0.005	0.015	0.014	0.025	0.017	0.030	0.030	0.02	0.75	0.02	0.01	0.26	0.00
4.5	0.025	H_m	0.009	0.050	0.009	0.008	0.051	0.007	0.028	0.024	0.043	0.032	0.053	0.052	0.03	0.65	0.03	0.02	0.26	0.01
4.5	0.035	H_m	0.012	0.071	0.012	0.010	0.069	0.010	0.040	0.037	0.059	0.046	0.074	0.069	0.04	0.63	0.05	0.03	0.25	0.01
4.5	0.045	H_m	0.015	0.090	0.016	0.012	0.086	0.013	0.052	0.047	0.073	0.057	0.096	0.089	0.05	0.64	0.06	0.04	0.25	0.01
5.0	0.015	H_m	0.009	0.037	0.009	0.009	0.034	0.008	0.030	0.028	0.029	0.024	0.039	0.034	0.02	0.65	0.03	0.02	0.38	0.01
5.0	0.025	H_m	0.015	0.062	0.014	0.014	0.056	0.014	0.051	0.048	0.048	0.038	0.065	0.056	0.04	0.63	0.05	0.03	0.36	0.01
5.0	0.035	H_m	0.019	0.087	0.020	0.019	0.076	0.019	0.069	0.067	0.067	0.052	0.090	0.076	0.06	0.62	0.07	0.04	0.35	0.02
5.5	0.015	H_m	0.013	0.025	0.013	0.014	0.017	0.014	0.040	0.041	0.036	0.020	0.026	0.016	0.02	0.61	0.03	0.02	0.49	0.01
5.5	0.025	H_m	0.020	0.043	0.021	0.022	0.030	0.021	0.068	0.067	0.057	0.033	0.043	0.024	0.04	0.61	0.05	0.03	0.47	0.02
6.0	0.015	H_m	0.020	0.048	0.020	0.020	0.051	0.021	0.034	0.037	0.037	0.024	0.047	0.049	0.03	0.55	0.04	0.02	0.64	0.02
6.0	0.025	H_m	0.032	0.078	0.030	0.032	0.083	0.033	0.056	0.059	0.061	0.036	0.077	0.082	0.06	0.55	0.06	0.03	0.58	0.03
6.5	0.015	H_m	0.023	0.025	0.025	0.025	0.032	0.023	0.033	0.034	0.039	0.032	0.024	0.032	0.03	0.54	0.03	0.01	0.69	0.02
6.5	0.,025	H_m	0.039	0.044	0.041	0.041	0.055	0.040	0.062	0.056	0.065	0.053	0.042	0.054	0.05	0.53	0.05	0.02	0.67	0.04

Table A.11: Data Analysis Results for unit case 6 B60d27.5

B60d27.5			Gauge1	Gauge2	Gauge3	Gauge5	Gauge6	Gauge7	Gauge8	Gauge11	Gauge12	Gauge13	Gauge15	Gauge16	Results below are in model scale					
Period (prototype)	Steepness		1	2	3	4	5	6	7	8	9	10	11	12	$H_{m\ (mean)}$	K_r	H_I	H_R	K_t	H_t
4.0	0.015	H_m	0.002	0.021	0.003	0.003	0.009	0.003	0.024	0.024	0.019	0.016	0.023	0.009	0.01	0.74	0.02	0.01	0.17	0.00
4.0	0.025	H_m	0.003	0.034	0.005	0.005	0.013	0.005	0.040	0.041	0.032	0.027	0.037	0.016	0.02	0.73	0.03	0.02	0.17	0.00
4.0	0.035	H_m	0.003	0.048	0.005	0.007	0.018	0.005	0.055	0.056	0.044	0.036	0.051	0.022	0.03	0.72	0.04	0.03	0.15	0.01
4.0	0.045	H_m	0.005	0.062	0.006	0.008	0.024	0.007	0.067	0.071	0.055	0.044	0.061	0.029	0.04	0.72	0.05	0.04	0.16	0.01
4.5	0.015	H_m	0.005	0.033	0.005	0.003	0.034	0.003	0.017	0.015	0.027	0.024	0.036	0.037	0.02	0.73	0.02	0.01	0.21	0.00
4.5	0.025	H_m	0.007	0.049	0.008	0.004	0.047	0.005	0.029	0.026	0.041	0.032	0.051	0.049	0.03	0.67	0.03	0.02	0.18	0.01
4.5	0.035	H_m	0.009	0.071	0.009	0.005	0.067	0.006	0.043	0.036	0.059	0.046	0.077	0.070	0.04	0.67	0.05	0.03	0.17	0.01
4.5	0.045	H_m	0.011	0.091	0.013	0.006	0.086	0.008	0.056	0.049	0.074	0.058	0.096	0.087	0.05	0.66	0.06	0.04	0.17	0.01
5.0	0.015	H_m	0.007	0.039	0.007	0.007	0.033	0.006	0.033	0.031	0.029	0.022	0.040	0.034	0.02	0.66	0.03	0.02	0.27	0.01
5.0	0.025	H_m	0.010	0.063	0.010	0.011	0.055	0.010	0.053	0.051	0.048	0.039	0.065	0.054	0.04	0.65	0.05	0.03	0.26	0.01
5.0	0.035	H_m	0.015	0.090	0.015	0.014	0.077	0.014	0.075	0.073	0.067	0.053	0.092	0.077	0.06	0.64	0.07	0.04	0.26	0.01
5.5	0.015	H_m	0.009	0.024	0.010	0.011	0.017	0.011	0.041	0.040	0.035	0.020	0.024	0.015	0.02	0.65	0.03	0.02	0.38	0.01
5.5	0.025	H_m	0.015	0.039	0.016	0.018	0.030	0.017	0.068	0.066	0.058	0.036	0.040	0.028	0.04	0.63	0.04	0.03	0.36	0.02
6.0	0.015	H_m	0.015	0.049	0.015	0.016	0.051	0.017	0.036	0.038	0.038	0.024	0.049	0.051	0.03	0.59	0.04	0.02	0.50	0.02
6.0	0.025	H_m	0.024	0.079	0.024	0.025	0.082	0.025	0.059	0.061	0.062	0.040	0.078	0.078	0.05	0.56	0.06	0.03	0.46	0.02
6.5	0.015	H_m	0.020	0.024	0.021	0.021	0.035	0.020	0.032	0.031	0.039	0.033	0.024	0.034	0.03	0.58	0.02	0.01	0.58	0.02
6.5	0.,025	H_m	0.032	0.044	0.032	0.032	0.059	0.031	0.055	0.053	0.064	0.055	0.042	0.059	0.05	0.55	0.04	0.02	0.53	0.03

Table A.12: Data Analysis Results for unit case 7 B80d7.5

B80d7.5			Gauge1	Gauge2	Gauge3	Gauge5	Gauge6	Gauge7	Gauge8	Gauge11	Gauge12	Gauge13	Gauge15	Gauge16	Results below are in model scale					
Period (prototype)	Steepness		1	2	3	4	5	6	7	8	9	10	11	12	$H_{m\ (mean)}$	K_r	H_I	H_R	K_t	H_t
4.0	0.015	H_m	0.004	0.026	0.005	0.006	0.018	0.006	0.014	0.016	0.021	0.014	0.027	0.020	0.01	0.67	0.02	0.01	0.33	0.01
4.0	0.025	H_m	0.007	0.044	0.008	0.010	0.030	0.009	0.023	0.026	0.035	0.022	0.043	0.032	0.02	0.67	0.03	0.02	0.32	0.01
4.0	0.035	H_m	0.010	0.061	0.010	0.013	0.043	0.011	0.032	0.036	0.048	0.030	0.059	0.043	0.03	0.64	0.04	0.03	0.33	0.01
4.0	0.045	H_m	0.012	0.080	0.013	0.015	0.056	0.013	0.040	0.045	0.060	0.039	0.074	0.053	0.04	0.63	0.05	0.03	0.33	0.01
4.5	0.015	H_m	0.005	0.025	0.007	0.009	0.031	0.008	0.015	0.012	0.026	0.017	0.022	0.030	0.02	0.61	0.02	0.01	0.39	0.01
4.5	0.025	H_m	0.012	0.044	0.013	0.014	0.056	0.013	0.023	0.021	0.044	0.030	0.040	0.052	0.03	0.64	0.03	0.02	0.42	0.01
4.5	0.035	H_m	0.017	0.059	0.018	0.017	0.074	0.017	0.030	0.028	0.062	0.044	0.060	0.077	0.04	0.63	0.04	0.02	0.41	0.02
4.5	0.045	H_m	0.020	0.074	0.021	0.020	0.093	0.020	0.036	0.036	0.078	0.053	0.078	0.098	0.05	0.62	0.05	0.03	0.38	0.02
5.0	0.015	H_m	0.011	0.036	0.011	0.011	0.038	0.010	0.022	0.019	0.031	0.021	0.038	0.039	0.02	0.63	0.02	0.01	0.48	0.01
5.0	0.025	H_m	0.019	0.059	0.018	0.017	0.062	0.018	0.036	0.034	0.050	0.035	0.062	0.064	0.04	0.63	0.04	0.03	0.47	0.02
5.0	0.035	H_m	0.026	0.083	0.025	0.025	0.087	0.025	0.052	0.051	0.069	0.049	0.085	0.090	0.06	0.63	0.06	0.04	0.46	0.02
5.5	0.015	H_m	0.015	0.032	0.015	0.015	0.023	0.015	0.044	0.042	0.034	0.016	0.033	0.022	0.03	0.62	0.03	0.02	0.54	0.01
5.5	0.025	H_m	0.025	0.057	0.025	0.025	0.040	0.025	0.075	0.075	0.060	0.027	0.058	0.039	0.04	0.58	0.06	0.03	0.56	0.03
6.0	0.015	H_m	0.021	0.044	0.019	0.021	0.049	0.021	0.024	0.028	0.035	0.019	0.041	0.048	0.03	0.56	0.03	0.02	0.64	0.02
6.0	0.025	H_m	0.035	0.072	0.035	0.035	0.082	0.036	0.042	0.047	0.061	0.036	0.069	0.081	0.05	0.56	0.05	0.03	0.66	0.03
6.5	0.015	H_m	0.027	0.025	0.027	0.028	0.027	0.026	0.041	0.041	0.040	0.026	0.027	0.024	0.03	0.53	0.03	0.02	0.77	0.03
6.5	0.025	H_m	0.034	0.037	0.036	0.037	0.046	0.034	0.065	0.062	0.063	0.068	0.039	0.045	0.05	0.57	0.04	0.03	0.60	0.04

Table A.13: Data Analysis Results for unit case 8 B80d17.5

B80d17.5			Gauge1	Gauge2	Gauge3	Gauge5	Gauge6	Gauge7	Gauge8	Gauge11	Gauge12	Gauge13	Gauge15	Gauge16	Results below are in model scale					
Period (prototype)	Steepness		1	2	3	4	5	6	7	8	9	10	11	12	$H_{m\ (mean)}$	K_r	H_I	H_R	K_t	H_t
4.0	0.015	H_m	0.004	0.027	0.004	0.004	0.017	0.004	0.017	0.018	0.021	0.021	0.029	0.019	0.02	0.73	0.02	0.01	0.25	0.00
4.0	0.025	H_m	0.004	0.042	0.005	0.006	0.026	0.005	0.026	0.030	0.035	0.035	0.043	0.029	0.02	0.70	0.03	0.02	0.19	0.01
4.0	0.035	H_m	0.005	0.060	0.006	0.009	0.037	0.006	0.037	0.042	0.049	0.049	0.059	0.038	0.03	0.70	0.04	0.03	0.21	0.01
4.0	0.045	H_m	0.006	0.079	0.008	0.010	0.048	0.008	0.046	0.051	0.061	0.062	0.077	0.049	0.04	0.69	0.05	0.03	0.21	0.01
4.5	0.015	H_m	0.005	0.026	0.006	0.006	0.031	0.005	0.011	0.010	0.027	0.028	0.027	0.033	0.02	0.68	0.02	0.01	0.29	0.01
4.5	0.025	H_m	0.008	0.042	0.009	0.008	0.050	0.008	0.018	0.014	0.044	0.047	0.045	0.053	0.03	0.69	0.02	0.02	0.27	0.01
4.5	0.035	H_m	0.011	0.058	0.012	0.011	0.069	0.011	0.025	0.021	0.061	0.065	0.064	0.075	0.04	0.66	0.04	0.02	0.26	0.01
4.5	0.045	H_m	0.013	0.074	0.014	0.013	0.086	0.012	0.034	0.030	0.075	0.079	0.081	0.093	0.05	0.64	0.05	0.03	0.24	0.01
5.0	0.015	H_m	0.009	0.038	0.009	0.008	0.039	0.008	0.022	0.023	0.031	0.030	0.037	0.038	0.02	0.65	0.02	0.02	0.36	0.01
5.0	0.025	H_m	0.014	0.060	0.013	0.013	0.060	0.013	0.039	0.038	0.050	0.050	0.063	0.063	0.04	0.65	0.04	0.03	0.33	0.01
5.0	0.035	H_m	0.018	0.086	0.019	0.017	0.083	0.017	0.054	0.055	0.069	0.072	0.087	0.086	0.06	0.64	0.06	0.04	0.32	0.02
5.5	0.015	H_m	0.012	0.032	0.012	0.012	0.020	0.012	0.044	0.045	0.035	0.023	0.032	0.019	0.02	0.66	0.03	0.02	0.44	0.01
5.5	0.025	H_m	0.018	0.050	0.020	0.020	0.032	0.019	0.072	0.072	0.059	0.043	0.054	0.033	0.04	0.63	0.05	0.03	0.43	0.02
6.0	0.015	H_m	0.017	0.044	0.016	0.017	0.050	0.018	0.028	0.031	0.037	0.028	0.043	0.050	0.03	0.59	0.03	0.02	0.54	0.02
6.0	0.025	H_m	0.028	0.074	0.028	0.029	0.083	0.028	0.046	0.050	0.057	0.050	0.072	0.082	0.05	0.61	0.05	0.03	0.52	0.03
6.5	0.015	H_m	0.021	0.020	0.023	0.023	0.028	0.022	0.039	0.038	0.039	0.041	0.023	0.027	0.03	0.56	0.03	0.02	0.63	0.02
6.5	0.025	H_m	0.034	0.037	0.036	0.037	0.046	0.034	0.065	0.062	0.063	0.068	0.039	0.045	0.05	0.57	0.04	0.03	0.60	0.04

Table A.14: Data Analysis Results for unit case 9 B80d27.5

B80d27.5			Gauge1	Gauge2	Gauge3	Gauge5	Gauge6	Gauge7	Gauge8	Gauge11	Gauge12	Gauge13	Gauge15	Gauge16	Results below are in model scale					
Period (prototype)	Steepness		1	2	3	4	5	6	7	8	9	10	11	12	$H_{m\,(mean)}$	K_r	H_I	H_R	K_t	H_t
4.0	0.015	H_m	0.002	0.025	0.003	0.004	0.016	0.003	0.017	0.018	0.020	0.013	0.027	0.018	0.01	0.70	0.02	0.01	0.19	0.00
4.0	0.025	H_m	0.001	0.042	0.003	0.006	0.026	0.004	0.028	0.029	0.033	0.024	0.045	0.029	0.02	0.72	0.03	0.02	0.15	0.00
4.0	0.035	H_m	0.002	0.058	0.004	0.008	0.036	0.005	0.036	0.040	0.045	0.032	0.060	0.038	0.03	0.71	0.04	0.03	0.15	0.01
4.0	0.045	H_m	0.003	0.077	0.005	0.010	0.046	0.007	0.046	0.051	0.058	0.040	0.075	0.047	0.04	0.71	0.05	0.04	0.15	0.01
4.5	0.015	H_m	0.004	0.024	0.004	0.003	0.028	0.004	0.011	0.008	0.026	0.018	0.026	0.031	0.02	0.70	0.01	0.01	0.19	0.00
4.5	0.025	H_m	0.005	0.045	0.008	0.006	0.051	0.007	0.017	0.013	0.044	0.033	0.046	0.055	0.03	0.71	0.02	0.02	0.21	0.01
4.5	0.035	H_m	0.008	0.064	0.009	0.008	0.072	0.009	0.023	0.018	0.060	0.046	0.066	0.066	0.04	0.69	0.04	0.02	0.19	0.01
4.5	0.045	H_m	0.008	0.087	0.011	0.009	0.102	0.011	0.023	0.013	0.085	0.064	0.094	0.097	0.05	0.79	0.04	0.03	0.18	0.01
5.0	0.015	H_m	0.007	0.038	0.006	0.006	0.036	0.006	0.026	0.025	0.030	0.022	0.038	0.030	0.02	0.70	0.03	0.02	0.26	0.01
5.0	0.025	H_m	0.011	0.063	0.010	0.010	0.062	0.009	0.042	0.041	0.050	0.037	0.064	0.051	0.04	0.70	0.04	0.03	0.25	0.01
5.0	0.035	H_m	0.015	0.087	0.016	0.013	0.085	0.013	0.058	0.057	0.068	0.052	0.088	0.070	0.05	0.68	0.06	0.04	0.26	0.01
5.5	0.015	H_m	0.009	0.031	0.008	0.010	0.018	0.010	0.045	0.044	0.035	0.016	0.031	0.014	0.02	0.70	0.03	0.02	0.33	0.01
5.5	0.025	H_m	0.016	0.050	0.015	0.016	0.027	0.015	0.075	0.074	0.060	0.028	0.052	0.023	0.04	0.69	0.05	0.04	0.34	0.02
6.0	0.015	H_m	0.015	0.048	0.015	0.016	0.048	0.016	0.030	0.033	0.036	0.017	0.047	0.044	0.03	0.64	0.03	0.02	0.49	0.02
6.0	0.025	H_m	0.023	0.079	0.023	0.024	0.079	0.025	0.050	0.053	0.059	0.032	0.076	0.071	0.05	0.61	0.06	0.03	0.44	0.02
6.5	0.015	H_m	0.018	0.021	0.019	0.019	0.027	0.018	0.038	0.038	0.040	0.031	0.021	0.023	0.03	0.61	0.03	0.02	0.53	0.02
6.5	0.025	H_m	0.030	0.037	0.032	0.032	0.046	0.031	0.064	0.061	0.064	0.051	0.038	0.038	0.04	0.57	0.04	0.03	0.52	0.03

Table A.15: K_t results

Ho/Lo Range 0.015 - 0.045		Width (prototype) (m)								
		8			12			16		
		Draft (prototype) (m)			Draft (prototype) (m)			Draft (prototype) (m)		
T_p (sec)		**1.5**	**3.5**	**5.5**	**1.5**	**3.5**	**5.5**	**1.5**	**3.5**	**5.5**
4	K_t (min)	0.42	0.20	0.13	0.32	0.18	0.15	0.32	0.19	0.15
	K_t (max)	0.44	0.22	0.17	0.35	0.23	0.17	0.33	0.25	0.19
	K_t (mean)	**0.43**	**0.21**	**0.15**	**0.34**	**0.21**	**0.16**	**0.33**	**0.21**	**0.16**
4.5	K_t (min)	0.49	0.27	0.16	0.42	0.25	0.17	0.38	0.24	0.18
	K_t (max)	0.55	0.30	0.20	0.53	0.26	0.21	0.42	0.29	0.21
	K_t (mean)	**0.51**	**0.29**	**0.18**	**0.46**	**0.26**	**0.18**	**0.40**	**0.26**	**0.19**
5	K_t (min)	0.57	0.39	0.27	0.49	0.35	0.26	0.46	0.32	0.25
	K_t (max)	0.60	0.42	0.29	0.54	0.38	0.27	0.48	0.36	0.26
	K_t (mean)	**0.59**	**0.41**	**0.28**	**0.52**	**0.36**	**0.26**	**0.47**	**0.34**	**0.26**
5.5	K_t (min)	0.70	0.54	0.38	0.61	0.47	0.36	0.54	0.43	0.33
	K_t (max)	0.71	0.56	0.40	0.62	0.49	0.38	0.56	0.44	0.34
	K_t (mean)	**0.71**	**0.55**	**0.39**	**0.62**	**0.48**	**0.37**	**0.55**	**0.44**	**0.34**
6	K_t (min)	0.81	0.65	0.49	0.69	0.58	0.46	0.64	0.52	0.44
	K_t (max)	0.82	0.70	0.57	0.77	0.64	0.50	0.66	0.54	0.49
	K_t (mean)	**0.82**	**0.68**	**0.53**	**0.73**	**0.61**	**0.48**	**0.65**	**0.53**	**0.47**
6.5	K_t (min)	0.87	0.70	0.56	0.78	0.67	0.53	0.60	0.60	0.52
	K_t (max)	0.90	0.74	0.57	0.82	0.69	0.58	0.77	0.63	0.53
	K_t (mean)	**0.88**	**0.72**	**0.57**	**0.80**	**0.68**	**0.55**	**0.68**	**0.61**	**0.53**

Table A.16: K_r results

H_o/L_o Range 0.015 - 0.045		Width (prototype) (m)								
		8			12			16		
		Draft (prototype) (m)			Draft (prototype) (m)			Draft (prototype) (m)		
T_p (sec)		**1.5**	**3.5**	**5.5**	**1.5**	**3.5**	**5.5**	**1.5**	**3.5**	**5.5**
4	K_r (min)	0.63	0.70	0.71	0.63	0.70	0.72	0.63	0.69	0.55
	K_r (max)	0.65	0.72	0.74	0.67	0.72	0.74	0.67	0.73	0.66
	K_r (mean)	**0.43**	**0.21**	**0.15**	**0.34**	**0.21**	**0.16**	**0.33**	**0.21**	**0.16**
4.5	K_r (min)	0.55	0.61	0.65	0.59	0.63	0.66	0.61	0.64	0.45
	K_r (max)	0.57	0.65	0.68	0.64	0.75	0.73	0.64	0.69	0.64
	K_r (mean)	**0.51**	**0.29**	**0.18**	**0.46**	**0.26**	**0.18**	**0.40**	**0.26**	**0.19**
5	K_r (min)	0.52	0.57	0.62	0.55	0.62	0.64	0.63	0.64	0.40
	K_r (max)	0.53	0.59	0.65	0.59	0.65	0.66	0.63	0.65	0.57
	K_r (mean)	**0.59**	**0.41**	**0.28**	**0.52**	**0.36**	**0.26**	**0.47**	**0.34**	**0.26**
5.5	K_r (min)	0.48	0.55	0.61	0.54	0.61	0.63	0.58	0.63	0.38
	K_r (max)	0.49	0.56	0.62	0.54	0.61	0.65	0.62	0.66	0.46
	K_r (mean)	**0.49**	**0.56**	**0.61**	**0.54**	**0.61**	**0.64**	**0.60**	**0.65**	**0.42**
6	K_r (min)	0.42	0.48	0.55	0.48	0.55	0.56	0.56	0.59	0.42
	K_r (max)	0.44	0.51	0.57	0.50	0.55	0.59	0.56	0.61	0.48
	K_r (mean)	**0.43**	**0.50**	**0.56**	**0.49**	**0.55**	**0.57**	**0.56**	**0.60**	**0.45**
6.5	K_r (min)	0.39	0.44	0.51	0.47	0.53	0.55	0.53	0.56	0.44
	K_r (max)	0.41	0.46	0.56	0.47	0.54	0.58	0.57	0.57	0.47
	K_r (mean)	**0.40**	**0.45**	**0.54**	**0.47**	**0.53**	**0.57**	**0.55**	**0.57**	**0.46**

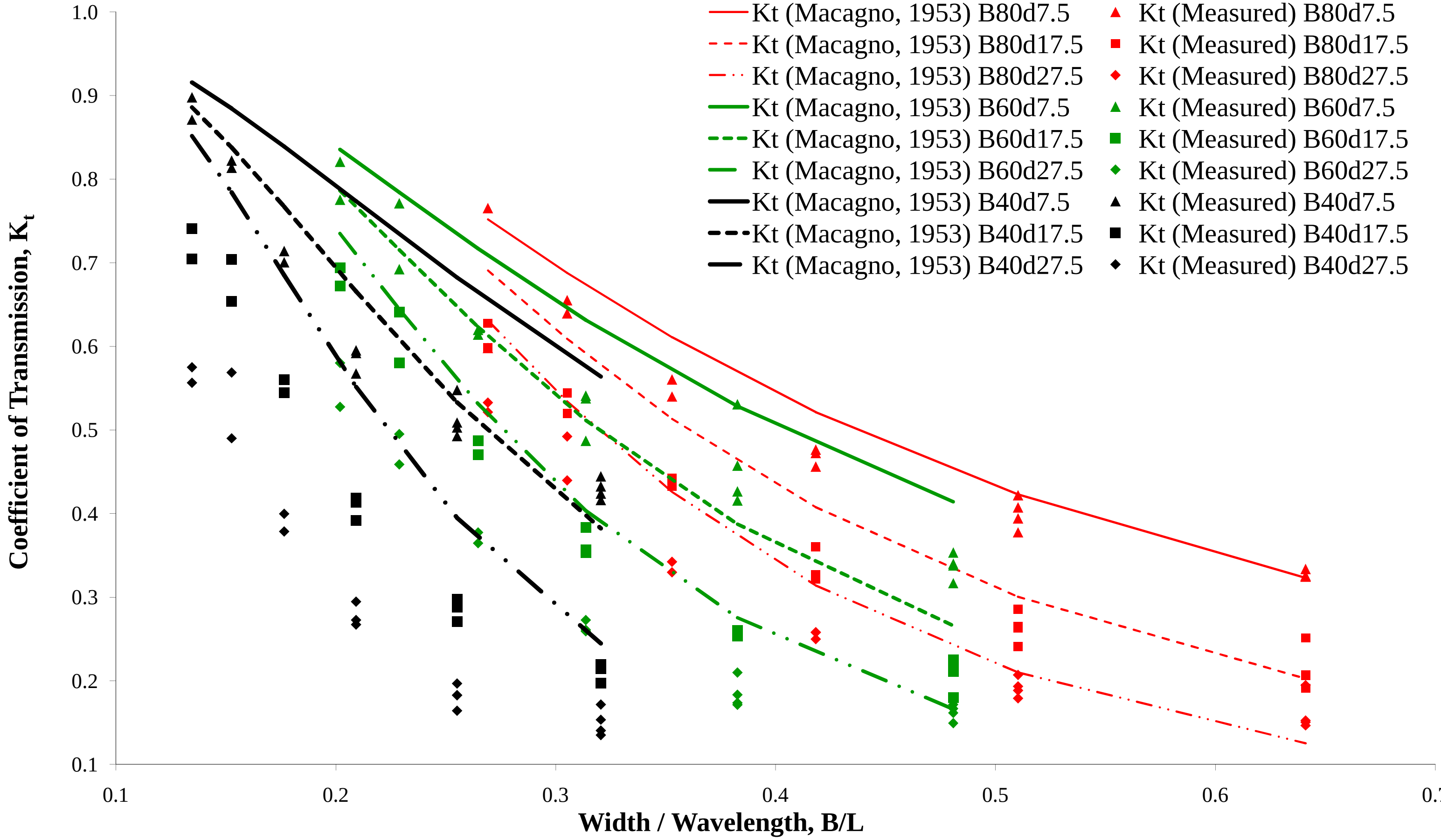

Figure A.2: Experimental K_t comparison with Macagno's Theory

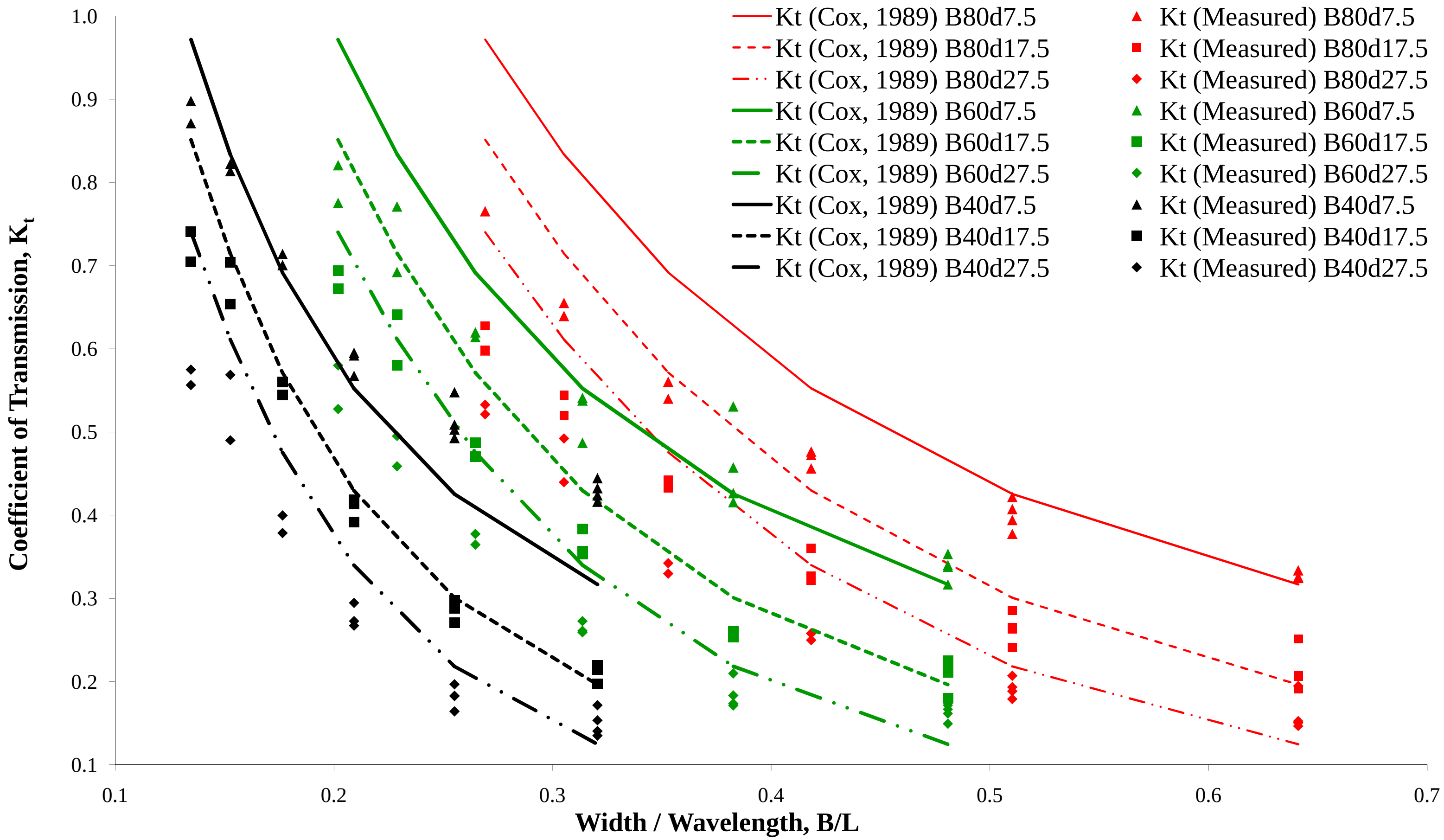

Figure A.3: Experimental K_t comparison with Cox's Theory

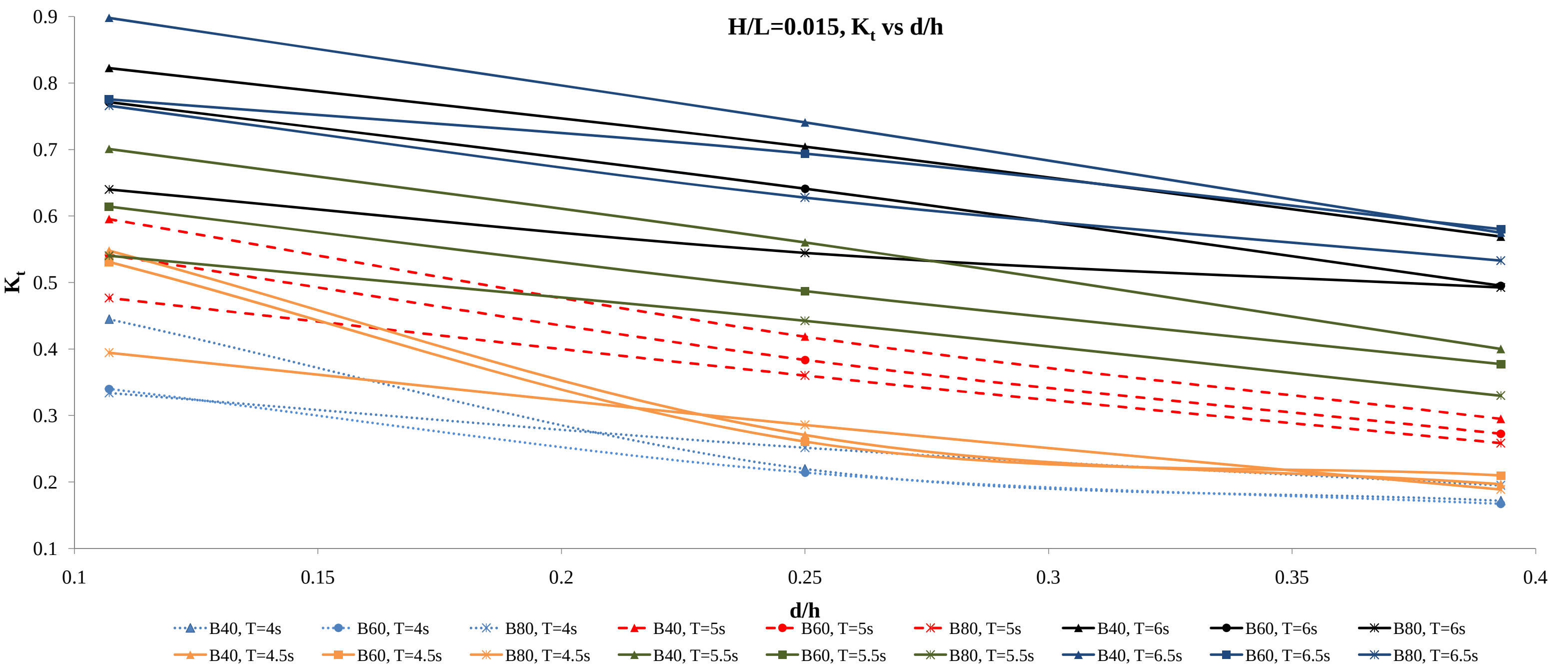

Figure A.4: K_t vs d/h for H/L=0.015 all periods

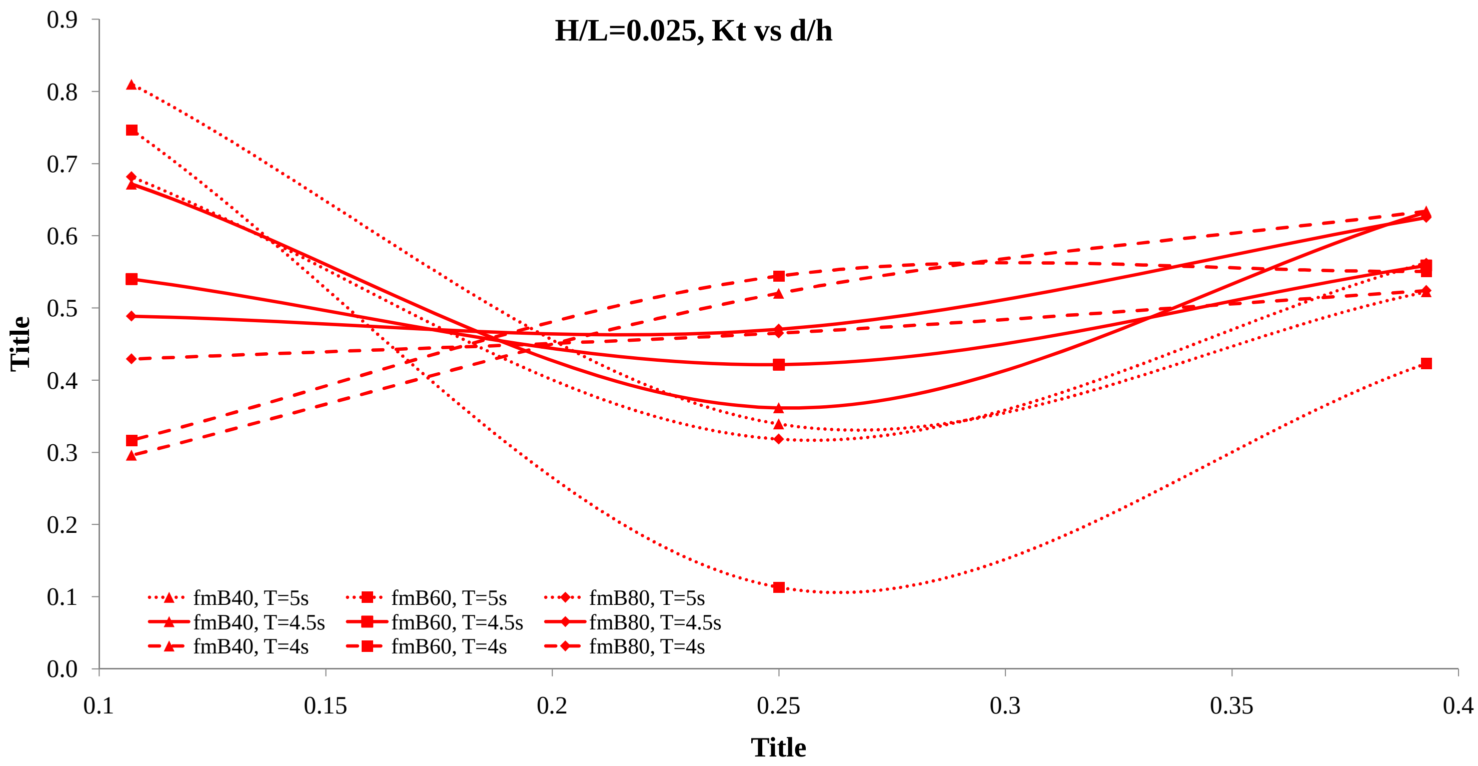

Figure A.5: K_t vs d/h for H/L=0.025 all periods

Table A.17: Data Analysis Results for chain moored case 1 B40d7.5

B40d7.5fm			Gauge1	Gauge2	Gauge3	Gauge5	Gauge6	Gauge7	Gauge8	Gauge11	Gauge12	Gauge13	Gauge15	Gauge16	Results below are in model scale					
Period (prototype)	Steepness		1	2	3	4	5	6	7	8	9	10	11	12	$H_{m\ (mean)}$	K_r	H_I	H_R	K_t	H_t
4.0	0.015	Hm	0.007	0.018	0.007	0.004	0.015	0.004	0.017	0.015	0.020	0.014	0.023	0.019	0.01	0.26	0.02	0.00	0.35	0.01
4.0	0.025	Hm	0.009	0.032	0.010	0.006	0.027	0.007	0.028	0.027	0.033	0.022	0.036	0.030	0.02	0.23	0.03	0.01	0.30	0.01
4.0	0.035	Hm	0.012	0.044	0.012	0.010	0.036	0.010	0.041	0.038	0.045	0.032	0.048	0.039	0.03	0.24	0.04	0.01	0.30	0.01
4.0	0.045	Hm	0.016	0.055	0.017	0.013	0.044	0.013	0.053	0.052	0.057	0.040	0.057	0.046	0.04	0.23	0.05	0.01	0.34	0.01
4.5	0.015	Hm	0.015	0.019	0.015	0.014	0.022	0.014	0.021	0.019	0.025	0.016	0.021	0.023	0.02	0.21	0.02	0.00	0.77	0.01
4.5	0.025	Hm	0.022	0.032	0.023	0.021	0.036	0.020	0.033	0.031	0.041	0.027	0.034	0.039	0.03	0.16	0.03	0.01	0.67	0.02
4.5	0.035	Hm	0.030	0.046	0.030	0.028	0.051	0.027	0.045	0.042	0.057	0.037	0.049	0.054	0.04	0.14	0.05	0.01	0.66	0.03
4.5	0.045	Hm	0.039	0.047	0.039	0.032	0.053	0.030	0.053	0.047	0.071	0.042	0.056	0.063	0.05	0.16	0.05	0.01	0.65	0.03
5.0	0.015	Hm	0.020	0.022	0.019	0.018	0.024	0.018	0.020	0.021	0.029	0.018	0.022	0.025	0.02	0.16	0.02	0.00	0.80	0.02
5.0	0.025	Hm	0.033	0.039	0.032	0.031	0.042	0.031	0.034	0.038	0.046	0.028	0.036	0.040	0.04	0.13	0.04	0.00	0.81	0.03
5.0	0.035	Hm	0.046	0.061	0.046	0.045	0.063	0.044	0.053	0.059	0.066	0.041	0.056	0.059	0.06	0.10	0.06	0.01	0.83	0.05
5.5	0.015	Hm	0.026	0.031	0.027	0.028	0.032	0.027	0.028	0.031	0.033	0.022	0.030	0.031	0.03	0.10	0.03	0.00	0.97	0.03
5.5	0.025	Hm	0.043	0.051	0.043	0.045	0.052	0.044	0.048	0.050	0.055	0.037	0.050	0.049	0.05	0.08	0.05	0.00	0.95	0.04
6.0	0.015	Hm	0.032	0.034	0.031	0.033	0.034	0.034	0.034	0.035	0.038	0.025	0.033	0.033	0.03	0.09	0.03	0.00	1.04	0.03
6.0	0.025	Hm	0.052	0.057	0.051	0.055	0.056	0.055	0.056	0.058	0.064	0.045	0.055	0.055	0.06	0.09	0.06	0.01	1.00	0.05
6.5	0.015	Hm	0.037	0.040	0.037	0.036	0.041	0.036	0.039	0.040	0.041	0.029	0.040	0.039	0.04	0.10	0.04	0.00	1.02	0.04
6.5	0.025	Hm	0.062	0.065	0.062	0.061	0.066	0.060	0.067	0.066	0.067	0.047	0.065	0.066	0.06	0.09	0.06	0.01	1.01	0.06

Table A.18: Data Analysis Results for chain moored case 3 B40d17.5

B40d17.5fm			Gauge1	Gauge2	Gauge3	Gauge5	Gauge6	Gauge7	Gauge8	Gauge11	Gauge12	Gauge13	Gauge15	Gauge16	Results below are in model scale					
Period (prototype)	Steepness		1	2	3	4	5	6	7	8	9	10	11	12	$H_{m\ (mean)}$	K_r	H_I	H_R	K_t	H_t
4.0	0.015	Hm	0.009	0.023	0.008	0.009	0.013	0.009	0.019	0.024	0.020	0.015	0.022	0.013	0.02	0.47	0.02	0.01	0.56	0.01
4.0	0.025	Hm	0.014	0.036	0.014	0.015	0.022	0.014	0.034	0.038	0.033	0.026	0.034	0.020	0.02	0.46	0.03	0.01	0.52	0.01
4.0	0.035	Hm	0.024	0.018	0.045	0.018	0.019	0.028	0.018	0.048	0.051	0.043	0.035	0.045	0.03	0.44	0.04	0.02	0.52	0.02
4.0	0.045	Hm	0.020	0.054	0.019	0.022	0.035	0.022	0.063	0.064	0.055	0.045	0.056	0.038	0.04	0.43	0.05	0.02	0.47	0.02
4.5	0.015	Hm	0.006	0.024	0.006	0.007	0.026	0.007	0.015	0.014	0.025	0.018	0.024	0.028	0.02	0.41	0.02	0.01	0.35	0.01
4.5	0.025	Hm	0.010	0.039	0.010	0.013	0.042	0.013	0.025	0.024	0.041	0.030	0.041	0.046	0.03	0.38	0.03	0.01	0.36	0.01
4.5	0.035	Hm	0.015	0.056	0.016	0.018	0.057	0.018	0.037	0.035	0.059	0.040	0.057	0.055	0.04	0.35	0.05	0.02	0.38	0.02
4.5	0.045	Hm	0.019	0.073	0.019	0.022	0.075	0.021	0.051	0.049	0.074	0.052	0.074	0.074	0.05	0.33	0.06	0.02	0.38	0.02
5.0	0.015	Hm	0.007	0.028	0.008	0.006	0.030	0.006	0.021	0.021	0.029	0.019	0.029	0.028	0.02	0.27	0.03	0.01	0.28	0.01
5.0	0.025	Hm	0.014	0.046	0.014	0.012	0.050	0.013	0.036	0.036	0.048	0.031	0.046	0.046	0.03	0.25	0.04	0.01	0.34	0.01
5.0	0.035	Hm	0.023	0.064	0.027	0.023	0.067	0.021	0.053	0.054	0.067	0.044	0.065	0.062	0.06	0.24	0.06	0.01	0.43	0.02
5.5	0.015	Hm	0.018	0.032	0.018	0.019	0.031	0.019	0.031	0.032	0.033	0.023	0.032	0.028	0.03	0.21	0.03	0.01	0.66	0.02
5.5	0.025	Hm	0.030	0.053	0.032	0.033	0.050	0.030	0.053	0.055	0.055	0.035	0.052	0.045	0.04	0.20	0.05	0.01	0.67	0.03
6.0	0.015	Hm	0.028	0.033	0.028	0.029	0.034	0.030	0.033	0.034	0.039	0.027	0.032	0.031	0.03	0.14	0.03	0.00	0.93	0.03
6.0	0.025	Hm	0.047	0.054	0.044	0.046	0.055	0.048	0.052	0.053	0.055	0.044	0.052	0.050	0.05	0.13	0.05	0.01	0.87	0.05
6.5	0.015	Hm	0.034	0.041	0.037	0.037	0.039	0.035	0.042	0.041	0.036	0.027	0.040	0.036	0.04	0.15	0.04	0.01	1.00	0.04
6.5	0.025	Hm	0.041	0.065	0.046	0.047	0.059	0.040	0.069	0.068	0.060	0.042	0.065	0.055	0.06	0.17	0.06	0.01	0.74	0.04

Table A.19: Data Analysis Results for chain moored case 3 B40d27.5

B40d27.5fm			Gauge1	Gauge2	Gauge3	Gauge5	Gauge6	Gauge7	Gauge8	Gauge11	Gauge12	Gauge13	Gauge15	Gauge16	Results below are in model scale					
Period (prototype)	Steepness		1	2	3	4	5	6	7	8	9	10	11	12	$H_{m\ (mean)}$	K_r	H_I	H_R	K_t	H_t
4.0	0.015	Hm	0.010	0.018	0.009	0.010	0.011	0.010	0.021	0.019	0.019	0.015	0.020	0.013	0.01	0.45	0.02	0.01	0.62	0.01
4.0	0.025	Hm	0.017	0.030	0.017	0.018	0.020	0.017	0.036	0.034	0.032	0.026	0.033	0.021	0.02	0.46	0.03	0.01	0.63	0.02
4.0	0.035	Hm	0.024	0.041	0.022	0.024	0.026	0.024	0.050	0.049	0.044	0.036	0.044	0.029	0.03	0.45	0.04	0.02	0.66	0.02
4.0	0.045	Hm	0.027	0.050	0.026	0.029	0.035	0.029	0.065	0.064	0.056	0.046	0.053	0.039	0.04	0.43	0.05	0.02	0.63	0.03
4.5	0.015	Hm	0.011	0.023	0.011	0.013	0.025	0.012	0.015	0.015	0.025	0.018	0.025	0.026	0.02	0.38	0.02	0.01	0.64	0.01
4.5	0.025	Hm	0.018	0.041	0.019	0.023	0.042	0.022	0.025	0.025	0.043	0.030	0.041	0.043	0.03	0.39	0.03	0.01	0.63	0.02
4.5	0.035	Hm	0.026	0.058	0.025	0.029	0.058	0.030	0.039	0.038	0.059	0.042	0.060	0.060	0.04	0.35	0.05	0.02	0.63	0.03
4.5	0.045	Hm	0.029	0.076	0.030	0.035	0.073	0.033	0.053	0.051	0.072	0.052	0.078	0.074	0.05	0.35	0.07	0.02	0.59	0.03
5.0	0.015	Hm	0.012	0.031	0.013	0.012	0.031	0.012	0.023	0.023	0.029	0.021	0.031	0.029	0.02	0.34	0.03	0.01	0.52	0.01
5.0	0.025	Hm	0.020	0.051	0.021	0.020	0.050	0.019	0.039	0.040	0.048	0.033	0.050	0.045	0.04	0.32	0.04	0.01	0.52	0.02
5.0	0.035	Hm	0.028	0.071	0.028	0.027	0.069	0.026	0.056	0.058	0.067	0.046	0.070	0.063	0.06	0.31	0.06	0.02	0.50	0.03
5.5	0.015	Hm	0.012	0.032	0.012	0.011	0.029	0.010	0.035	0.036	0.034	0.022	0.032	0.025	0.02	0.32	0.03	0.01	0.41	0.01
5.5	0.025	Hm	0.023	0.051	0.022	0.022	0.047	0.021	0.058	0.061	0.056	0.034	0.051	0.041	0.04	0.29	0.05	0.01	0.48	0.02
6.0	0.015	Hm	0.019	0.033	0.019	0.019	0.036	0.019	0.030	0.031	0.038	0.027	0.032	0.032	0.03	0.21	0.03	0.01	0.62	0.02
6.0	0.025	Hm	0.035	0.056	0.034	0.035	0.062	0.034	0.051	0.052	0.061	0.044	0.054	0.055	0.05	0.20	0.05	0.01	0.65	0.03
6.5	0.015	Hm	0.028	0.040	0.030	0.029	0.039	0.027	0.041	0.042	0.042	0.029	0.039	0.034	0.04	0.15	0.04	0.01	0.79	0.03
6.5	0.025	Hm	0.044	0.065	0.047	0.046	0.063	0.043	0.069	0.068	0.069	0.043	0.065	0.057	0.06	0.15	0.06	0.01	0.78	0.05

Table A.20: Data Analysis Results for chain moored case 4 B60d7.5

B60d7.5fm			Gauge1	Gauge2	Gauge3	Gauge5	Gauge6	Gauge7	Gauge8	Gauge11	Gauge12	Gauge13	Gauge15	Gauge16	Results below are in model scale					
Period (prototype)	Steepness		1	2	3	4	5	6	7	8	9	10	11	12	$H_{m\ (mean)}$	K_r	H_I	H_R	K_t	H_t
4.0	0.015	Hm	0.008	0.019	0.008	0.006	0.019	0.006	0.016	0.014	0.019	0.013	0.021	0.021	0.01	0.26	0.02	0.00	0.42	0.01
4.0	0.025	Hm	0.010	0.031	0.010	0.008	0.029	0.008	0.025	0.024	0.033	0.021	0.036	0.034	0.02	0.21	0.03	0.01	0.32	0.01
4.0	0.035	Hm	0.011	0.041	0.011	0.009	0.038	0.009	0.035	0.033	0.045	0.030	0.047	0.044	0.03	0.20	0.04	0.01	0.28	0.01
4.0	0.045	Hm	0.013	0.053	0.013	0.010	0.048	0.009	0.045	0.044	0.057	0.039	0.058	0.052	0.04	0.18	0.05	0.01	0.25	0.01
4.5	0.015	Hm	0.012	0.018	0.012	0.012	0.021	0.011	0.020	0.018	0.024	0.016	0.020	0.022	0.02	0.16	0.02	0.00	0.62	0.01
4.5	0.025	Hm	0.018	0.031	0.019	0.017	0.033	0.016	0.034	0.031	0.040	0.026	0.033	0.036	0.03	0.14	0.03	0.00	0.54	0.02
4.5	0.035	Hm	0.024	0.045	0.025	0.023	0.049	0.021	0.047	0.042	0.056	0.037	0.046	0.052	0.04	0.13	0.05	0.01	0.54	0.02
4.5	0.045	Hm	0.030	0.059	0.031	0.028	0.063	0.026	0.060	0.056	0.072	0.046	0.061	0.067	0.05	0.12	0.06	0.01	0.52	0.03
5.0	0.015	Hm	0.019	0.024	0.020	0.019	0.027	0.018	0.024	0.023	0.028	0.019	0.024	0.027	0.02	0.15	0.02	0.00	0.80	0.02
5.0	0.025	Hm	0.029	0.040	0.030	0.029	0.042	0.028	0.037	0.037	0.046	0.029	0.040	0.043	0.04	0.12	0.04	0.00	0.75	0.03
5.0	0.035	Hm	0.041	0.059	0.041	0.041	0.061	0.039	0.054	0.053	0.065	0.041	0.058	0.061	0.06	0.12	0.06	0.01	0.73	0.04
5.5	0.015	Hm	0.025	0.031	0.025	0.026	0.031	0.025	0.028	0.030	0.033	0.022	0.030	0.029	0.03	0.11	0.03	0.00	0.91	0.03
5.5	0.025	Hm	0.038	0.051	0.041	0.042	0.051	0.039	0.047	0.050	0.054	0.036	0.049	0.048	0.05	0.11	0.05	0.01	0.88	0.04
6.0	0.015	Hm	0.031	0.033	0.030	0.032	0.034	0.033	0.034	0.034	0.038	0.027	0.032	0.034	0.03	0.10	0.03	0.00	1.02	0.03
6.0	0.025	Hm	0.051	0.055	0.049	0.053	0.056	0.053	0.056	0.057	0.063	0.041	0.054	0.055	0.05	0.09	0.05	0.00	0.96	0.05
6.5	0.015	Hm	0.035	0.039	0.037	0.036	0.040	0.036	0.038	0.038	0.040	0.028	0.039	0.039	0.04	0.12	0.04	0.00	1.01	0.04
6.5	0.025	Hm	0.059	0.065	0.060	0.060	0.065	0.059	0.065	0.065	0.067	0.046	0.065	0.064	0.06	0.11	0.06	0.01	0.99	0.06

Table A.21: Data Analysis Results for unit chain moored case 5 B60d17.5

B60d17.5fm			Gauge1	Gauge2	Gauge3	Gauge5	Gauge6	Gauge7	Gauge8	Gauge11	Gauge12	Gauge13	Gauge15	Gauge16	Results below are in model scale					
Period (prototype)	Steepness		1	2	3	4	5	6	7	8	9	10	11	12	$H_{m\,(mean)}$	K_r	H_I	H_R	K_t	H_t
4.0	0.015	Hm	0.009	0.024	0.008	0.007	0.018	0.008	0.015	0.015	0.020	0.014	0.025	0.018	0.02	0.53	0.02	0.01	0.51	0.01
4.0	0.025	Hm	0.016	0.044	0.015	0.014	0.031	0.014	0.026	0.031	0.035	0.025	0.044	0.032	0.03	0.51	0.03	0.02	0.54	0.01
4.0	0.035	Hm	0.019	0.050	0.017	0.017	0.035	0.018	0.037	0.037	0.045	0.033	0.054	0.038	0.03	0.47	0.04	0.02	0.50	0.02
4.0	0.045	Hm	0.022	0.065	0.020	0.020	0.043	0.021	0.048	0.050	0.057	0.043	0.066	0.046	0.04	0.44	0.05	0.02	0.48	0.02
4.5	0.015	Hm	0.009	0.019	0.009	0.010	0.024	0.009	0.019	0.016	0.025	0.016	0.020	0.026	0.02	0.36	0.02	0.01	0.49	0.01
4.5	0.025	Hm	0.012	0.033	0.013	0.015	0.040	0.014	0.031	0.027	0.042	0.029	0.034	0.043	0.03	0.32	0.03	0.01	0.42	0.01
4.5	0.035	Hm	0.015	0.050	0.016	0.018	0.057	0.017	0.042	0.037	0.058	0.041	0.050	0.061	0.04	0.28	0.05	0.01	0.37	0.02
4.5	0.045	Hm	0.016	0.067	0.017	0.020	0.075	0.018	0.052	0.047	0.073	0.051	0.067	0.077	0.05	0.27	0.06	0.02	0.32	0.02
5.0	0.015	Hm	0.006	0.028	0.005	0.005	0.029	0.006	0.022	0.021	0.029	0.020	0.027	0.030	0.02	0.22	0.03	0.01	0.22	0.01
5.0	0.025	Hm	0.005	0.046	0.007	0.008	0.049	0.005	0.035	0.036	0.048	0.033	0.044	0.048	0.03	0.21	0.04	0.01	0.11	0.00
5.0	0.035	Hm	0.009	0.063	0.011	0.011	0.067	0.005	0.051	0.053	0.066	0.045	0.062	0.065	0.06	0.19	0.06	0.01	0.12	0.01
5.5	0.015	Hm	0.015	0.032	0.015	0.015	0.029	0.016	0.032	0.034	0.034	0.022	0.031	0.028	0.03	0.22	0.03	0.01	0.55	0.02
5.5	0.025	Hm	0.026	0.053	0.023	0.024	0.048	0.025	0.052	0.056	0.056	0.035	0.051	0.047	0.04	0.20	0.05	0.01	0.53	0.02
6.0	0.015	Hm	0.024	0.032	0.025	0.026	0.034	0.025	0.028	0.031	0.039	0.026	0.031	0.034	0.03	0.19	0.03	0.01	0.81	0.03
6.0	0.025	Hm	0.038	0.055	0.038	0.041	0.059	0.041	0.051	0.052	0.064	0.043	0.053	0.059	0.05	0.18	0.05	0.01	0.75	0.04
6.5	0.015	Hm	0.031	0.039	0.033	0.033	0.038	0.031	0.042	0.041	0.041	0.030	0.039	0.038	0.04	0.11	0.04	0.00	0.92	0.03
6.5	0.025	Hm	0.050	0.064	0.053	0.054	0.063	0.050	0.068	0.071	0.068	0.043	0.064	0.063	0.06	0.11	0.06	0.01	0.88	0.05

Table A.22: Data Analysis Results for unit chain moored case 6 B60d27.5

B60d27.5fm			Gauge1	Gauge2	Gauge3	Gauge5	Gauge6	Gauge7	Gauge8	Gauge11	Gauge12	Gauge13	Gauge15	Gauge16	Results below are in model scale					
Period (prototype)	Steepness		1	2	3	4	5	6	7	8	9	10	11	12	$H_{m\ (mean)}$	K_r	H_I	H_R	K_t	H_t
4.0	0.015	Hm	0.012	0.021	0.009	0.008	0.017	0.010	0.017	0.014	0.020	0.015	0.026	0.020	0.02	0.40	0.02	0.01	0.61	0.01
4.0	0.025	Hm	0.019	0.035	0.014	0.013	0.029	0.015	0.026	0.023	0.034	0.021	0.040	0.030	0.03	0.39	0.03	0.01	0.55	0.01
4.0	0.035	Hm	0.024	0.049	0.019	0.017	0.039	0.020	0.035	0.032	0.046	0.031	0.054	0.040	0.03	0.38	0.04	0.02	0.56	0.02
4.0	0.045	Hm	0.029	0.062	0.023	0.020	0.047	0.024	0.045	0.043	0.058	0.040	0.066	0.048	0.04	0.38	0.05	0.02	0.56	0.02
4.5	0.015	Hm	0.010	0.020	0.010	0.014	0.022	0.011	0.019	0.017	0.026	0.017	0.020	0.025	0.02	0.28	0.02	0.01	0.59	0.01
4.5	0.025	Hm	0.016	0.034	0.015	0.021	0.039	0.019	0.031	0.027	0.041	0.028	0.034	0.041	0.03	0.27	0.03	0.01	0.56	0.02
4.5	0.035	Hm	0.022	0.048	0.020	0.027	0.055	0.026	0.043	0.037	0.057	0.040	0.049	0.058	0.04	0.26	0.05	0.01	0.55	0.02
4.5	0.045	Hm	0.023	0.063	0.022	0.032	0.070	0.029	0.053	0.047	0.074	0.048	0.063	0.072	0.05	0.24	0.06	0.01	0.49	0.03
5.0	0.015	Hm	0.008	0.027	0.010	0.013	0.027	0.013	0.023	0.023	0.029	0.020	0.026	0.028	0.02	0.18	0.03	0.00	0.46	0.01
5.0	0.025	Hm	0.012	0.045	0.016	0.020	0.045	0.019	0.036	0.038	0.047	0.029	0.043	0.045	0.03	0.18	0.04	0.01	0.42	0.02
5.0	0.035	Hm	0.012	0.066	0.017	0.028	0.068	0.025	0.052	0.055	0.066	0.044	0.065	0.067	0.06	0.18	0.06	0.01	0.37	0.02
5.5	0.015	Hm	0.003	0.029	0.004	0.007	0.028	0.008	0.033	0.033	0.034	0.021	0.028	0.025	0.02	0.22	0.03	0.01	0.19	0.01
5.5	0.025	Hm	0.011	0.051	0.009	0.011	0.047	0.009	0.056	0.055	0.056	0.033	0.050	0.041	0.04	0.24	0.05	0.01	0.21	0.01
6.0	0.015	Hm	0.014	0.036	0.015	0.017	0.038	0.017	0.030	0.031	0.037	0.026	0.032	0.037	0.03	0.21	0.03	0.01	0.50	0.02
6.0	0.025	Hm	0.025	0.060	0.022	0.028	0.063	0.026	0.049	0.054	0.062	0.041	0.056	0.061	0.05	0.19	0.06	0.01	0.46	0.02
6.5	0.015	Hm	0.025	0.036	0.025	0.023	0.035	0.024	0.042	0.041	0.041	0.026	0.037	0.036	0.03	0.14	0.04	0.01	0.68	0.02
6.5	0.025	Hm	0.042	0.060	0.040	0.039	0.060	0.038	0.070	0.066	0.068	0.043	0.062	0.061	0.06	0.14	0.06	0.01	0.65	0.04

Table A.23: Data Analysis Results for unit chain moored case 7 B80d7.5

B80d7.5fm			Gauge1	Gauge2	Gauge3	Gauge5	Gauge6	Gauge7	Gauge8	Gauge11	Gauge12	Gauge13	Gauge15	Gauge16	Results below are in model scale					
Period (prototype)	Steepness		1	2	3	4	5	6	7	8	9	10	11	12	$H_{m\ (mean)}$	K_r	H_I	H_R	K_t	H_t
4.0	0.015	Hm	0.010	0.016	0.010	0.008	0.020	0.008	0.017	0.015	0.021	0.012	0.019	0.024	0.02	0.36	0.02	0.01	0.55	0.01
4.0	0.025	Hm	0.013	0.030	0.013	0.011	0.035	0.011	0.027	0.025	0.035	0.023	0.034	0.039	0.02	0.30	0.03	0.01	0.43	0.01
4.0	0.035	Hm	0.014	0.040	0.014	0.012	0.046	0.013	0.035	0.033	0.046	0.030	0.046	0.052	0.03	0.27	0.04	0.01	0.37	0.01
4.0	0.045	Hm	0.016	0.054	0.015	0.013	0.059	0.013	0.043	0.041	0.061	0.039	0.057	0.062	0.04	0.25	0.05	0.01	0.33	0.01
4.5	0.015	Hm	0.011	0.019	0.012	0.011	0.019	0.010	0.024	0.022	0.025	0.017	0.021	0.021	0.02	0.18	0.02	0.00	0.60	0.01
4.5	0.025	Hm	0.016	0.031	0.017	0.014	0.033	0.014	0.038	0.034	0.041	0.026	0.033	0.035	0.03	0.16	0.03	0.01	0.49	0.02
4.5	0.035	Hm	0.020	0.044	0.022	0.020	0.047	0.018	0.054	0.049	0.058	0.037	0.046	0.049	0.04	0.14	0.05	0.01	0.45	0.02
4.5	0.045	Hm	0.025	0.058	0.025	0.023	0.059	0.021	0.068	0.063	0.074	0.048	0.060	0.063	0.05	0.14	0.06	0.01	0.44	0.02
5.0	0.015	Hm	0.017	0.024	0.017	0.017	0.027	0.016	0.024	0.023	0.029	0.018	0.024	0.026	0.02	0.14	0.02	0.00	0.72	0.02
5.0	0.025	Hm	0.027	0.041	0.028	0.026	0.043	0.026	0.040	0.039	0.047	0.030	0.041	0.043	0.04	0.12	0.04	0.00	0.68	0.03
5.0	0.035	Hm	0.011	0.036	0.059	0.038	0.036	0.062	0.035	0.055	0.054	0.067	0.042	0.058	0.06	0.11	0.06	0.01	0.66	0.04
5.5	0.015	Hm	0.021	0.032	0.024	0.024	0.032	0.023	0.029	0.030	0.033	0.024	0.031	0.031	0.03	0.11	0.03	0.00	0.83	0.02
5.5	0.025	Hm	0.033	0.053	0.038	0.039	0.050	0.038	0.048	0.051	0.055	0.037	0.051	0.050	0.05	0.12	0.05	0.01	0.81	0.04
6.0	0.015	Hm	0.028	0.033	0.030	0.032	0.033	0.032	0.035	0.035	0.040	0.027	0.032	0.033	0.03	0.12	0.03	0.00	0.98	0.03
6.0	0.025	Hm	0.045	0.056	0.047	0.051	0.055	0.053	0.059	0.059	0.065	0.045	0.056	0.055	0.05	0.10	0.06	0.01	0.92	0.05
6.5	0.015	Hm	0.032	0.041	0.037	0.037	0.041	0.036	0.040	0.042	0.043	0.030	0.042	0.040	0.04	0.11	0.04	0.00	0.98	0.04
6.5	0.025	Hm	0.052	0.067	0.061	0.061	0.066	0.058	0.067	0.067	0.068	0.046	0.068	0.067	0.06	0.12	0.07	0.01	0.96	0.06

Table A.24: Data Analysis Results for unit chain moored case 8 B80d17.5

B80d17.5fm			Gauge1	Gauge2	Gauge3	Gauge5	Gauge6	Gauge7	Gauge8	Gauge11	Gauge12	Gauge13	Gauge15	Gauge16	Results below are in model scale					
Period (prototype)	Steepness		1	2	3	4	5	6	7	8	9	10	11	12	$H_{m\ (mean)}$	K_r	H_I	H_R	K_t	H_t
4.0	0.015	Hm	0.009	0.024	0.008	0.008	0.023	0.007	0.011	0.009	0.022	0.013	0.026	0.025	0.02	0.63	0.02	0.01	0.50	0.01
4.0	0.025	Hm	0.014	0.043	0.013	0.012	0.038	0.013	0.016	0.017	0.034	0.020	0.044	0.040	0.03	0.58	0.03	0.02	0.47	0.01
4.0	0.035	Hm	0.019	0.057	0.017	0.016	0.051	0.016	0.025	0.023	0.049	0.029	0.059	0.053	0.04	0.54	0.04	0.02	0.47	0.02
4.0	0.045	Hm	0.021	0.070	0.020	0.019	0.060	0.019	0.035	0.031	0.061	0.038	0.073	0.063	0.04	0.50	0.05	0.03	0.44	0.02
4.5	0.015	Hm	0.009	0.014	0.010	0.011	0.021	0.010	0.024	0.021	0.025	0.016	0.015	0.024	0.02	0.42	0.02	0.01	0.52	0.01
4.5	0.025	Hm	0.014	0.026	0.015	0.017	0.036	0.015	0.039	0.034	0.042	0.027	0.027	0.040	0.03	0.39	0.03	0.01	0.47	0.01
4.5	0.035	Hm	0.018	0.039	0.019	0.021	0.052	0.019	0.051	0.046	0.059	0.039	0.041	0.057	0.04	0.33	0.04	0.01	0.43	0.02
4.5	0.045	Hm	0.019	0.055	0.020	0.024	0.069	0.022	0.057	0.056	0.076	0.050	0.057	0.073	0.05	0.28	0.06	0.02	0.39	0.02
5.0	0.015	Hm	0.010	0.025	0.010	0.010	0.027	0.011	0.022	0.022	0.030	0.020	0.024	0.027	0.02	0.20	0.02	0.00	0.43	0.01
5.0	0.025	Hm	0.010	0.043	0.013	0.013	0.047	0.015	0.035	0.039	0.049	0.033	0.041	0.047	0.03	0.19	0.04	0.01	0.32	0.01
5.0	0.035	Hm	0.011	0.063	0.011	0.012	0.067	0.015	0.048	0.053	0.068	0.045	0.060	0.066	0.04	0.18	0.06	0.01	0.22	0.01
5.5	0.015	Hm	0.012	0.033	0.013	0.013	0.030	0.013	0.029	0.034	0.034	0.022	0.032	0.029	0.02	0.19	0.03	0.01	0.45	0.01
5.5	0.025	Hm	0.020	0.054	0.020	0.020	0.049	0.020	0.048	0.057	0.056	0.037	0.052	0.048	0.04	0.18	0.05	0.01	0.42	0.02
6.0	0.015	Hm	0.021	0.032	0.021	0.023	0.036	0.023	0.029	0.032	0.039	0.029	0.031	0.035	0.03	0.20	0.03	0.01	0.70	0.02
6.0	0.025	Hm	0.034	0.055	0.033	0.036	0.061	0.036	0.049	0.052	0.062	0.047	0.054	0.059	0.05	0.20	0.05	0.01	0.65	0.03
6.5	0.015	Hm	0.029	0.041	0.030	0.030	0.039	0.029	0.039	0.043	0.042	0.028	0.041	0.038	0.04	0.19	0.04	0.01	0.83	0.03
6.5	0.025	Hm	0.047	0.068	0.047	0.047	0.061	0.048	0.069	0.075	0.068	0.048	0.068	0.061	0.06	0.17	0.06	0.01	0.78	0.05

Table A.25: Data Analysis Results for unit chain moored case 9 B80d27.5

B80d27.5fm			Gauge1	Gauge2	Gauge3	Gauge5	Gauge6	Gauge7	Gauge8	Gauge11	Gauge12	Gauge13	Gauge15	Gauge16	Results below are in model scale					
Period (prototype)	Steepness		1	2	3	4	5	6	7	8	9	10	11	12	$H_{m\ (mean)}$	K_r	H_I	H_R	K_t	H_t
4.0	0.015	Hm	0.010	0.024	0.010	0.005	0.023	0.007	0.010	0.010	0.021	0.011	0.025	0.022	0.02	0.58	0.02	0.01	0.49	0.01
4.0	0.025	Hm	0.017	0.041	0.016	0.010	0.037	0.014	0.016	0.019	0.034	0.020	0.042	0.038	0.03	0.54	0.03	0.02	0.52	0.01
4.0	0.035	Hm	0.023	0.053	0.022	0.016	0.047	0.019	0.025	0.024	0.047	0.028	0.056	0.048	0.03	0.54	0.04	0.02	0.56	0.02
4.0	0.045	Hm	0.027	0.072	0.026	0.020	0.060	0.023	0.033	0.035	0.060	0.039	0.071	0.058	0.04	0.50	0.05	0.03	0.55	0.02
4.5	0.015	Hm	0.012	0.017	0.013	0.013	0.024	0.012	0.024	0.020	0.026	0.017	0.017	0.026	0.02	0.47	0.02	0.01	0.67	0.01
4.5	0.025	Hm	0.019	0.029	0.020	0.021	0.041	0.019	0.037	0.032	0.042	0.028	0.028	0.043	0.03	0.42	0.03	0.01	0.63	0.02
4.5	0.035	Hm	0.025	0.042	0.026	0.028	0.055	0.026	0.048	0.043	0.058	0.040	0.041	0.058	0.04	0.36	0.04	0.02	0.61	0.03
4.5	0.045	Hm	0.030	0.056	0.030	0.034	0.071	0.032	0.056	0.052	0.074	0.051	0.057	0.074	0.05	0.31	0.06	0.02	0.57	0.03
5.0	0.015	Hm	0.014	0.025	0.015	0.014	0.029	0.016	0.023	0.022	0.030	0.018	0.025	0.028	0.02	0.22	0.02	0.01	0.62	0.01
5.0	0.025	Hm	0.022	0.043	0.021	0.022	0.047	0.023	0.036	0.036	0.048	0.030	0.041	0.046	0.04	0.21	0.04	0.01	0.56	0.02
5.0	0.035	Hm	0.026	0.063	0.024	0.024	0.068	0.027	0.050	0.048	0.066	0.044	0.061	0.066	0.05	0.18	0.06	0.01	0.46	0.03
5.5	0.015	Hm	0.010	0.032	0.009	0.010	0.028	0.011	0.033	0.035	0.035	0.023	0.031	0.028	0.02	0.22	0.03	0.01	0.36	0.01
5.5	0.025	Hm	0.011	0.053	0.014	0.012	0.046	0.011	0.055	0.057	0.057	0.037	0.051	0.045	0.04	0.21	0.05	0.01	0.26	0.01
6.0	0.015	Hm	0.015	0.036	0.015	0.015	0.039	0.015	0.030	0.030	0.038	0.027	0.033	0.039	0.03	0.27	0.03	0.01	0.48	0.01
6.0	0.025	Hm	0.026	0.060	0.022	0.025	0.066	0.026	0.050	0.050	0.064	0.043	0.057	0.063	0.05	0.24	0.06	0.01	0.46	0.02
6.5	0.015	Hm	0.021	0.038	0.022	0.022	0.034	0.022	0.044	0.045	0.042	0.029	0.039	0.035	0.03	0.25	0.04	0.01	0.60	0.02
6.5	0.025	Hm	0.036	0.061	0.036	0.035	0.057	0.037	0.073	0.072	0.068	0.046	0.063	0.057	0.05	0.24	0.06	0.01	0.59	0.04

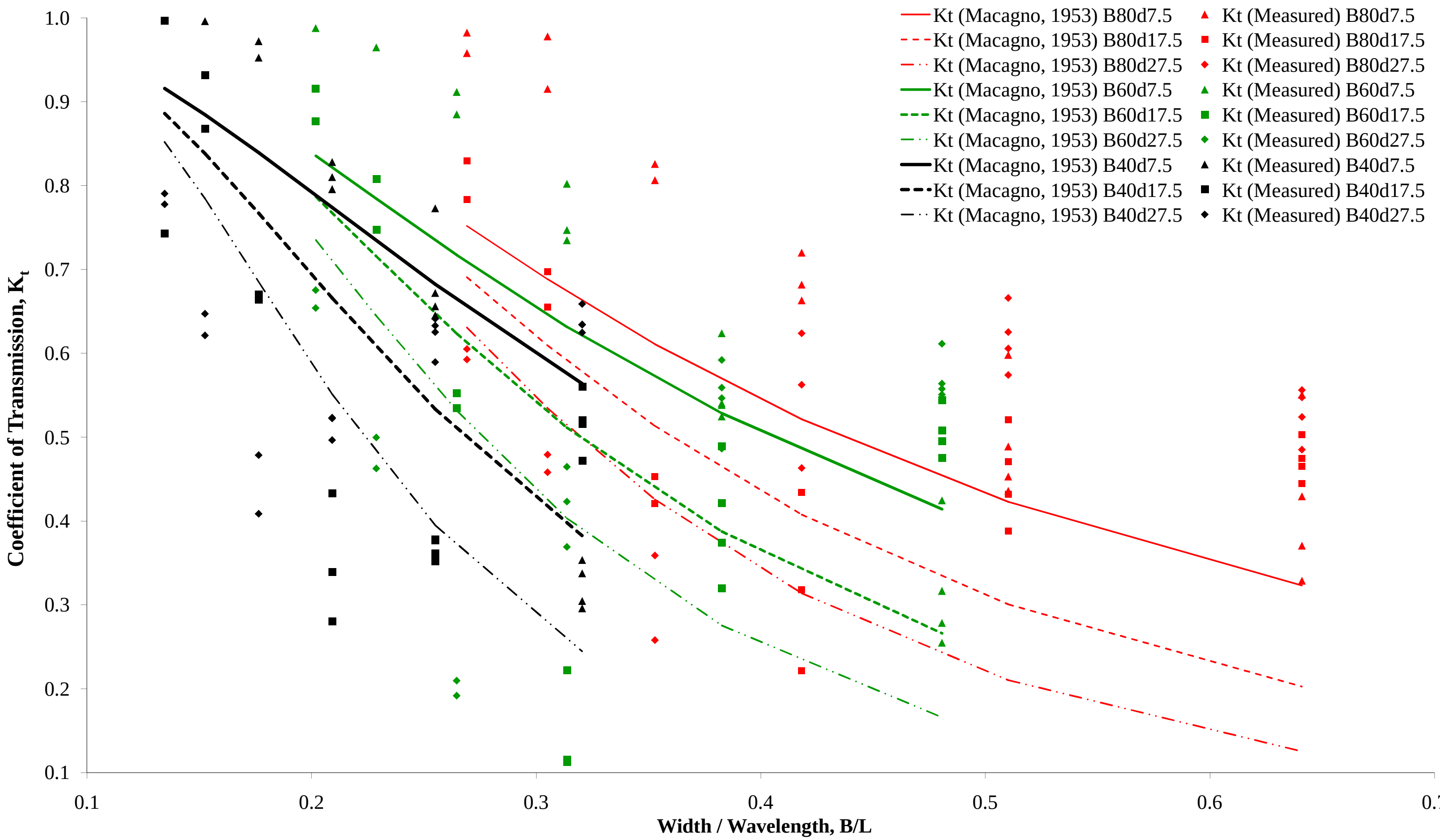

Figure A.6: Experimental K_t comparison with Macagno's Theory for chain moored cases

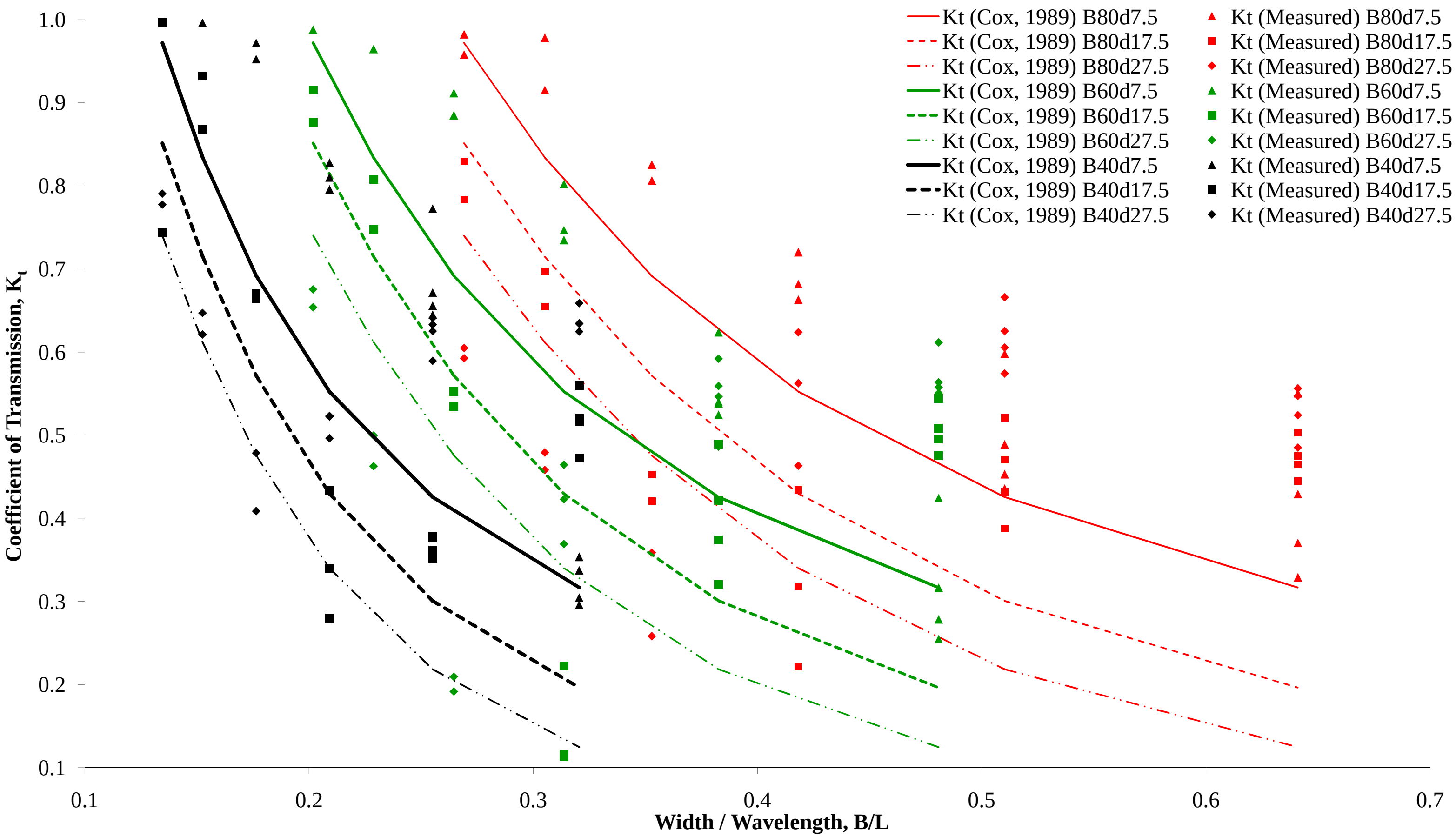

Figure A.7: Experimental K_t comparison with Cox's Theory for chain moored cases

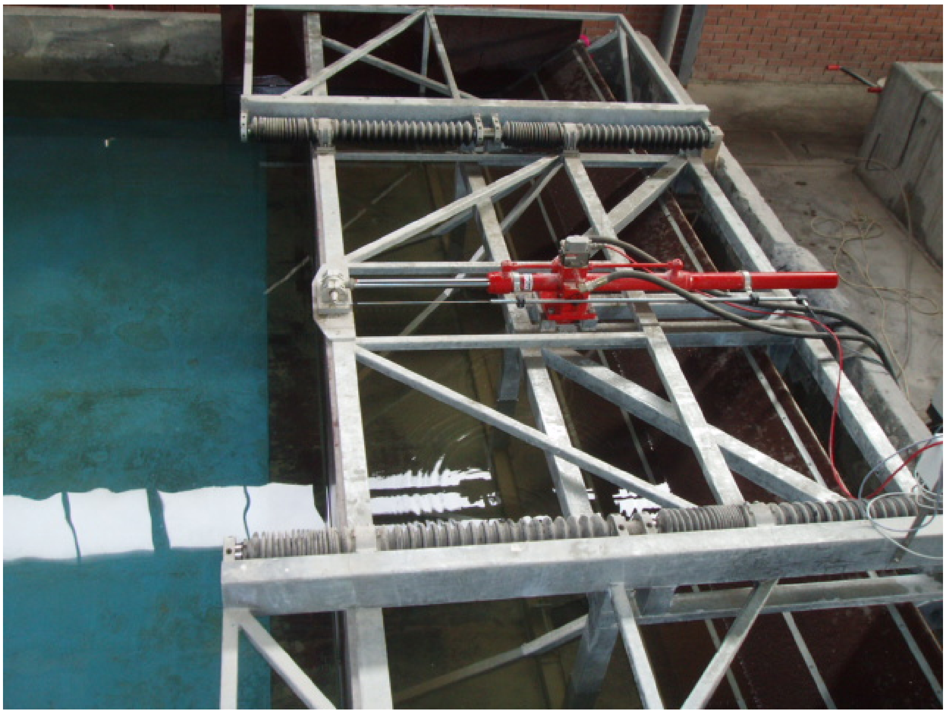

Figure A.8: Piston type wave generator

Figure A.9: Model Units in the wave flume